SAND2016-4765C

Applications of EBSD in Materials Science

Joseph R. Michael

Materials Science and Engineering Center, Sandia National Laboratories, Albuquerque, NM

Sandia is a multiprogram laboratory operated by Sandia Corporation, a Lockheed Martin Company, for the United States Department of Energy under contract DE-AC04-94AL85000.

Gibeon Meteorite – Microstructure over a huge difference in length scales

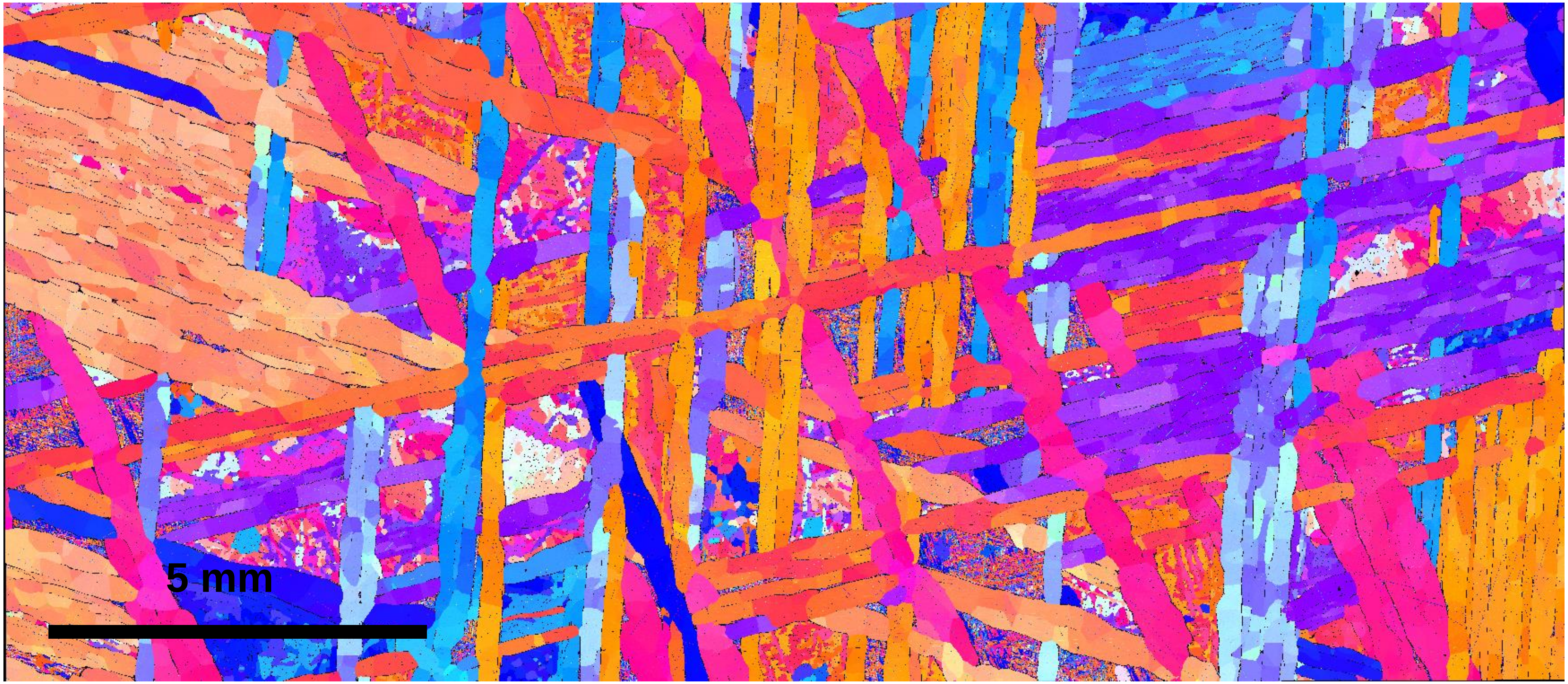

EBSD and TKD allow a large range of length scales to be studied! We can collect data that covers mm and with nearly the same technique we can collect data on the nm scale!

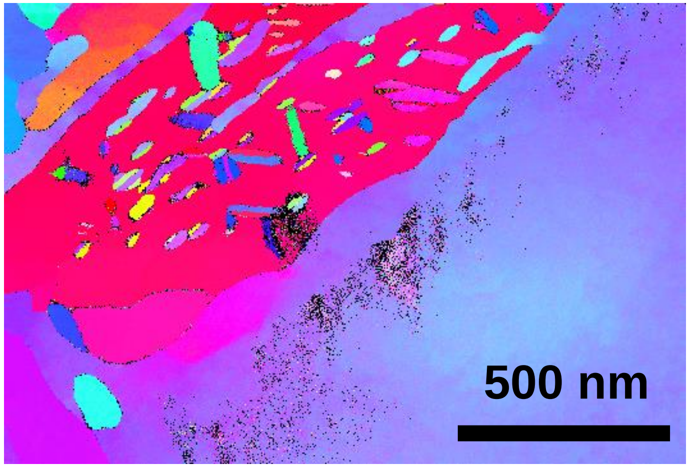

Using EBSD "cleaning" routines – ethical or not?

"EBSD seems to be one of the few techniques in electron microscopy where the extensive interpolation and modification of data through filtering of cleaning routines may be accepted without careful comment about the process."

There are no perfect (at least I have not seen one) EBSD maps with no missing or mis-indexed pixels as acquired, but there are many in the literature.

How many of these papers with perfect EBSD maps tell you what they did to make them that way?

The vendors of EBSD tools encourage this by supplying the "Easy button" that removes random mis-indexed pixels and then fills in the pixels that do not get indexed.

***Brewer and Michael, Risks of "cleaning" EBSD data, Microscopy Today, 2010, March, p. 10-15.**

EBSD cleaning routines

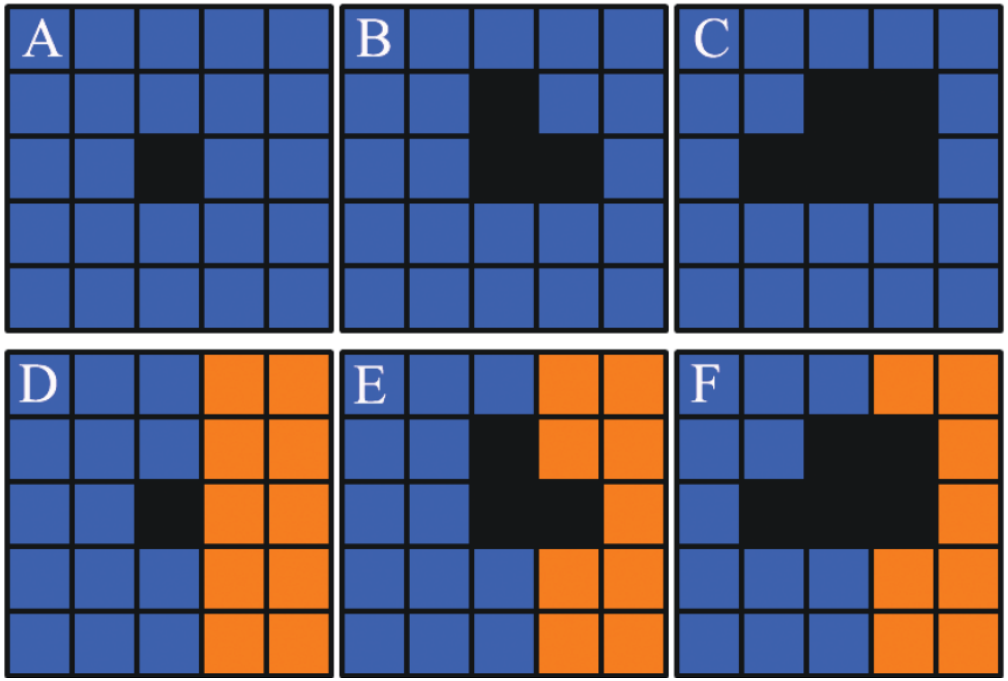

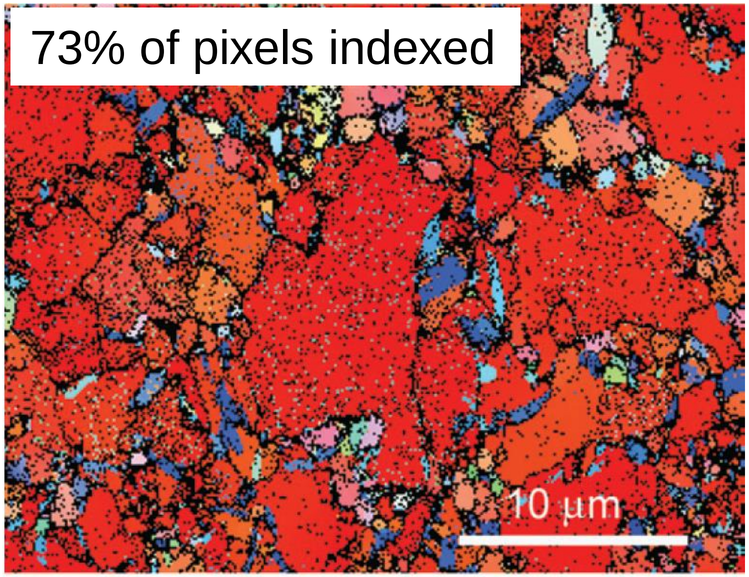

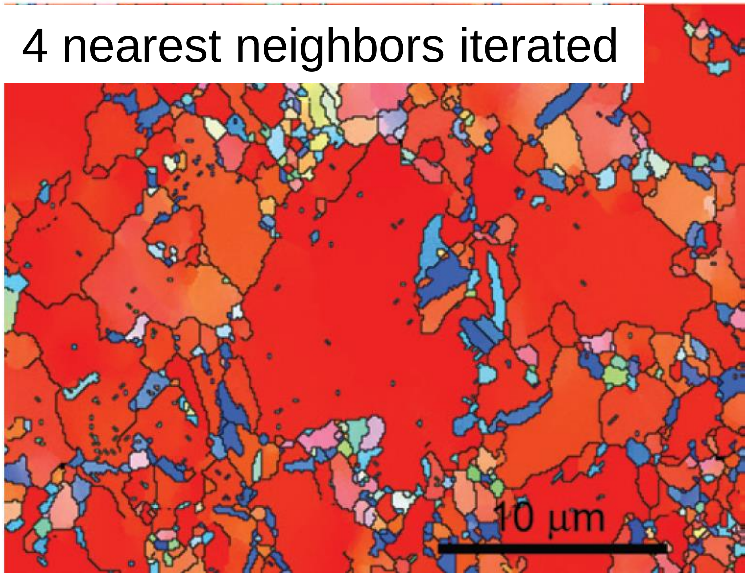

Be careful how the nearest neighbor hole filling routines are applied – can end up with some odd looking microstructures.

Raw data

8 neighbors

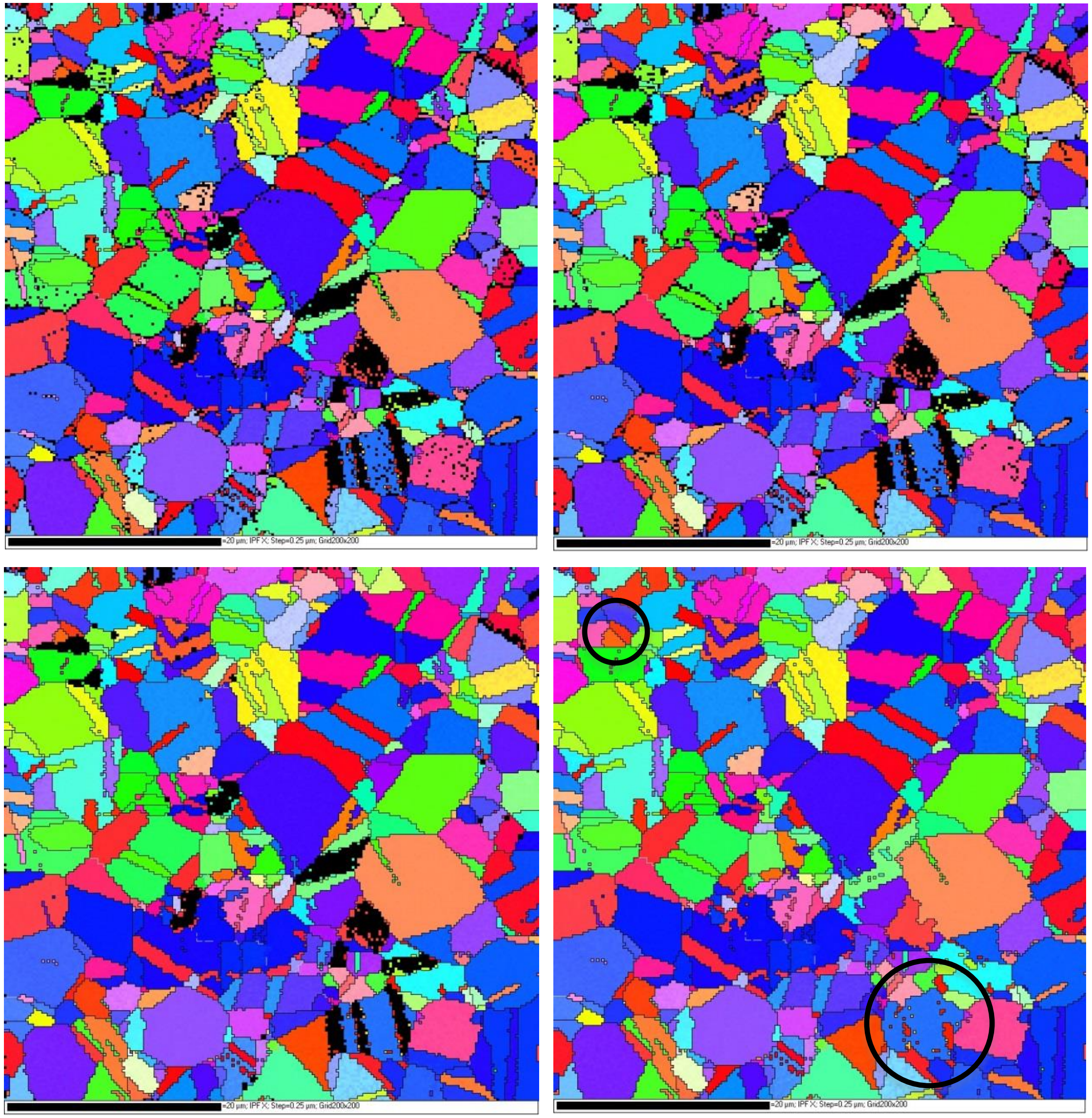

6 neighbors

4 neighbors

Impact of kernel size used to fill in pixels.

Extreme data cleaning -

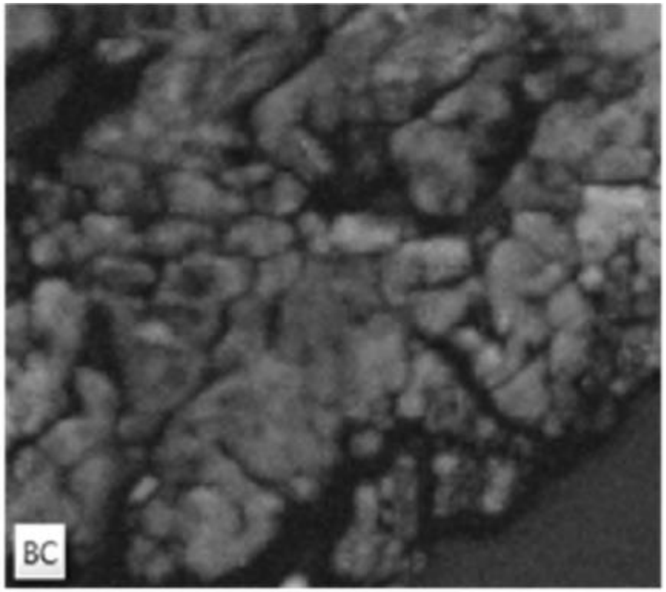

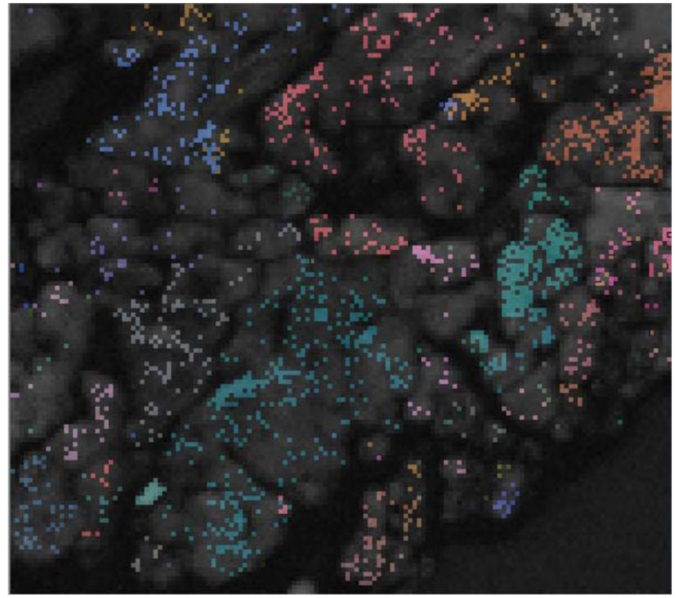

Actual indexed pixels

TKD example of what I consider to be “probably” too much data cleaning.

Maybe make a better sample of figure out why there are issues.

Cleaned data!

Things we (as EBSD experts and peer reviewers) can do to ensure that EBSD remains a strong, vibrant and trusted technique

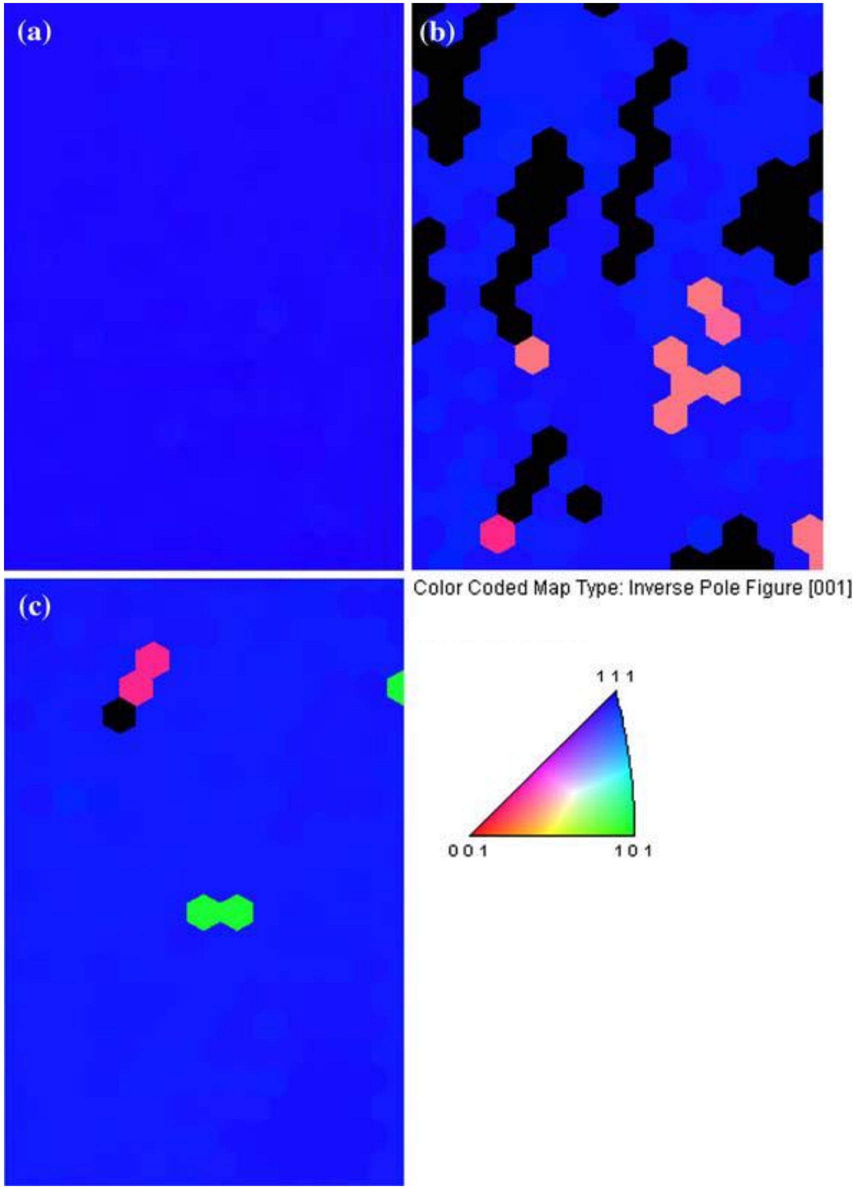

Why do maps like this get published?

No description of processing applied, orientation of sample or even a scale bar in the text or figure caption!

We must and we need to do better than this.

Using EBSD "cleaning" routines – ethical or not?

At the very least, each of us should fully disclose how the EBSD data were treated and why.

For example (and for many of the maps shown in this presentation):

The EBSD data was:

1. Filtered to remove mis-indexed or rogue pixels
2. An 8 nearest neighbors hole filling routine was used to fill in the pixels that were not indexed.
3. If interfaces are important – more aggressive hole filling was applied to ensure that the grain boundaries or interphase interfaces were complete.

Know your frames of reference!

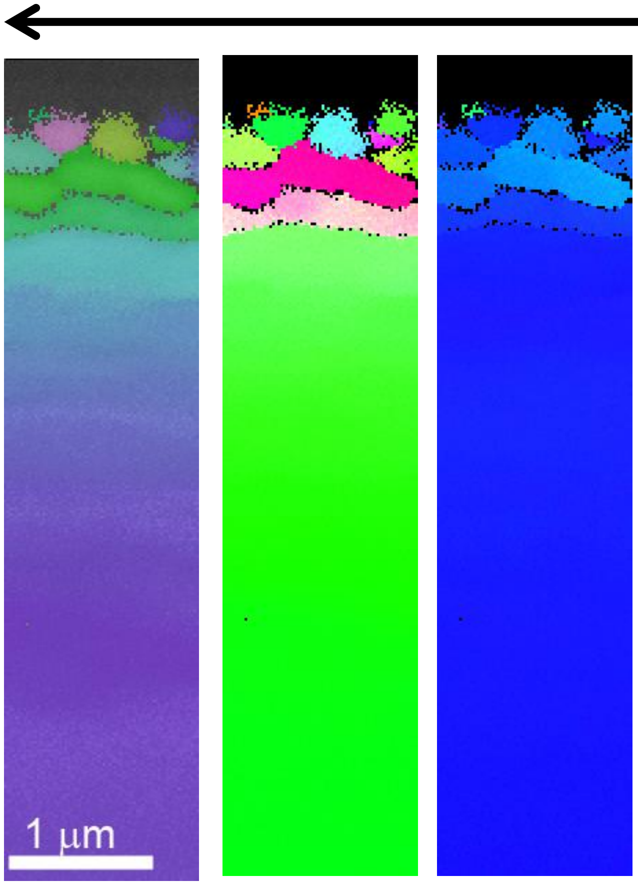

Wear surface of Ni worn in the <211> on (101) plane

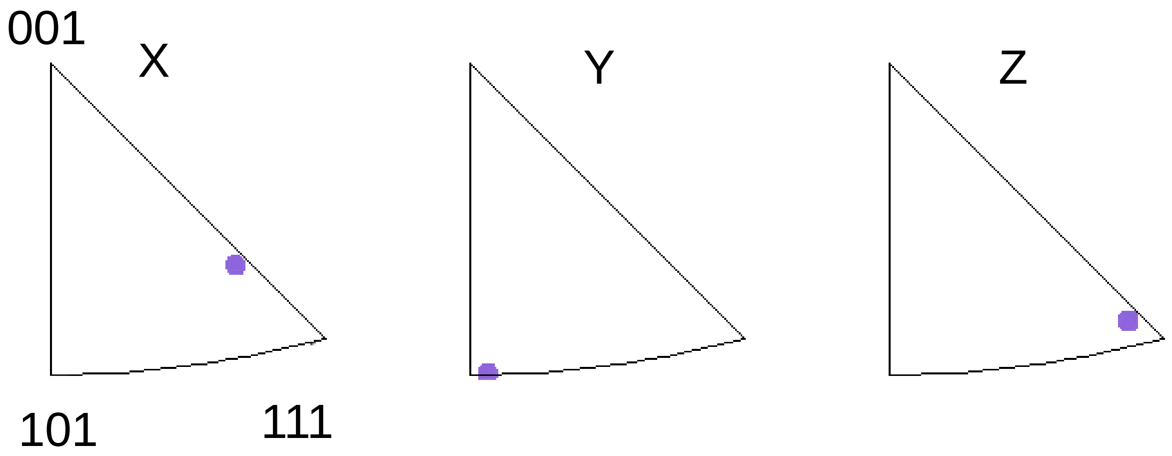

Periodically check to ensure that the data makes sense with respect to what we know about the sample.

In this case we knew we had a (101) single crystal surface and the wear scar was oriented along the <211>. The orientation data supports this.

Know your frames of reference!

Au and Mg layers deposited on a (001) Si wafer

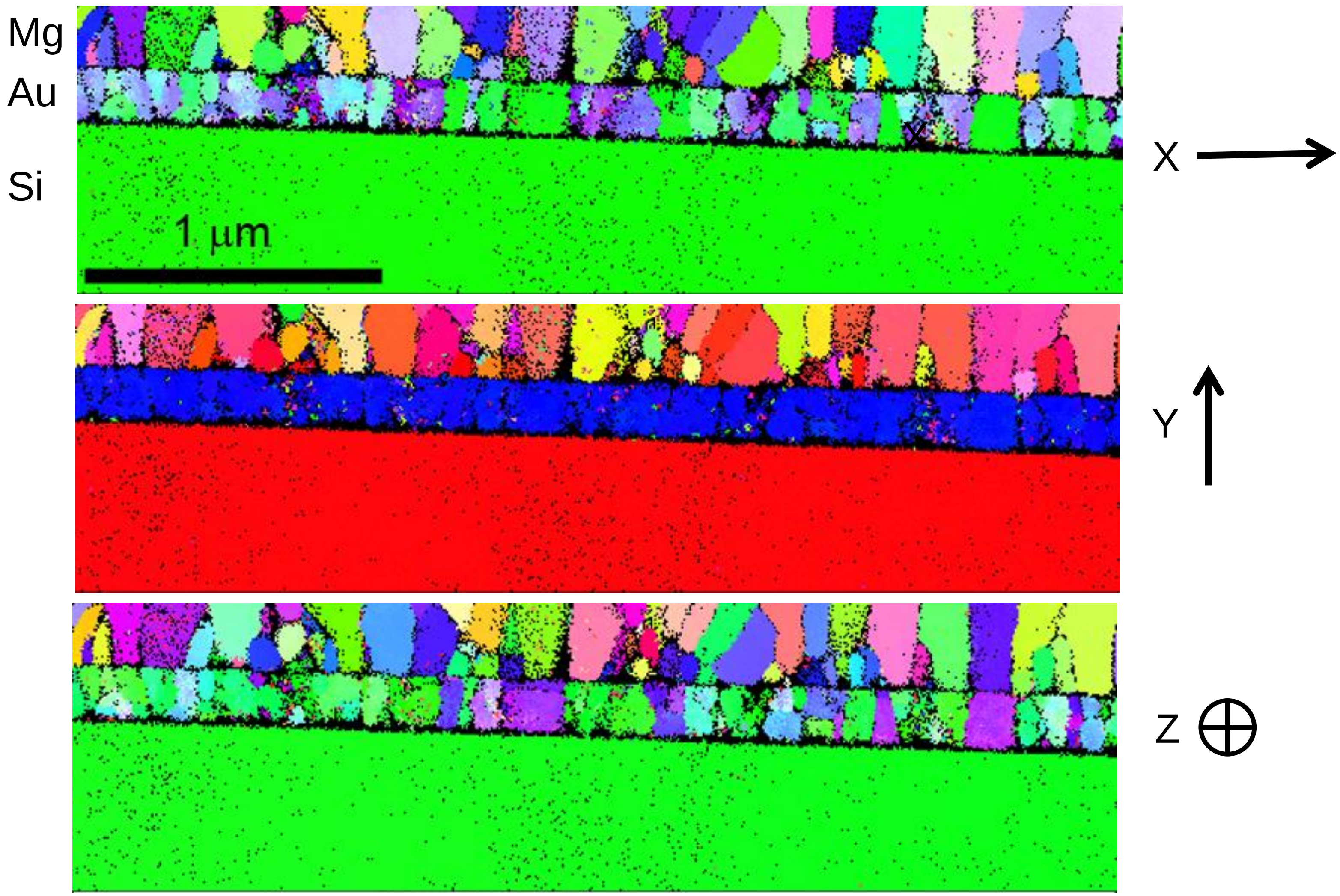

Wilkinson, A. J., T. B. Britton, J. Jiang, Y. Guo, A. Vilalta-Clemente, D. Wallis, L. N. Hansen, and A. Winkelmann. "Tutorial: crystal orientations and EBSD–or which way is up?." *Materials Characterization* (2016).

Analysis of linear feature in strained Al-Si

Sample was subjected to high strain rate deformation

Appearance of linear microstructural features – what are they?

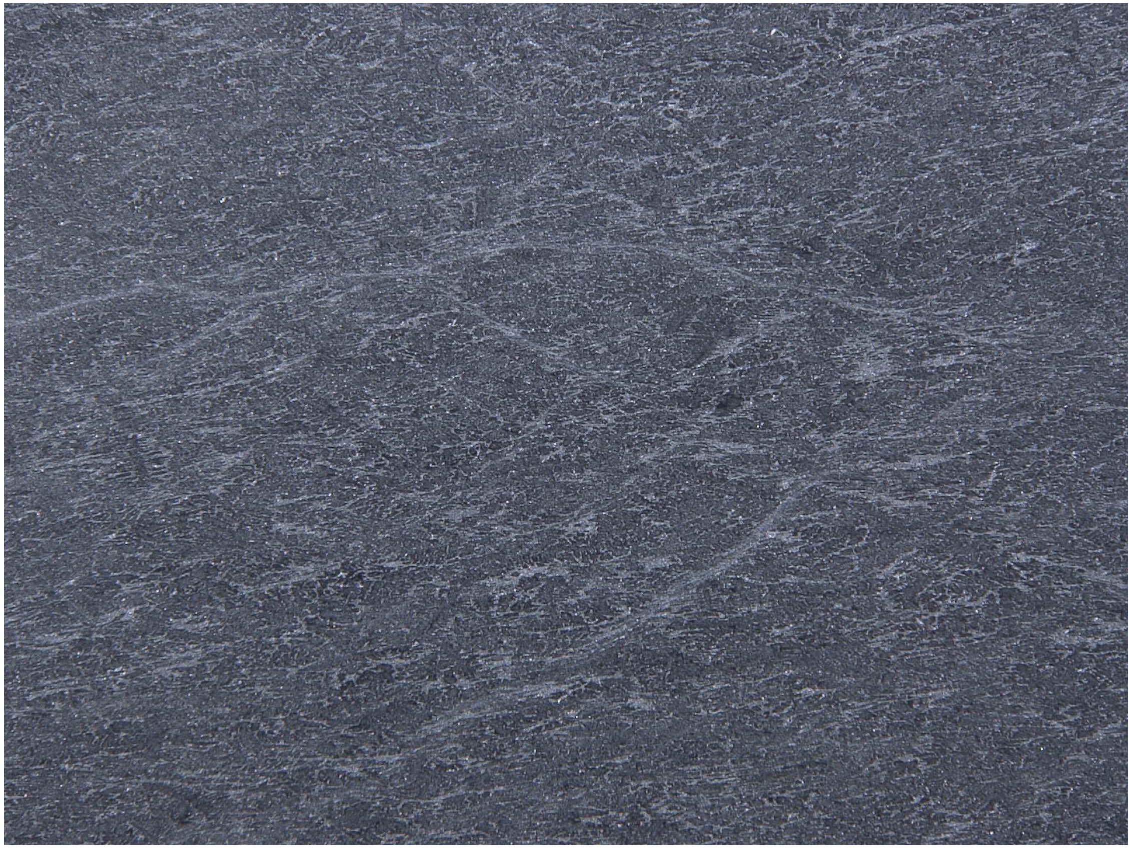

Macrograph of etched surface of sample

Adiabatic shear bands in an Al-Si alloy

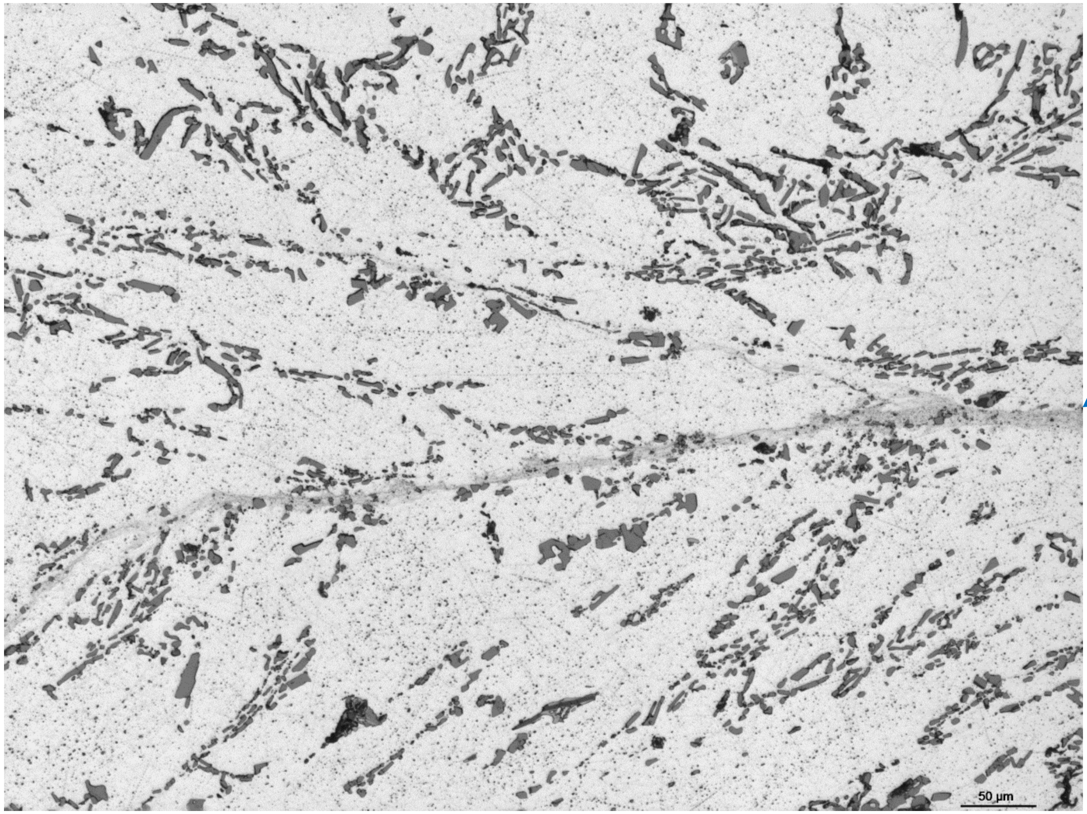

What is this linear feature?

Adiabatic shear band – region of rapid high deformation where slip occurs and causes local temperature rise. Combination of heat and deformation results in dynamic recrystallization in ASB

Adiabatic shear bands in an Al-Si alloy

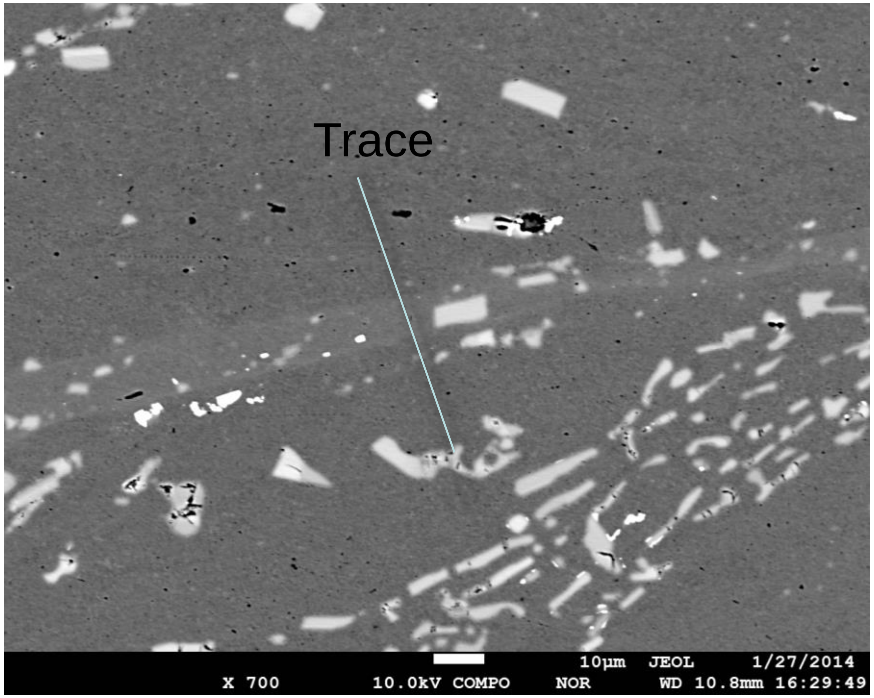

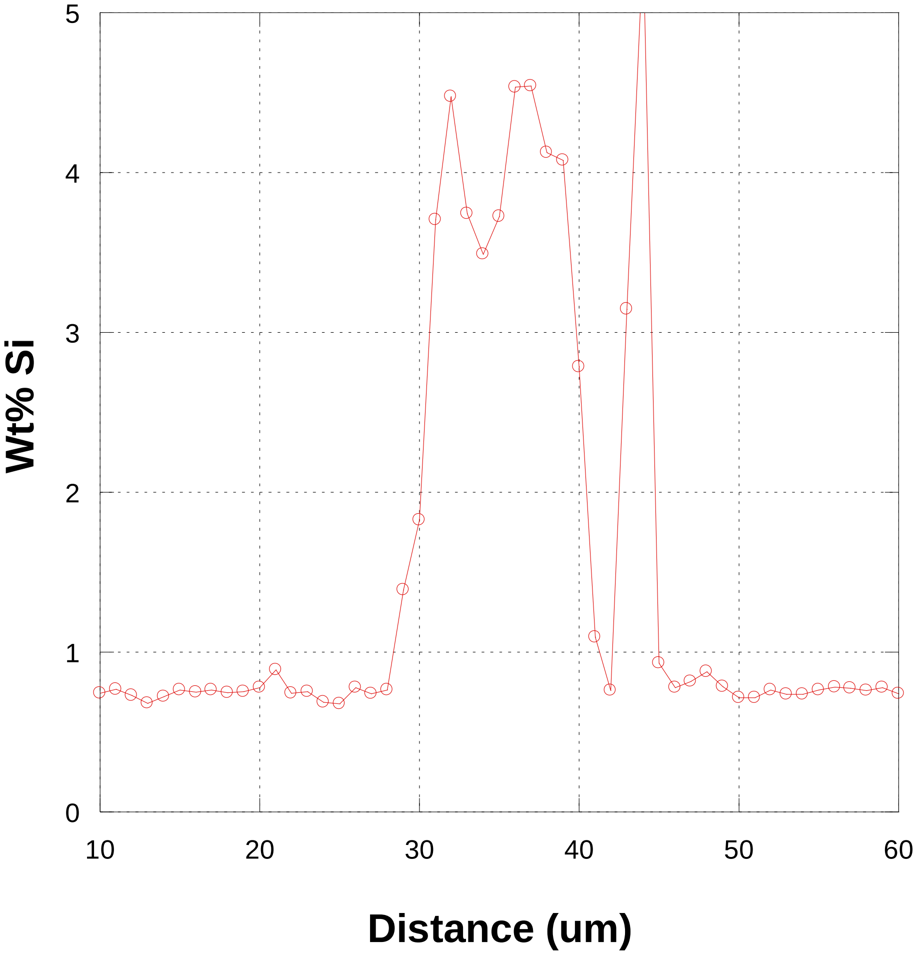

EPMA quantitative analysis shows an increase in Si in linear feature

Consistent with local heating followed by rapid cooling.

EBSD of deformed Al-Si alloy

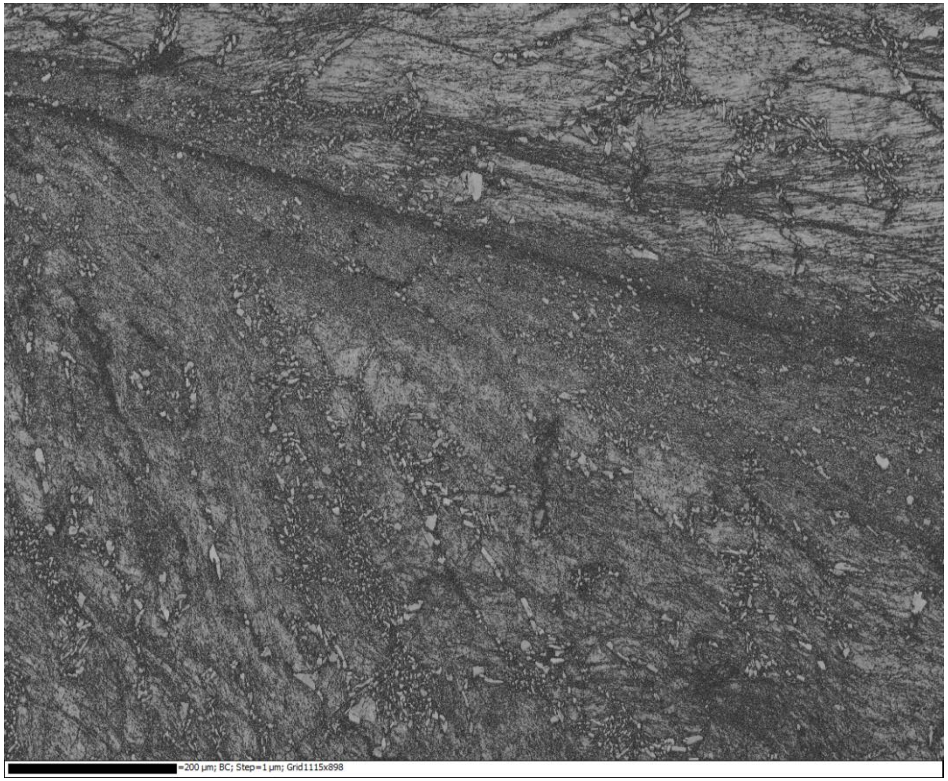

Band Contrast

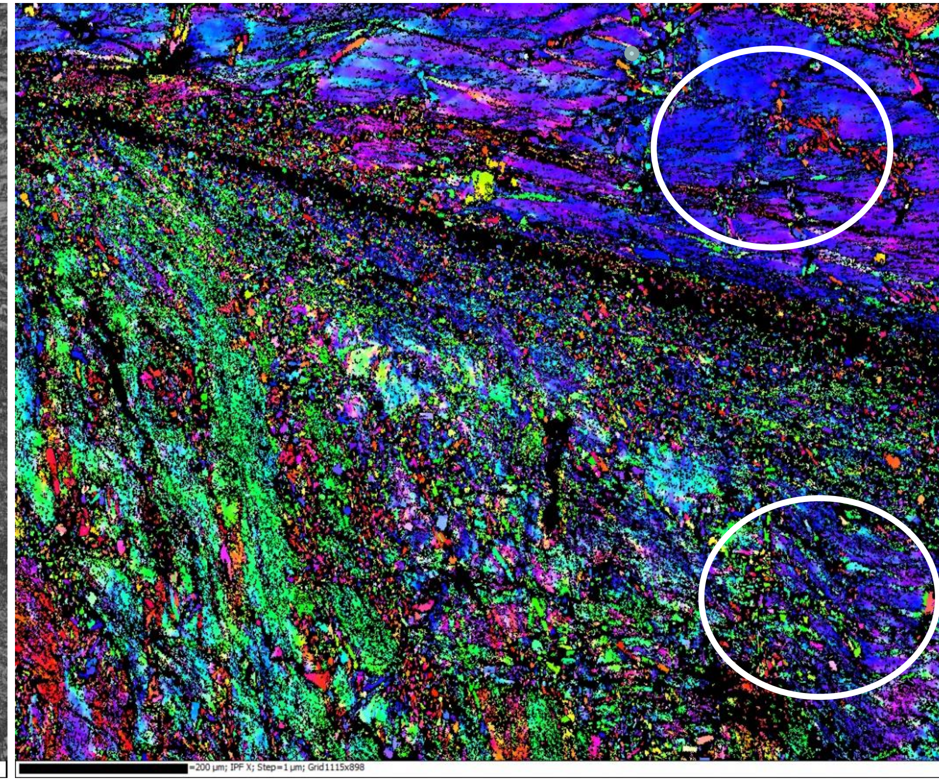

IPF X

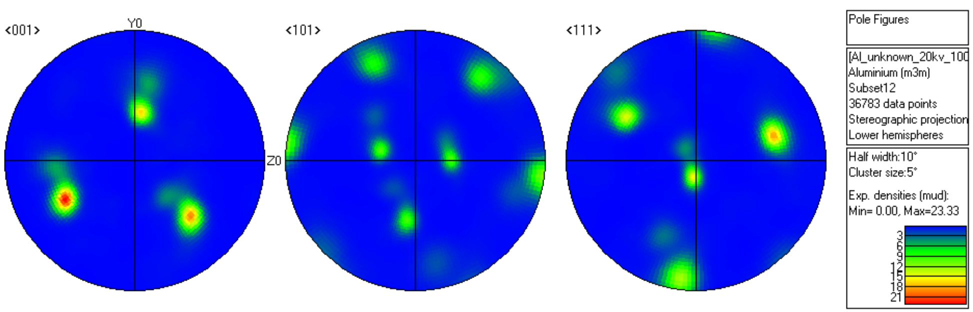

Pole figures show that regions across linear feature have similar orientations. Shear band cut across a grain.

EBSD of deformed Al-Si alloy – TKD from FIB prepared sample in linear band

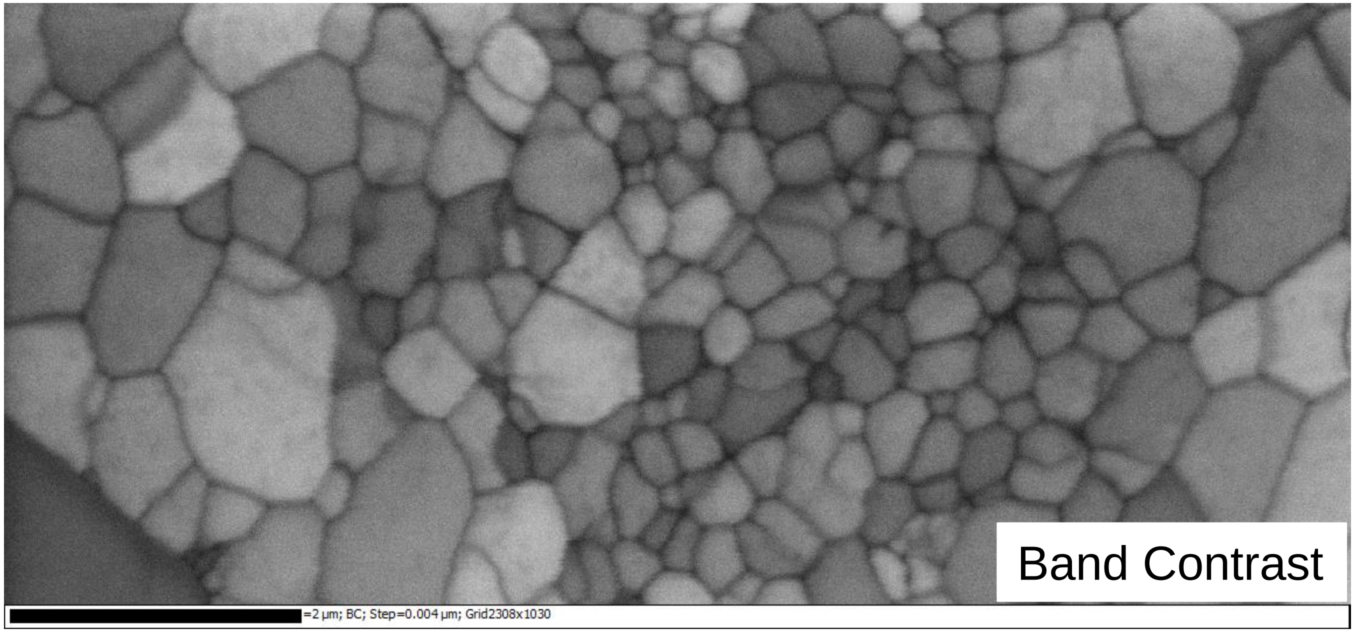

Small equiaxed, recrystallized grains in linear feature.

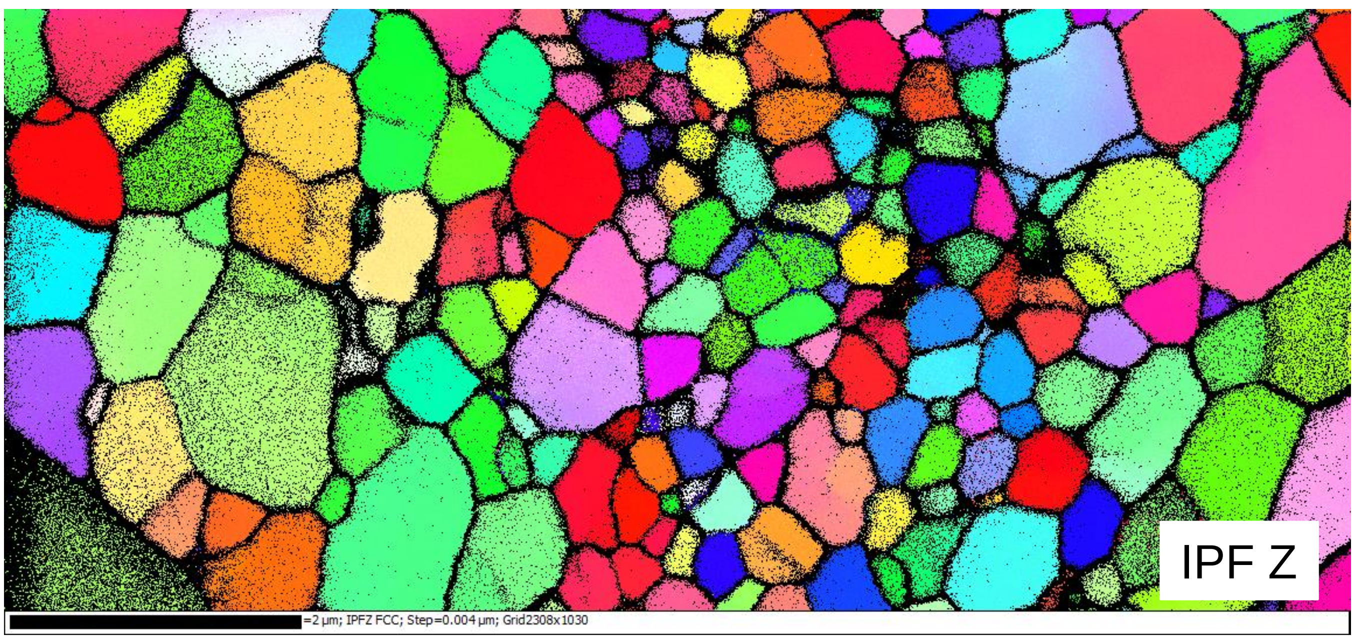

TKD map acquired at 4 nm step size

Analysis of linear features in Al-Si

Linear features are consistent with ASB’s because:

1. Evidence of deformation

2. Evidence of local heating – Si dissolved in local region

3. Evidence of recrystallization in shear band – TKD shows fine equiaxed grains in ASB region

EBSD characterization of whiskers offer many unique challenges:

Spatial resolution – whiskers have one dimension that is quite small

Geometry – Whiskers may cast shadows on detector screen that appear as bands adding indexing difficulties

We may want to know the whisker geometry with respect to the growth surface

Out-of-plane geometries are more difficult to deal with than planar (polished) samples.

Goal is to correlate crystallographic growth directions with physical growth angles

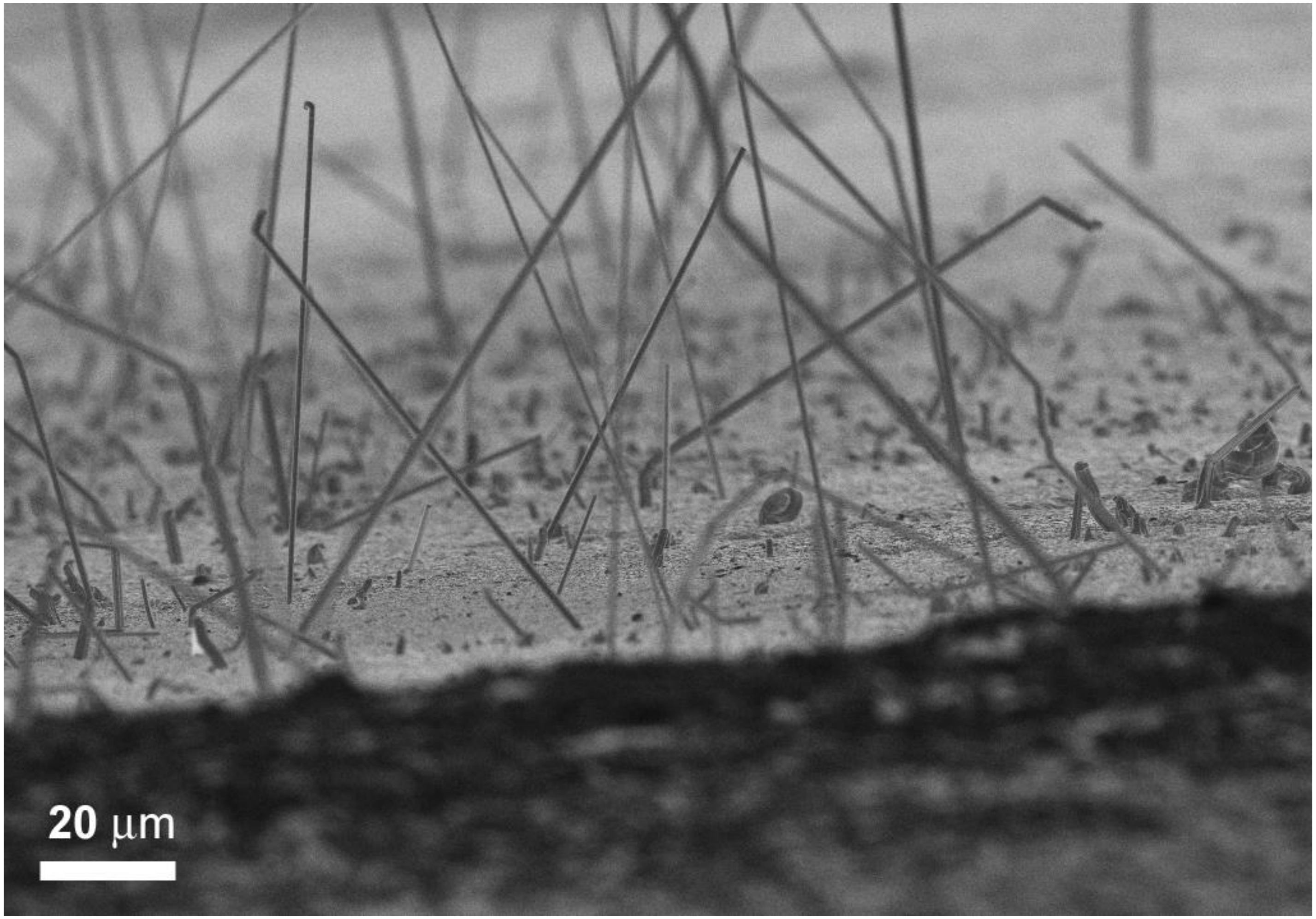

Sn whiskers can be reliability concern in electronic devices due to possibility of forming shorts.

Whiskers "in-situ" aligned with tilt axis and independent measurement of growth angle

1. Image whiskers un-tilted and align axis with tilt axis of SEM stage. Measure projected length of whisker.
2. Tilt sample to EBSD geometry and collect and index patterns from whisker. Measure projected height of whisker tip.
3. Use parallax and geometry to determine whisker angle.
4. Collect EBSD patterns and index. Mathematically rotate orientation matrix by measured whisker angle about Y axis to bring growth axis onto Z axis of pole figure.
5. Plot inverse pole figure of Z-direction

Advantages – retains whisker geometry, allows whisker axis to be unambiguously identified, independent measurement of whisker angle wrt sample surface, can use inverse pole figures for display

Disadvantages – neither fast or easy - about 40 whiskers per day

Whiskers "in-situ" aligned with tilt axis

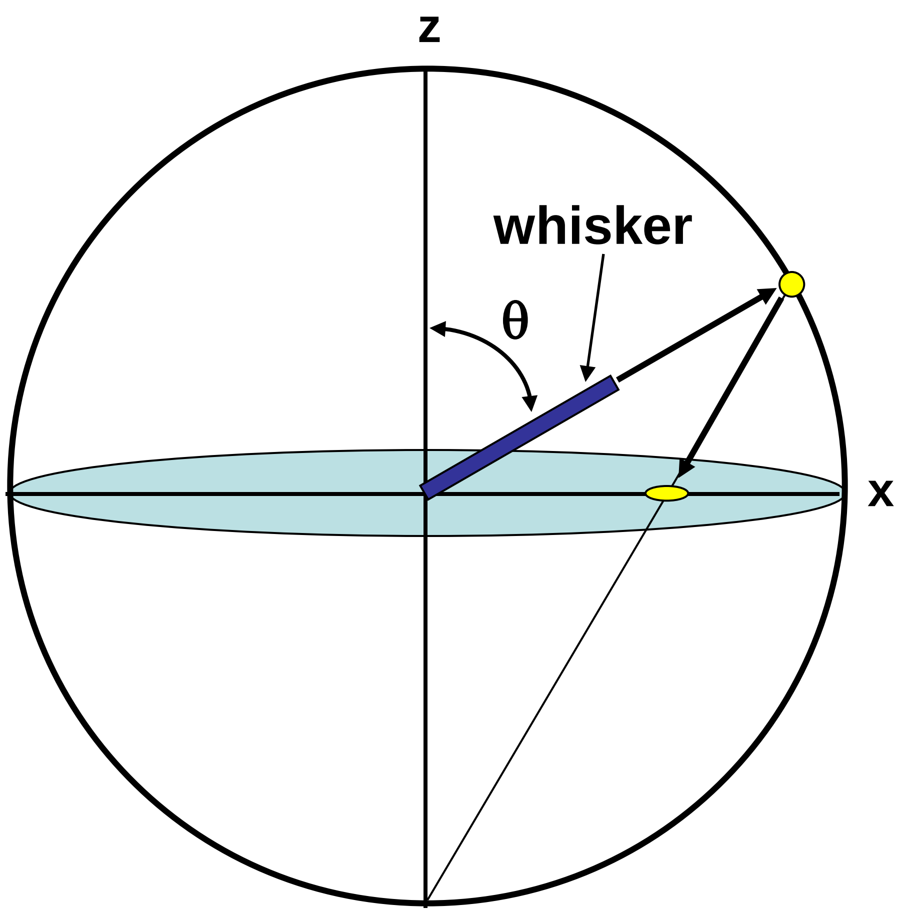

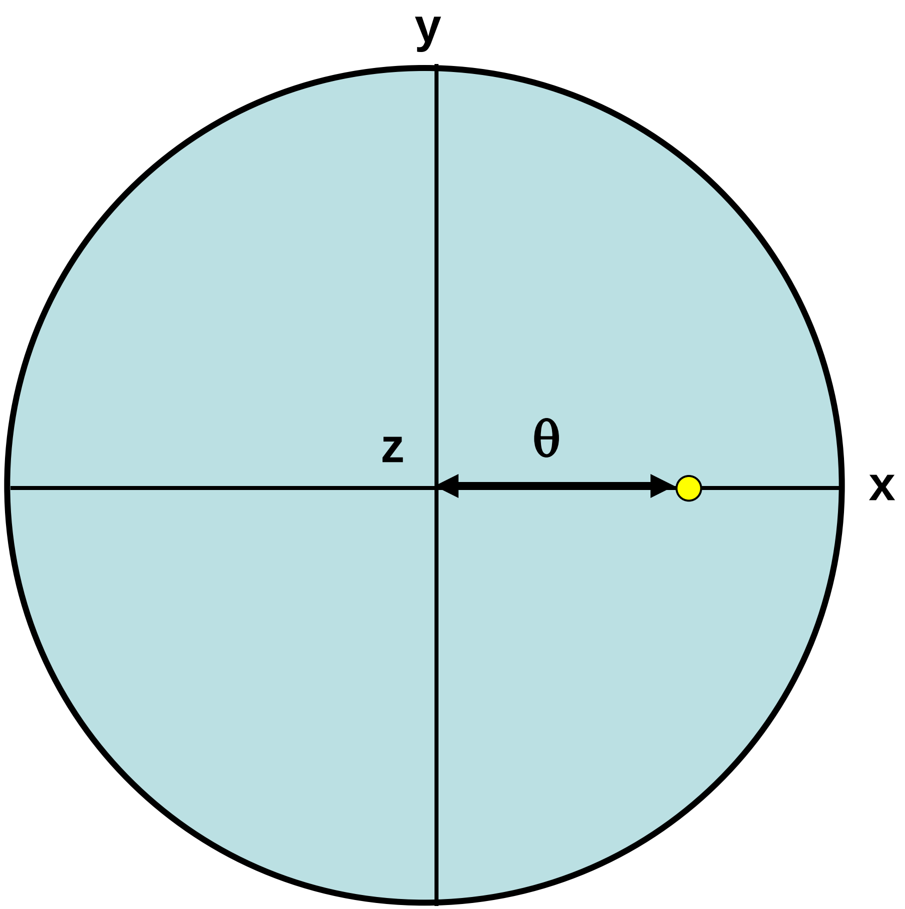

Whisker is in the x-z plane

Pole figure or stereographic projection

Use Stereographic projections to determine whisker growth axis

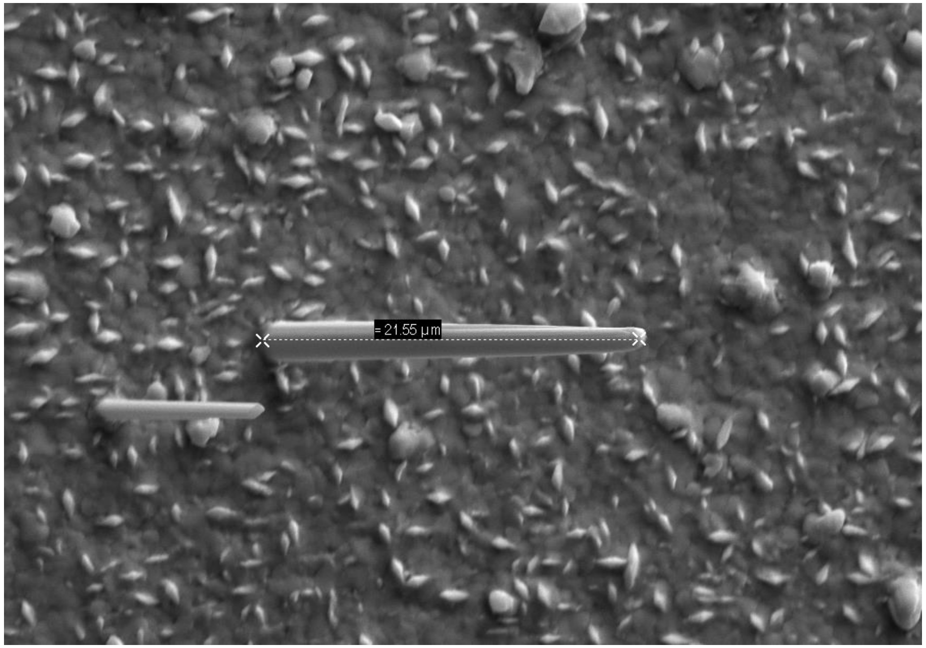

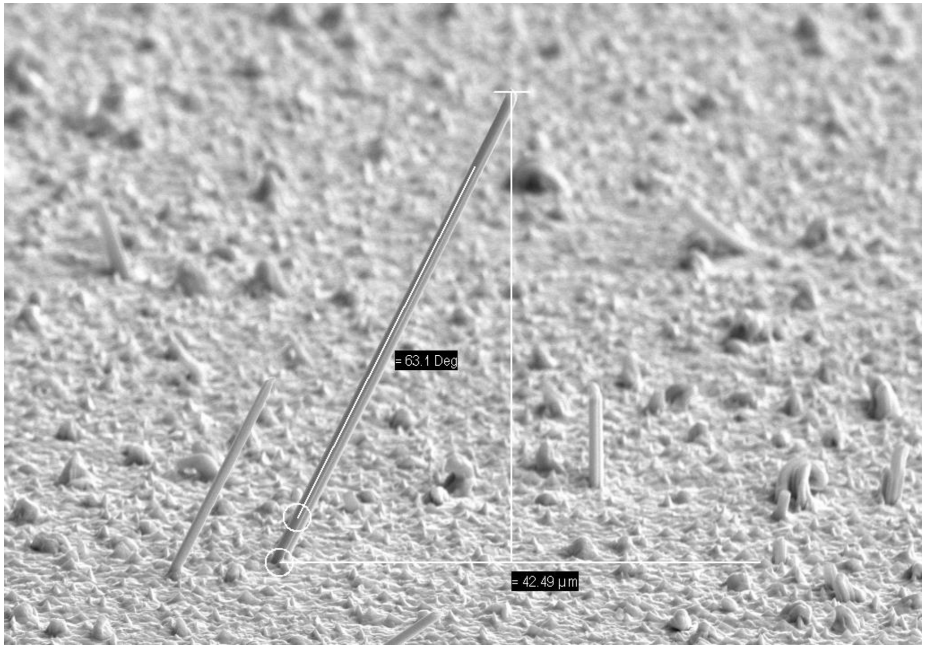

Determine whisker normal trace from two views of sample. In this case with no tilt and with 70º tilt.

Use Stereographic projections to determine whisker growth axis

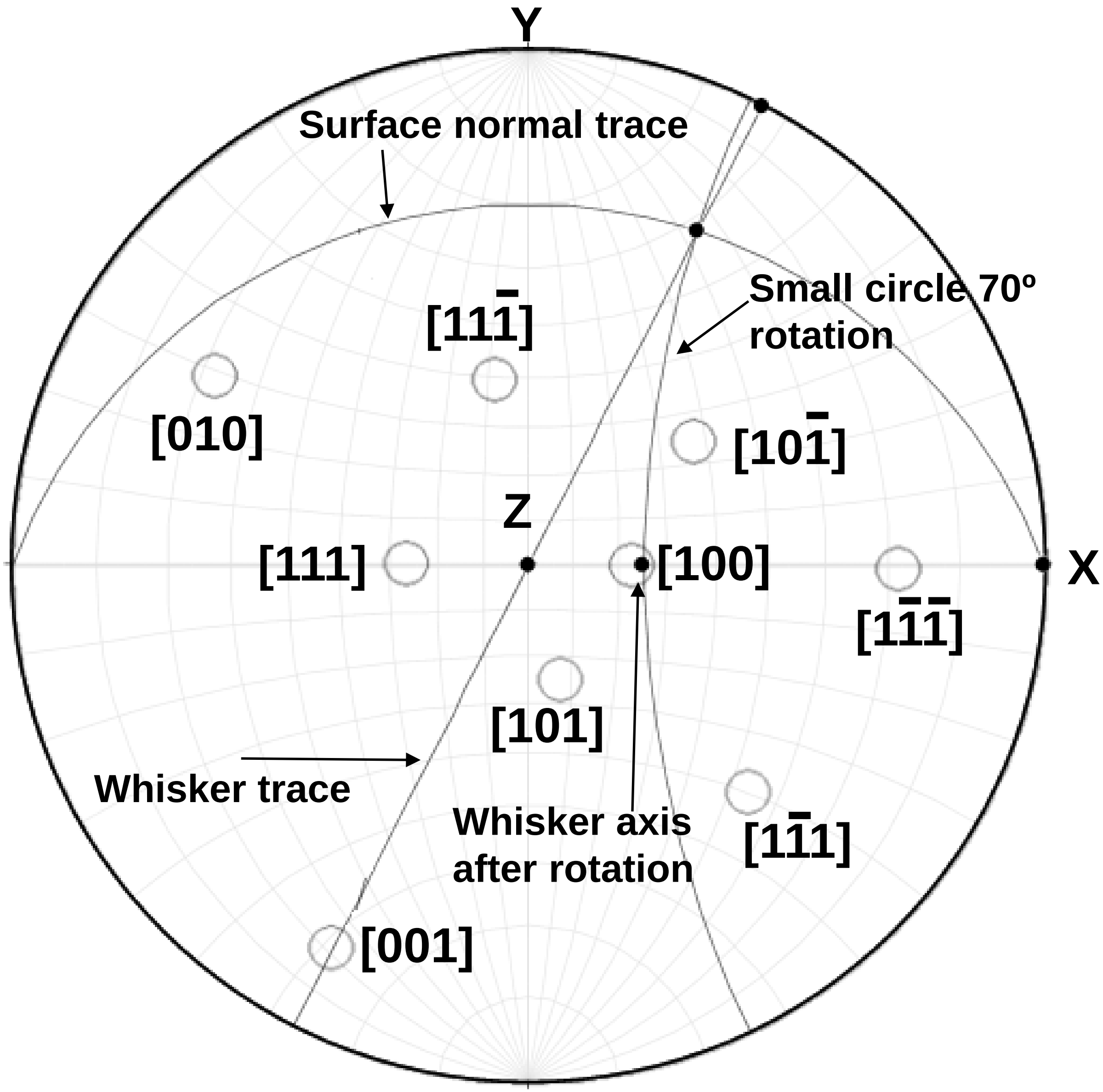

Surface normal plane contains whisker axis

Whisker axis is also contained in plane through the beam direction and inclined 63.1º to the x-axis

Draw great circles representing these planes and the intersection is the whisker axis.

Rotate axis (about tilt axis) along small circle -70º to get equivalent orientation to EBSD

Whiskers “in-situ” aligned with tilt axis

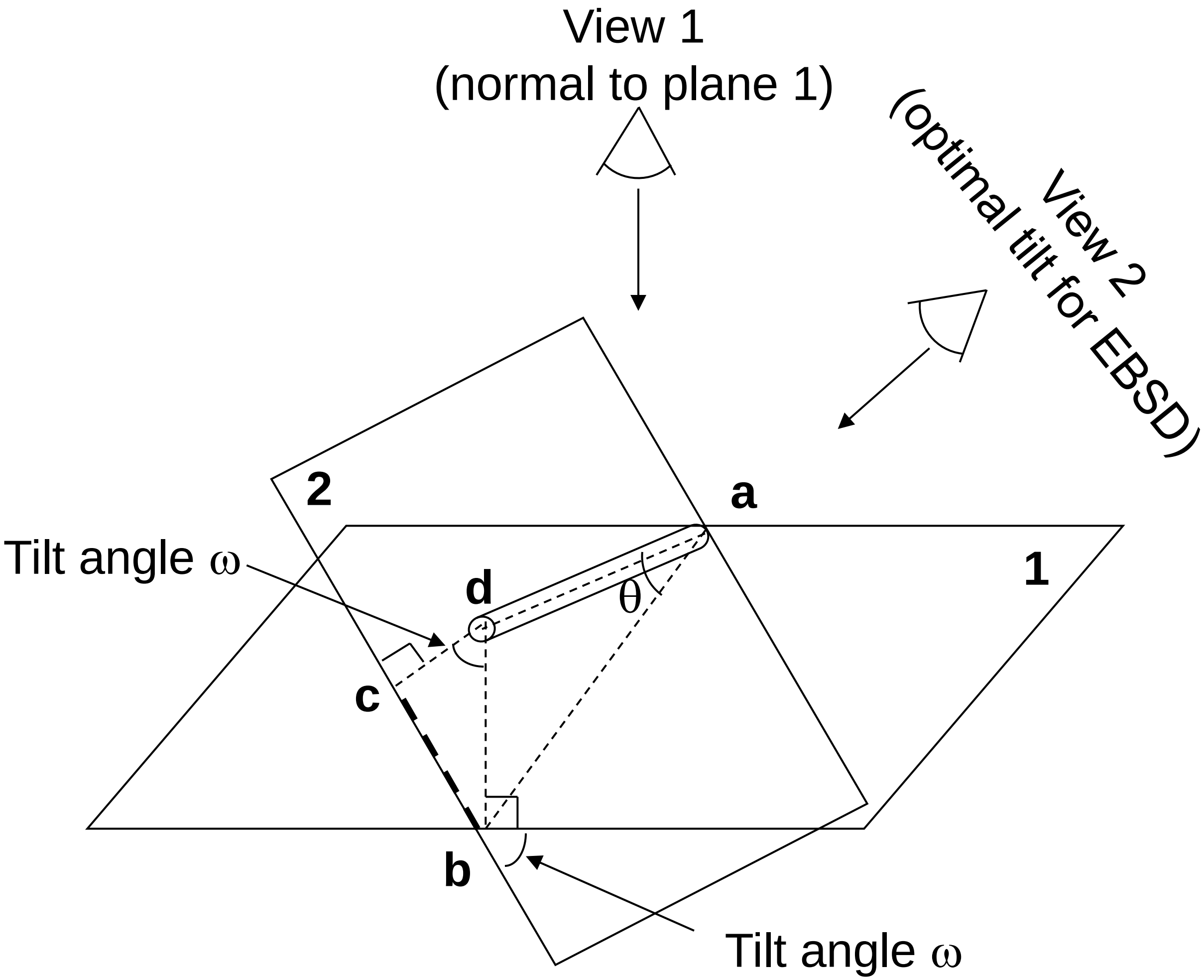

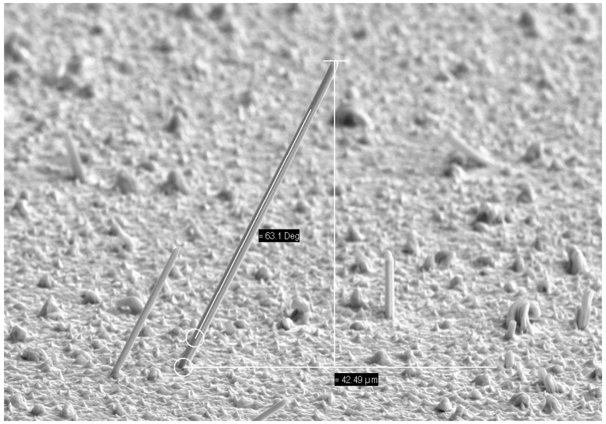

Tilt corrected height = measured height (at tilt)/ cos(90º-tilt angle)

Tilt corrected height(db) = 42.5(cb)/cos(90º-70º) = 45.3 µm

Whisker angle = ArcTan (tilt corrected height(db)/projected length(ab))

Whisker angle from surface = ArcTan(45.3/21.5)= 64.6º

Orientation matrix rotation (for Oxford/HKL systems)

$$OM_{uvw} = \begin{bmatrix} a_1 & b_1 & c_1 \\ a_2 & b_2 & c_2 \\ a_3 & b_3 & c_3 \end{bmatrix}$$

Where the columns represent the uvw with respect to x, y and z

$$OM_{ortho} = \begin{bmatrix} 5.82 & 0 & 0 \\ 0 & 5.82 & 0 \\ 0 & 0 & 3.17 \end{bmatrix} \begin{bmatrix} a_1 & b_1 & c_1 \\ a_2 & b_2 & c_2 \\ a_3 & b_3 & c_3 \end{bmatrix}$$

Multiply OM by the transformation matrix for Tin to get Cartesian coordinates

$$OM_{ROT} = OM_{ortho} \begin{bmatrix} \cos\theta & 0 & -\sin\theta \\ 0 & 1 & 0 \\ \sin\theta & 0 & \cos\theta \end{bmatrix}$$

Rotate OM about y-axis, angle is between sample normal and whisker axis.

$$OM_{final} = \begin{bmatrix} 0.1718 & 0 & 0 \\ 0 & 0.1718 & 0 \\ 0 & 0 & 0.3155 \end{bmatrix} OM_{ROT}$$

Multiply rotated OM by the inverse metric tensor for Tin so that columns of OM_{final} are UVW with respect to x, y and z.

If we get this correct the growth axis is aligned with the z axis!

Characterization of 102 whiskers in-situ on three samples

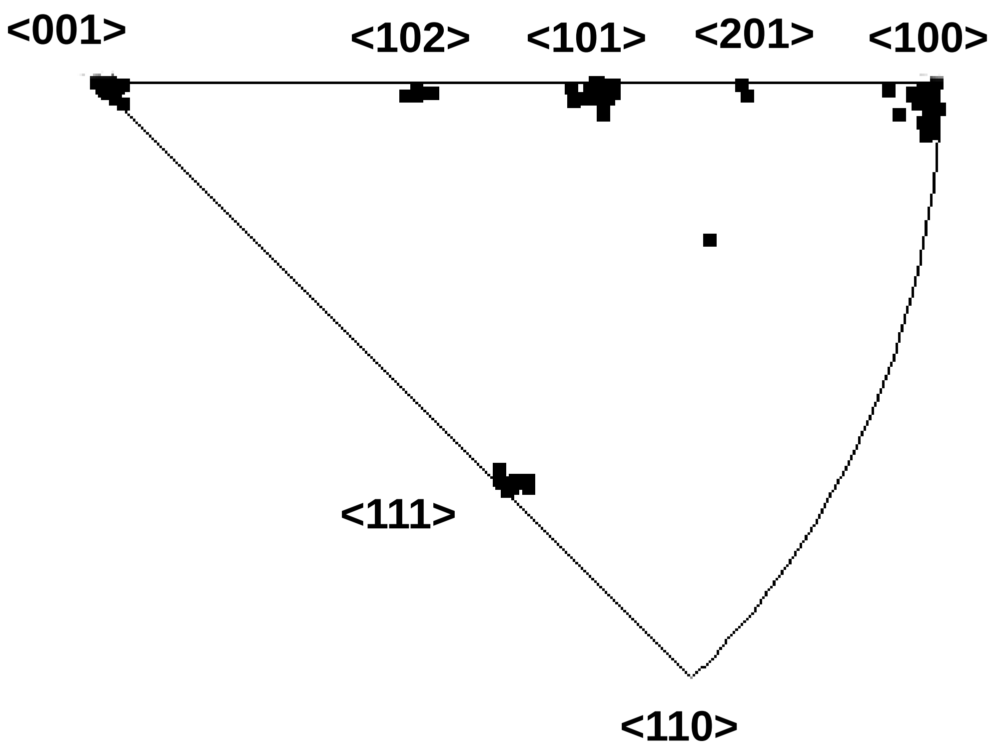

Distribution of growth axes for Sn Whiskers

<001> 45

<010> 19

<101> 18

<111> 11

<102> 6

<201> 2

EBSD's contribution to our understanding of the origins of the universe

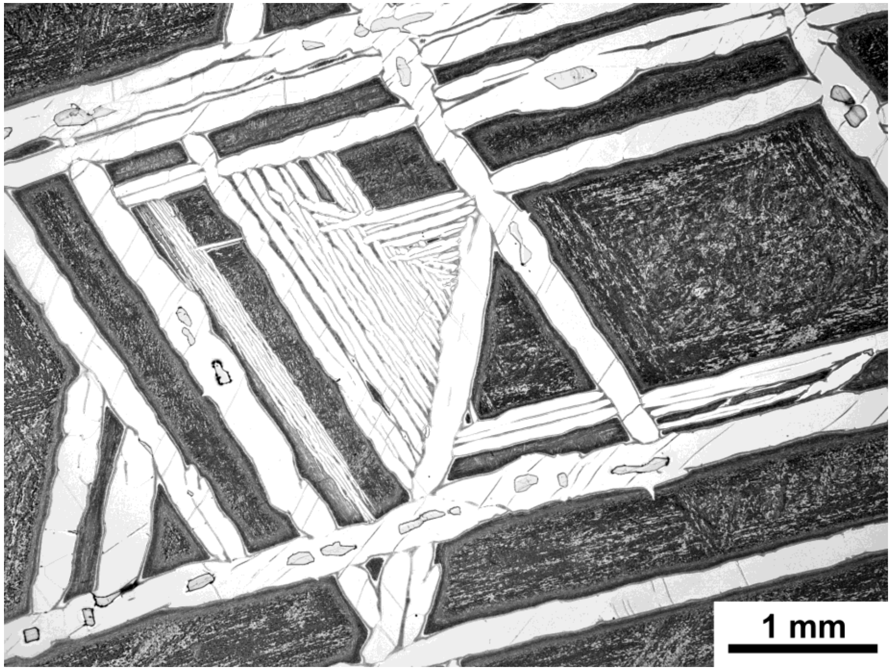

Carlton

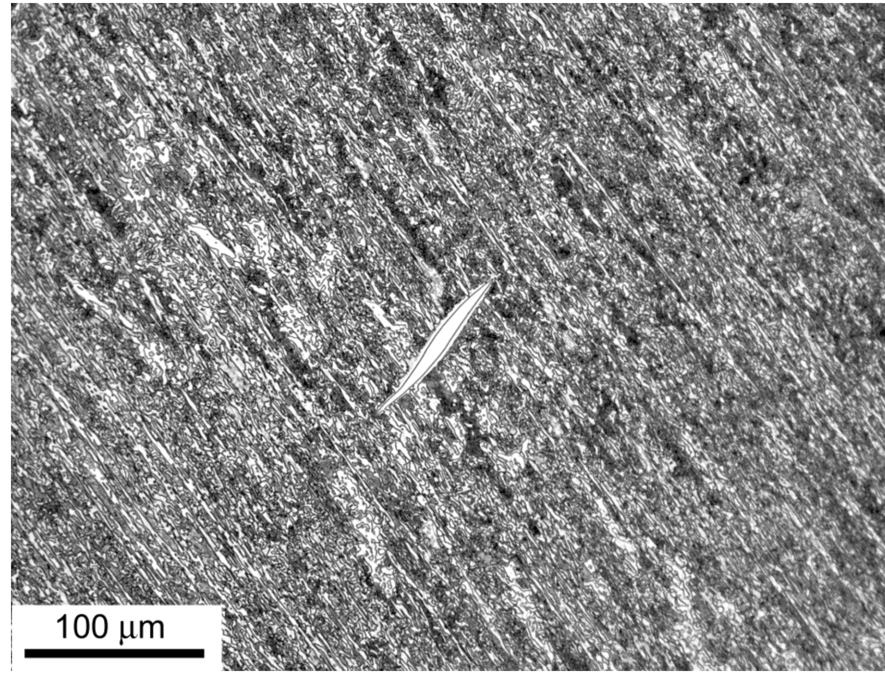

Cape of Good Hope

Microstructures of IVb Meteorites consist of Widmanstatten ferrite plus plessite (two phase mixture of austenite (taenite) and ferrite (kamacite).

Microstructural studies can help develop an understanding of the cooling history of the meteorite.

Orientation mapping of iron meteorites

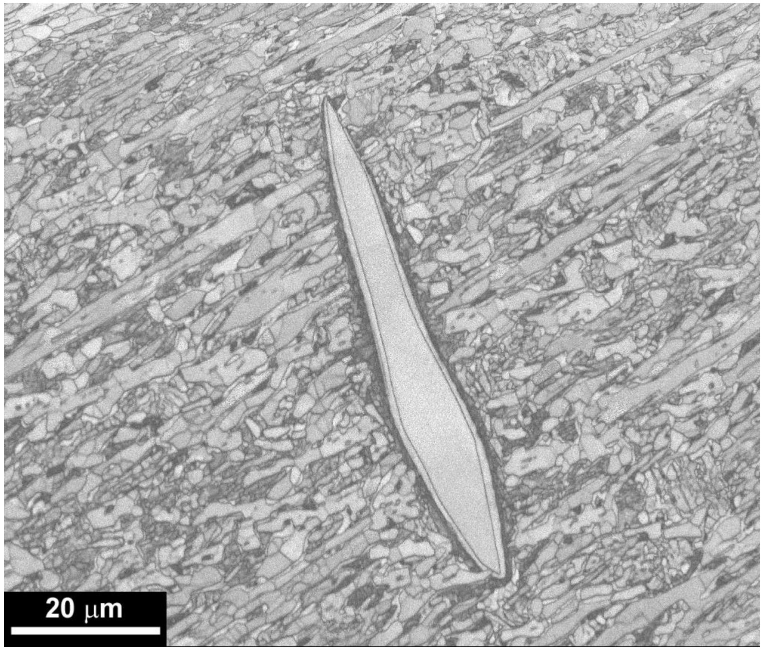

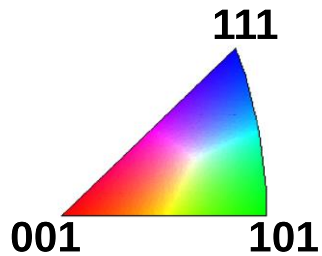

bcc

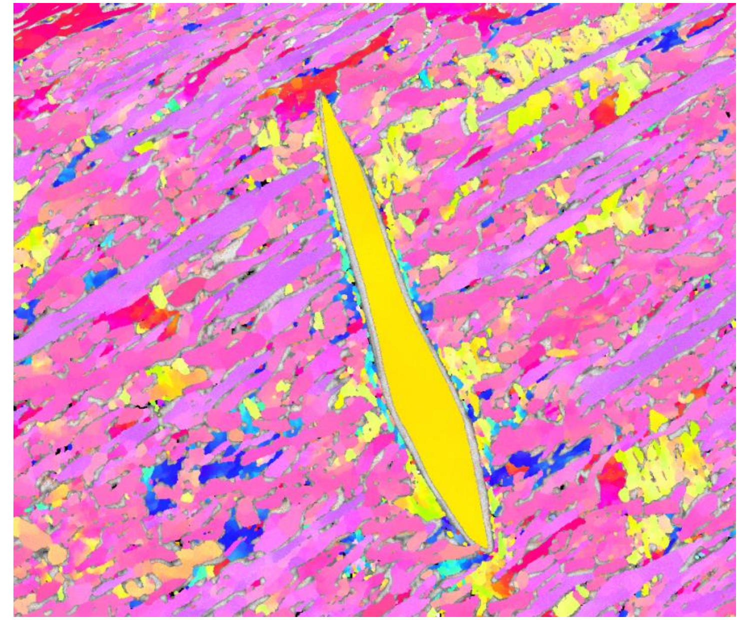

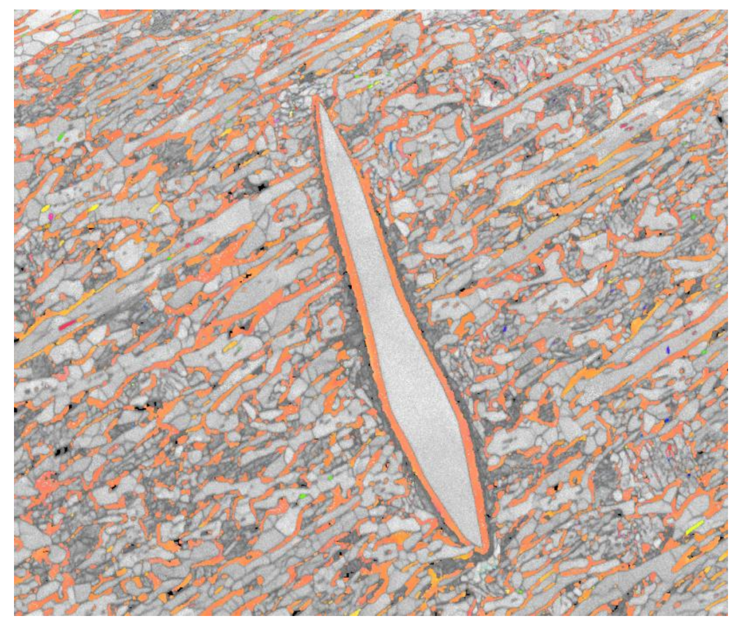

fcc

We can easily identify the fcc from the bcc phases of iron using EBSD.

All fcc has the same orientation!

Appears to be retained austenite from a martensitic transformation

Plessite in IVb Meteorites – IPF maps of austenite phase

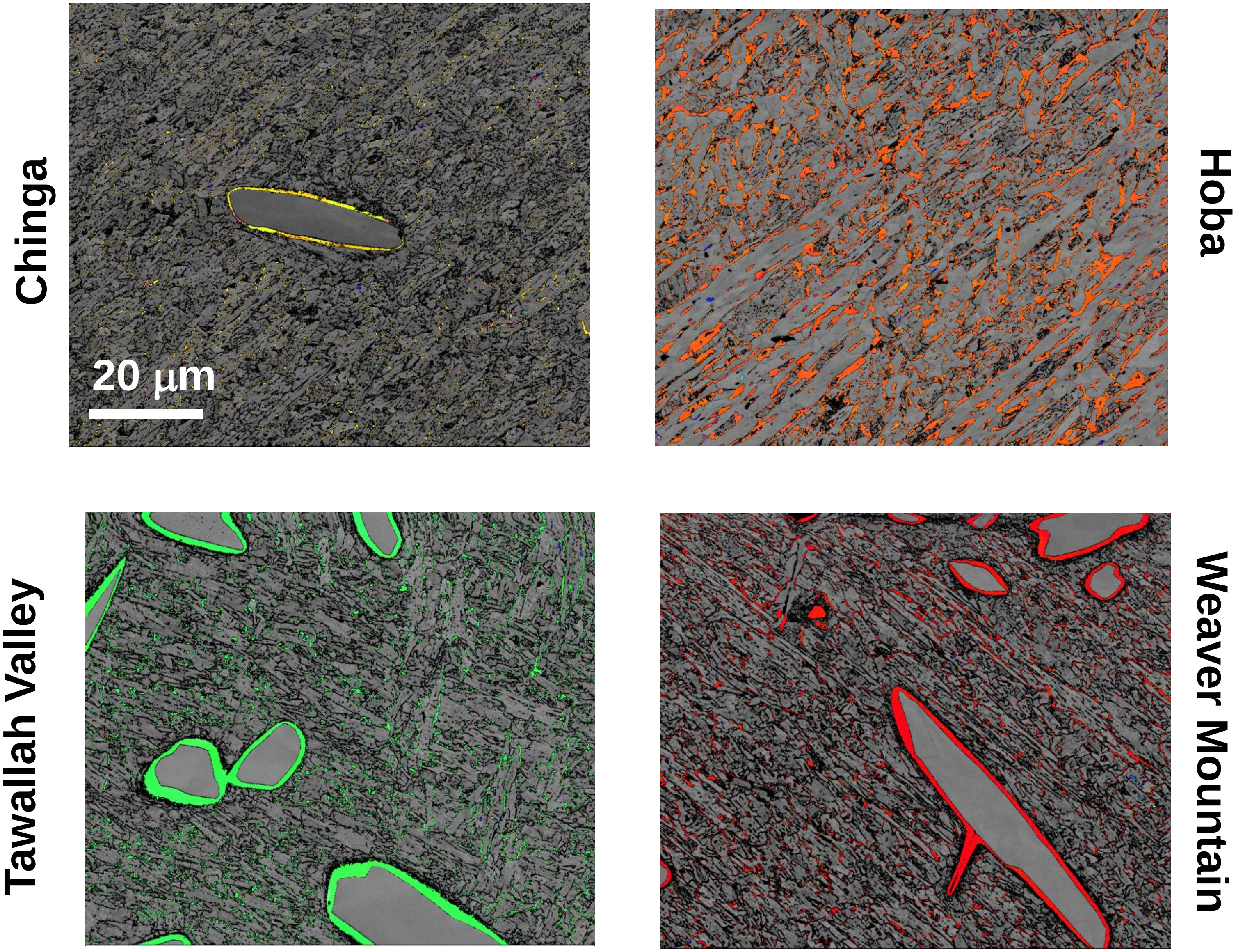

Note that in all cases all taenite (austenite) in a meteorite has the same orientation

Orientation relationships between Ferrite and austenite

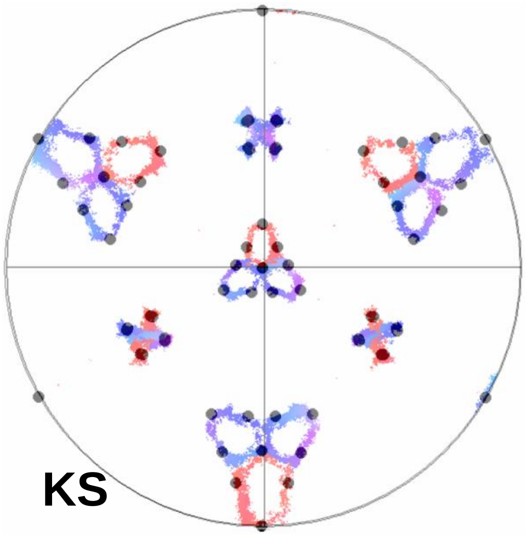

KS

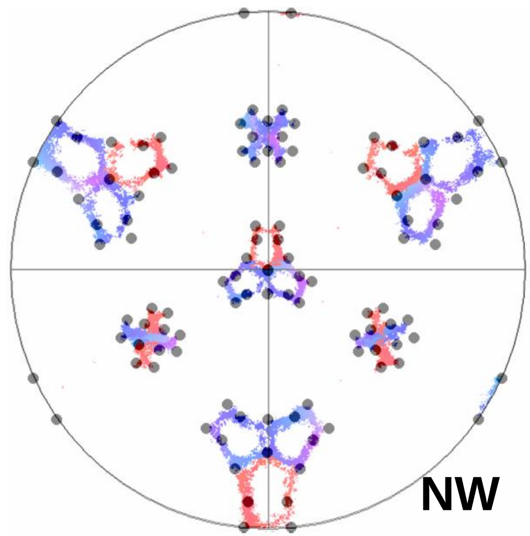

NW

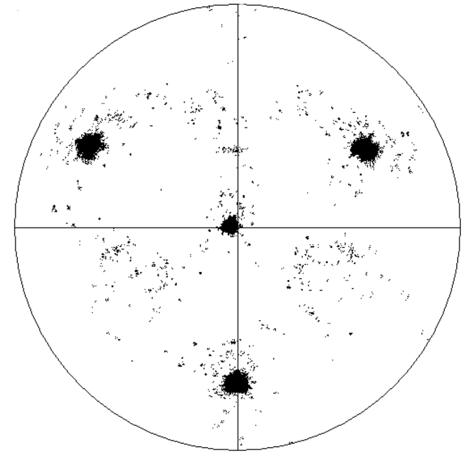

111
fcc Pole figure

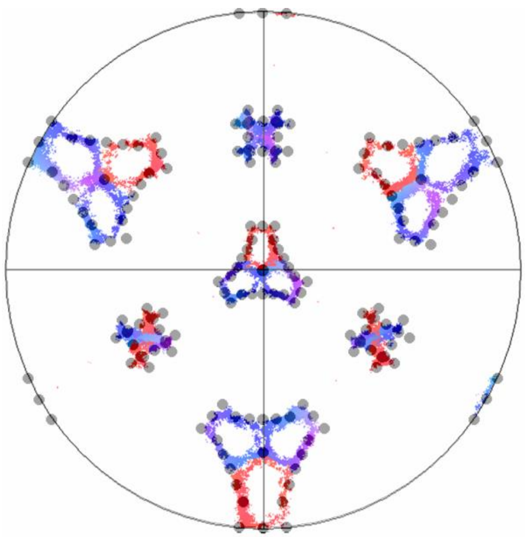

KS +NW
bcc <110>Pole figure

Complex <110>bcc pole figures indicate the orientation relationship between the fcc and the bcc phases is given by:

Kurdjumov-Sachs		Nishiyama-Wasserman
$\langle 110 \rangle_\gamma \parallel \langle 111 \rangle_\alpha$	or	$\langle 011 \rangle_\gamma \parallel \langle 001 \rangle_\alpha$
$(111)_\gamma \parallel (110)_\alpha$		$(111)_\gamma \parallel (110)_\alpha$

Or some combination of KS + NW

Large area mapping of Gibeon confirms the previous results

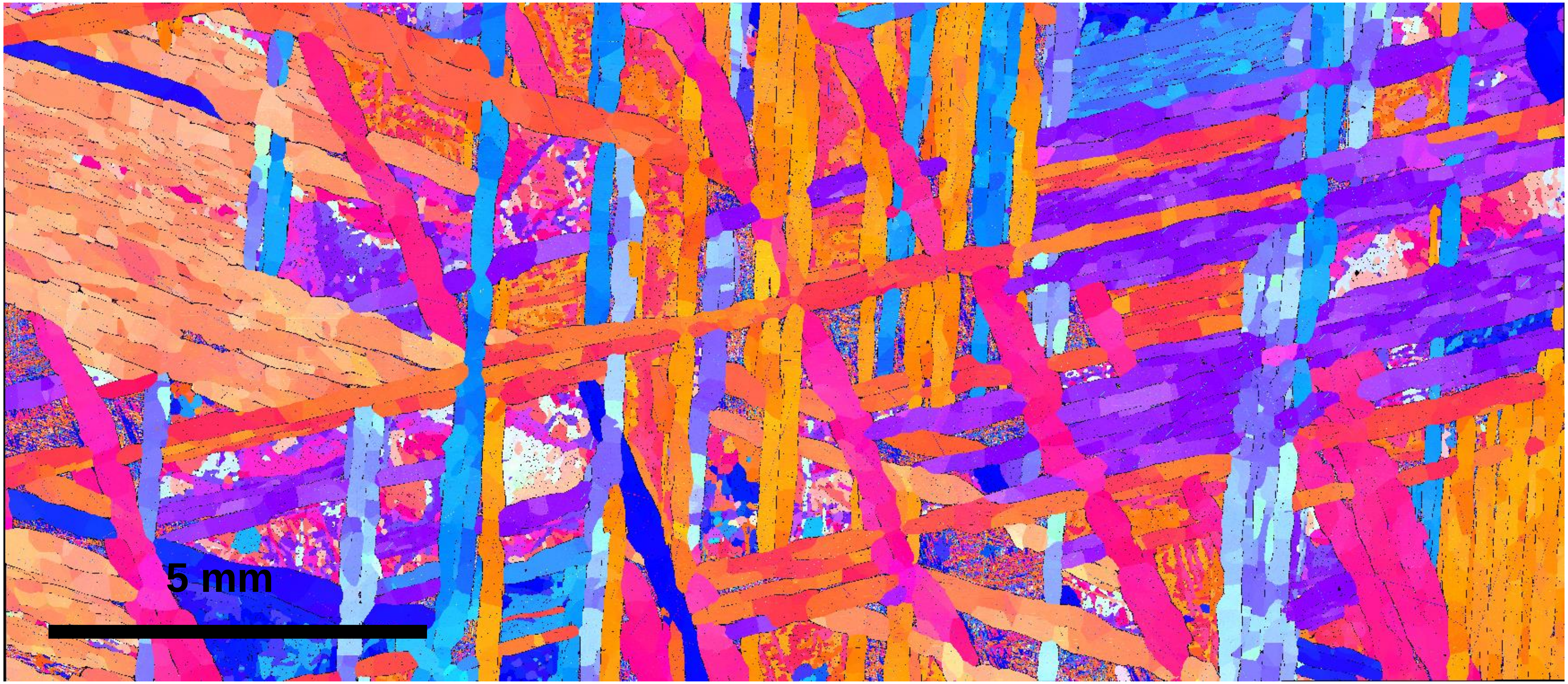

Polished section of Gibeon mapped over large area using 3 μm steps.
Large Widmanstatten ferrite plates formed during slow cooling.

Large area mapping of Gibeon confirms the previous results

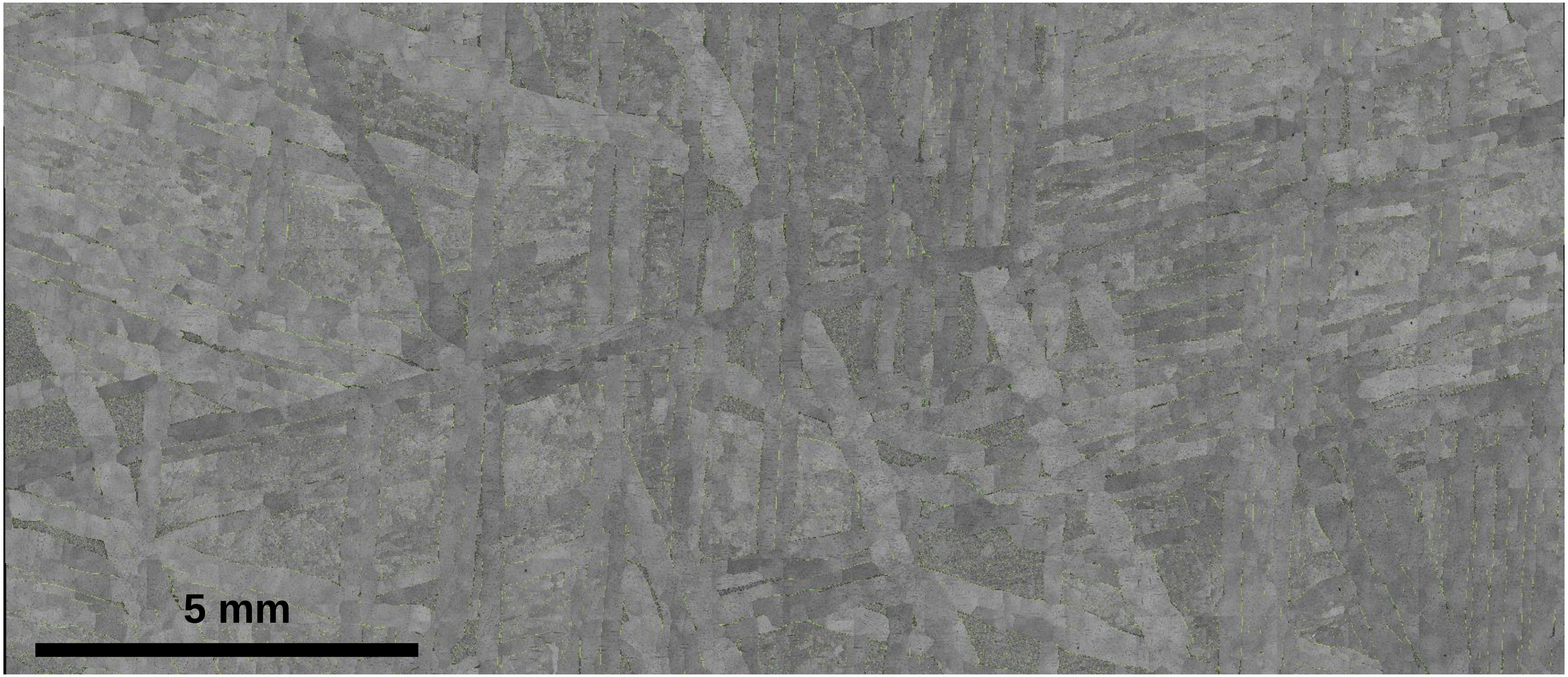

Along the Widmanstatten plates remains prior high temperature austenite all of the same orientation. This must be residual austenite from a grain that was larger than 22 mm across.

Pole figures of the Austenite and ferrite in the Gibeon meteorite

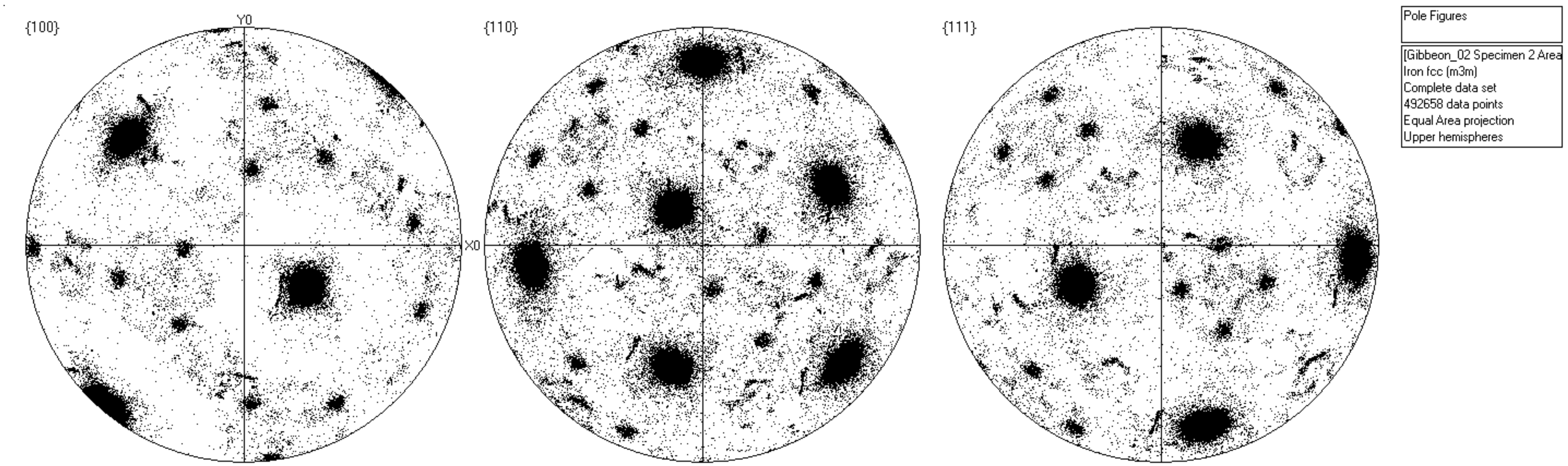

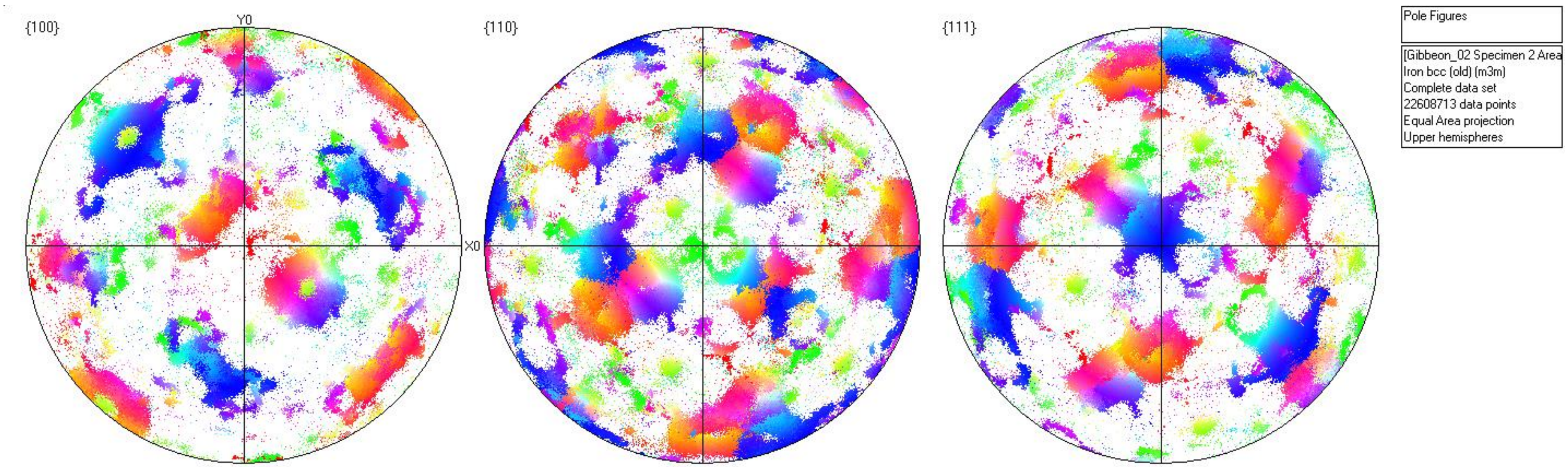

Consistent with results from smaller areas.

Iron-Nickel Phase diagram

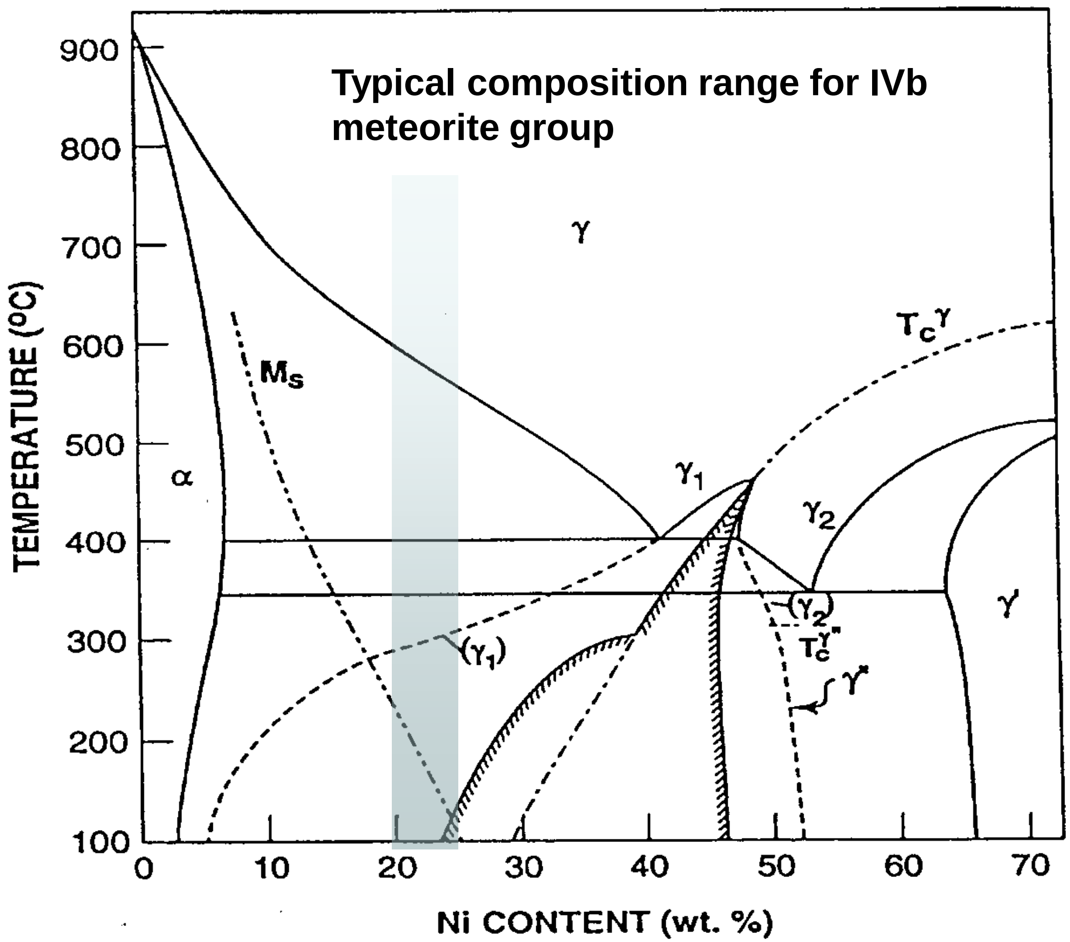

EBSD results gave a new insight to how plessite (a two phase region in meterorites containing both kamacite (bcc or ferrite to metallurgists) and taenite (fcc or austenite).

$\gamma \rightarrow \alpha_2$(martensite)$\rightarrow \alpha + \gamma$ inconsistent with EBSD results

$\gamma \rightarrow \alpha_2$(martensite) + $\gamma \rightarrow \alpha + \gamma$ consistent with EBSD results

Understanding Austenitic Stainless Steel Weld Mechanical Behavior Variation Requires Accurate Knowledge of Phase Distribution

- 60-70% of mechanical behavior variation attributed to non-metallurgical factors (e.g., weld shape, joint geo., etc.)

- Characterization of property variation due to metallurgical factors requires accurate characterization of phase constitution

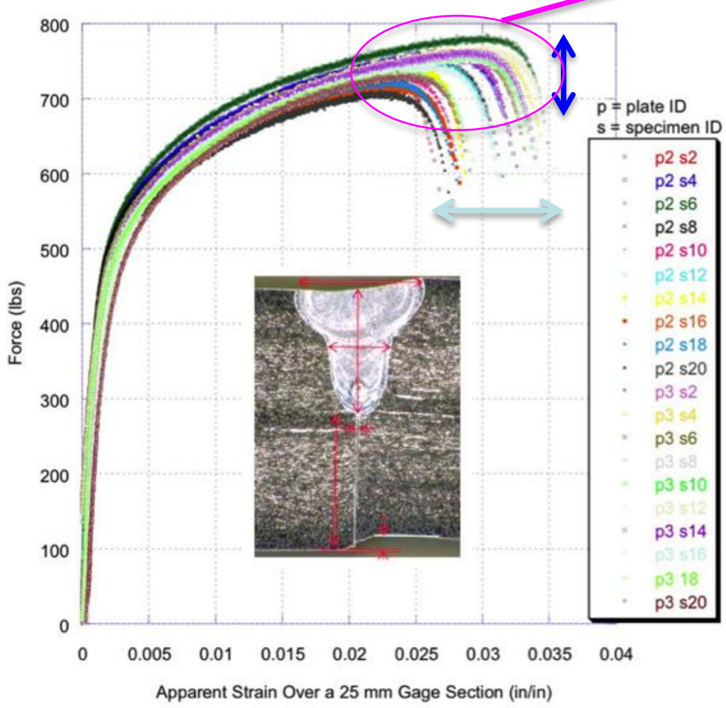

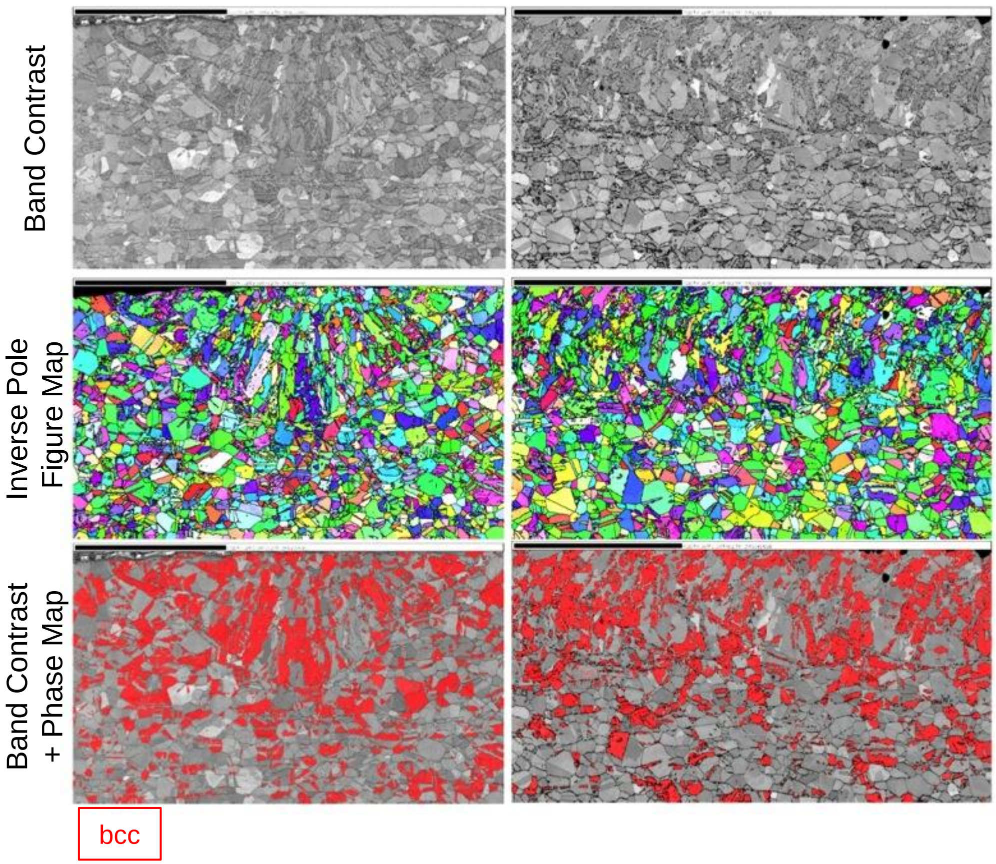

Metallographic Preparation for EBSD Phase Distribution Requires Additional Scrutiny

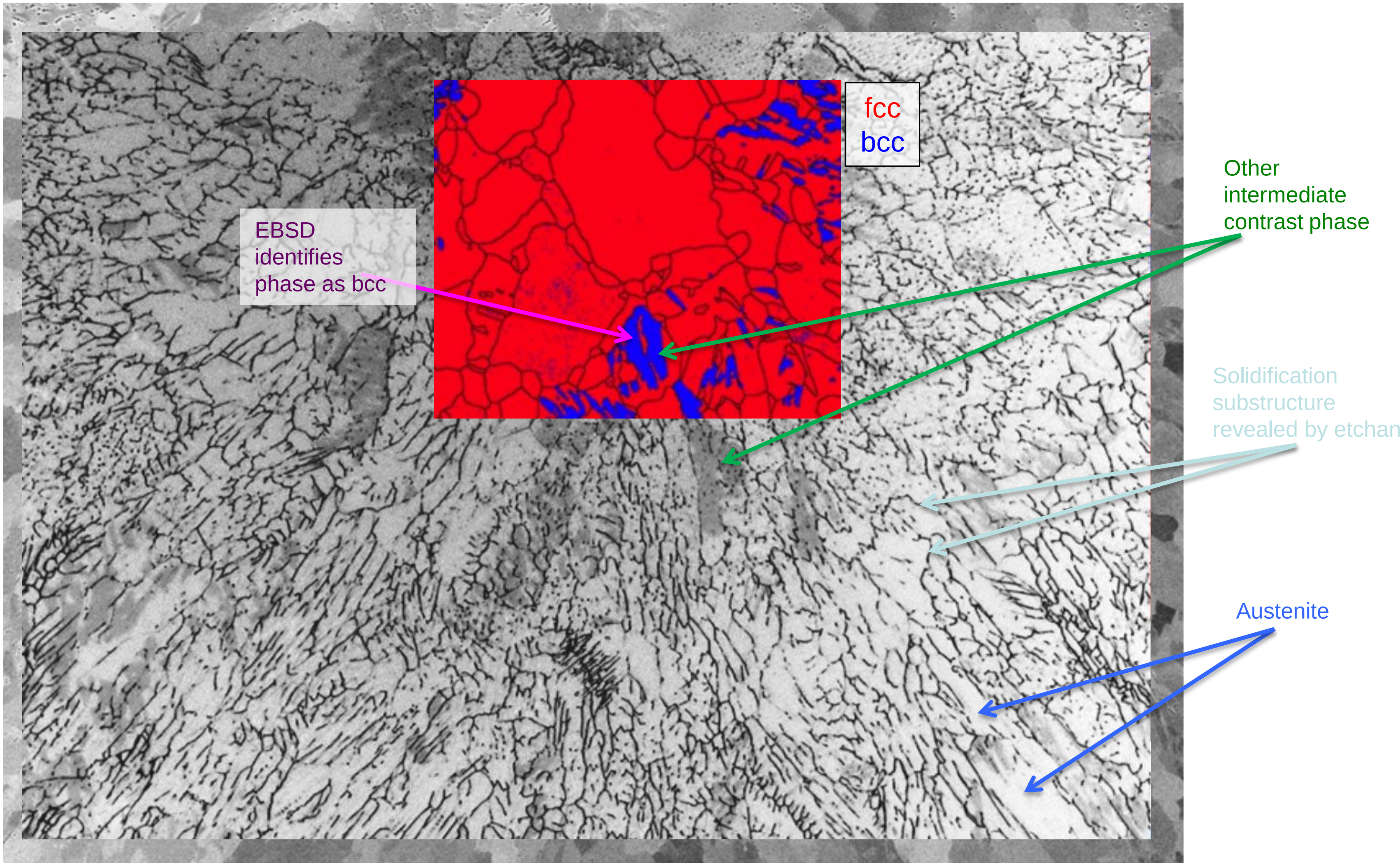

304L laser weld mechanically polished using conventional metallographic practices

Sample preparation possibilities – Electropolishing vs. mechanical methods

Standard metallographic procedure

grind, polish, and finish with 3 hours on vibratory polishing

Electropolishing

Bath – 80% phosphoric 20% Butanol

Bath Temp - 70C

Applied current - 600mA/cm^2

Polishing time – 2min

Di water rinse and N2 blow dry

Note that electropolishing requires no preliminary surface preparation and is really fast!

Bead on plate welds –Comparison of electropolished and metallographic polishing

Band contrast image with ferrite in red (0.1 area % ferrite)

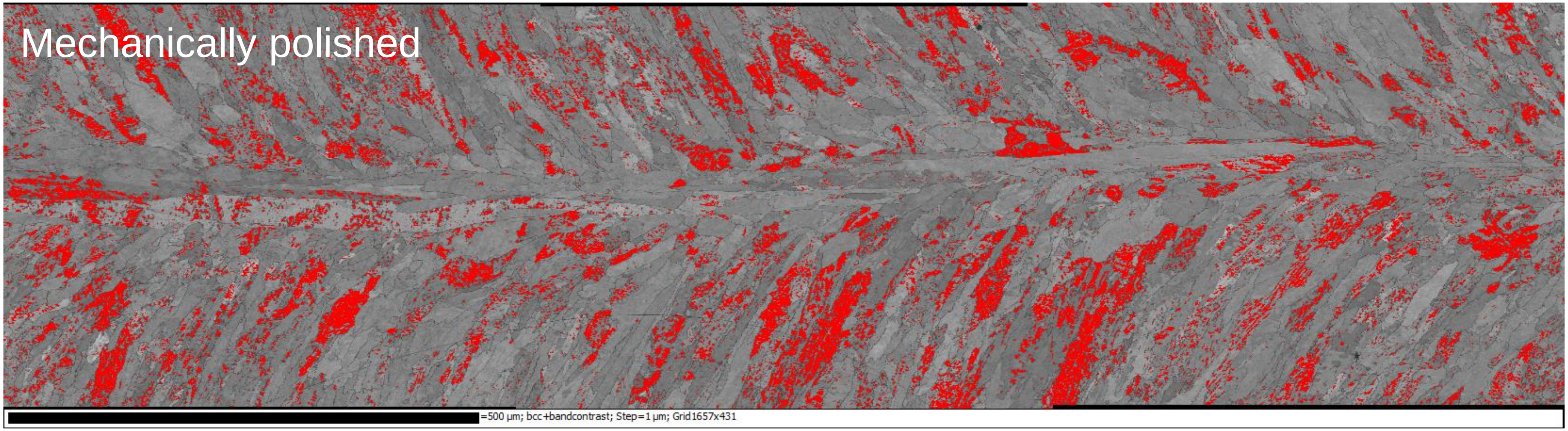

Band contrast image with ferrite in red (12 area % ferrite)!

304L Shear Test Specimens Exhibit Deformation-Induced Martensite

- Controlled shear loading of commercial wrought 304L leads to room-temperature deformation-induced martensite

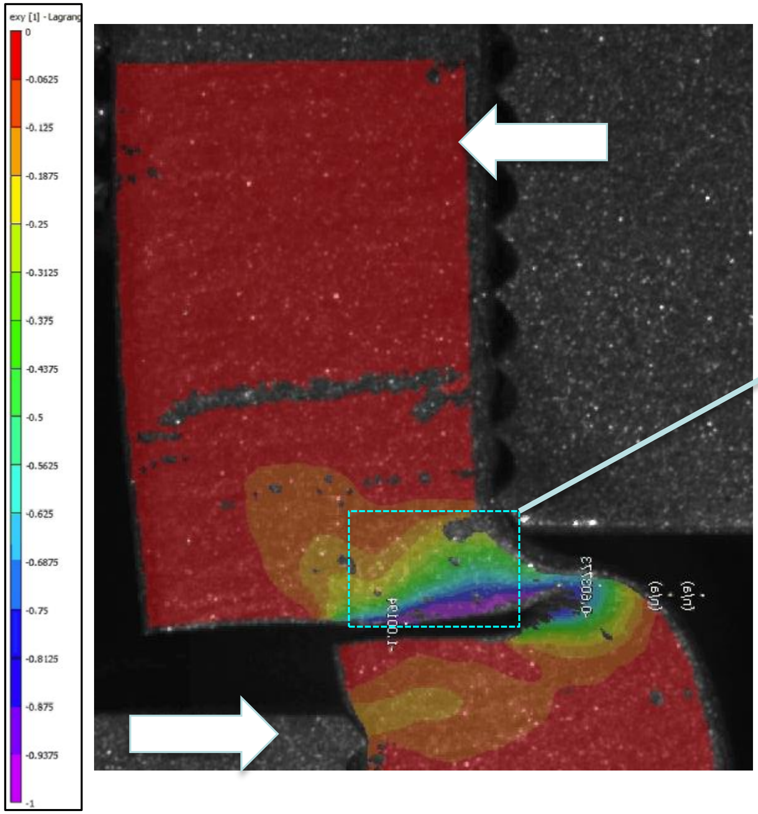

Optical micrograph of shear specimen (*electropolished*)

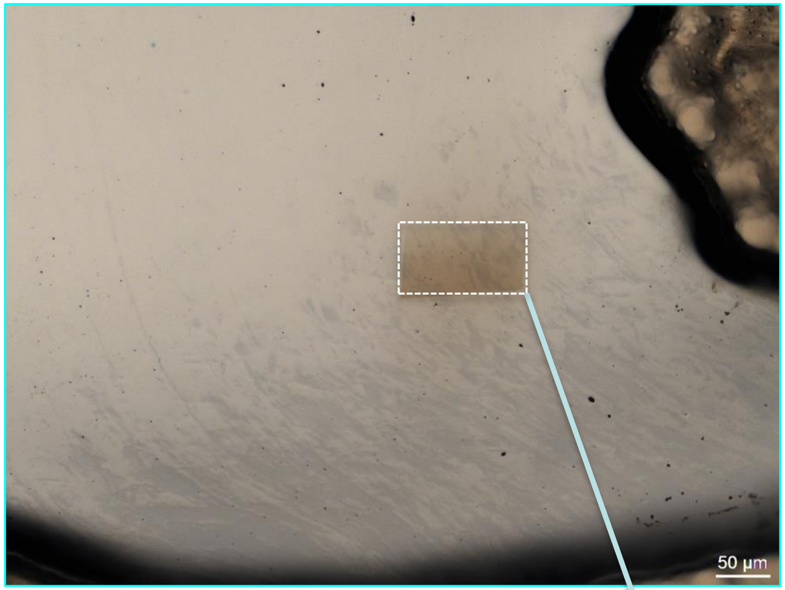

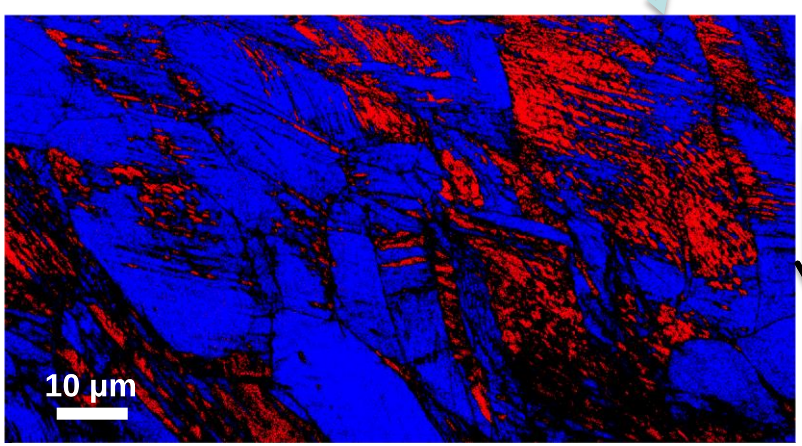

Phase Map: **fcc**; **bcc**

- Increasing Shear Strain
- Decreasing Diffraction Indexing Accuracy
- Increasing Martensite Fraction

Deformation-Induced Martensite Dependent on Local Shear Strain Level Irrespective of Loading Condition

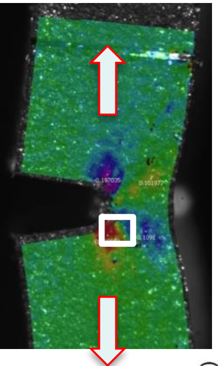

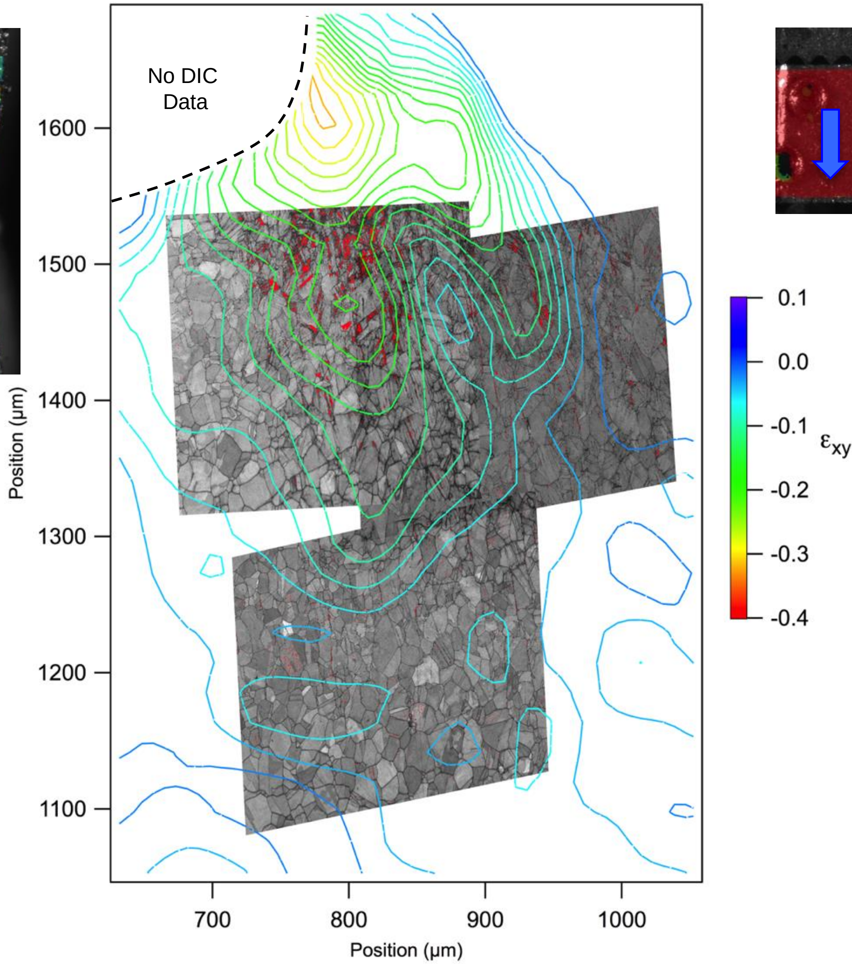

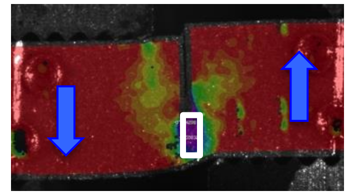

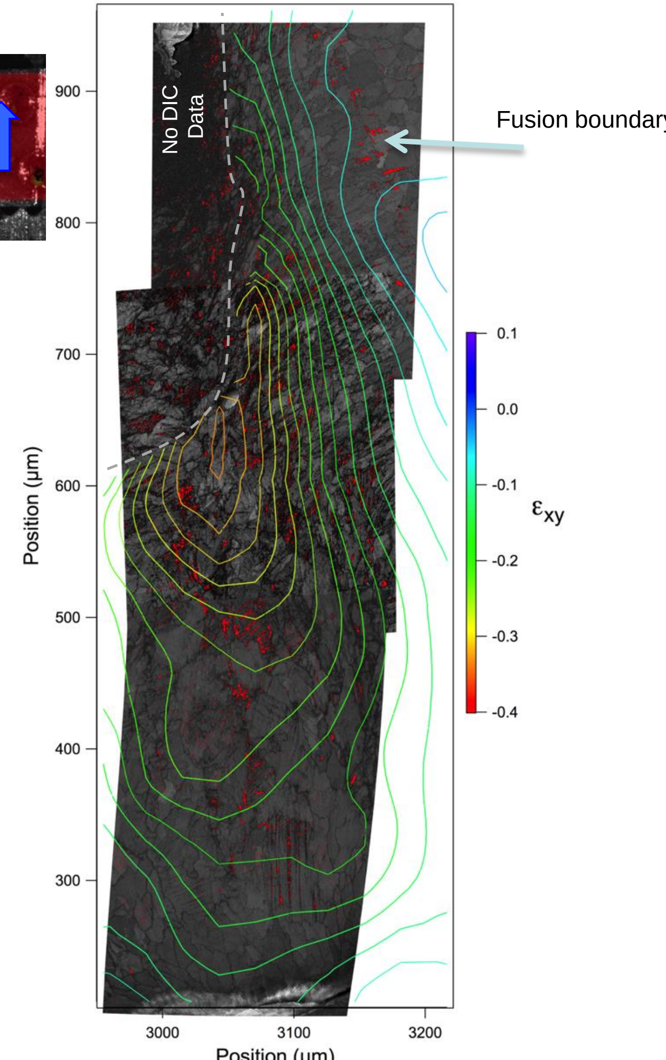

- Deformation-induced martensite dependent on local ε_{xy} level irrespective of loading condition
- Higher ε_{xy} magnitude resulting from shear loading likely leads to larger volume fraction
- Image correlation framework utilized for development of shear-strain dependent transformation model

Unambiguous determination of ferrite content with EBSD in 304 steels

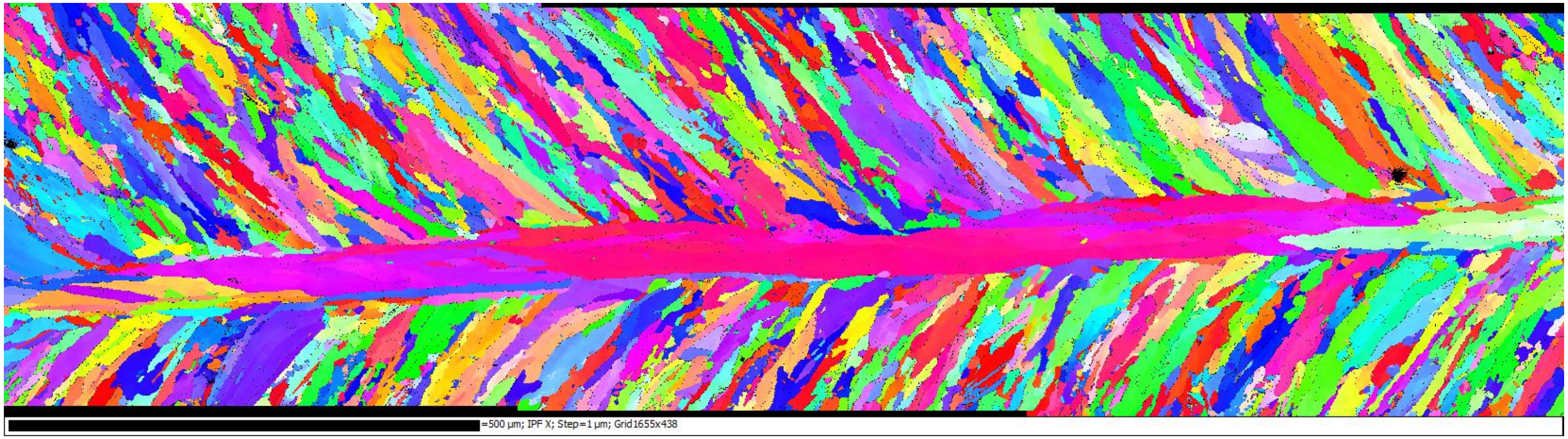

Mechanical polishing does not produce representative samples!

Unambiguous determination of ferrite content via EBSD requires electropolishing.

Shear strains can promote room temperature martensite in 304 stainless steels

.

Application of EBSD to understanding the structure of Additively Manufactured 304L

Understanding of solidification modes and microstructures needed as input to materials models.

Samples produced using direct metal deposition (DED) method

Application of EBSD to understanding the structure of Additively Manufactured 304L

Understanding of solidification modes and microstructures needed as input to materials models.

Samples produced using direct metal deposition (DED) method

Used DED to produce 2.5 x 2.5 x 10 cm blocks

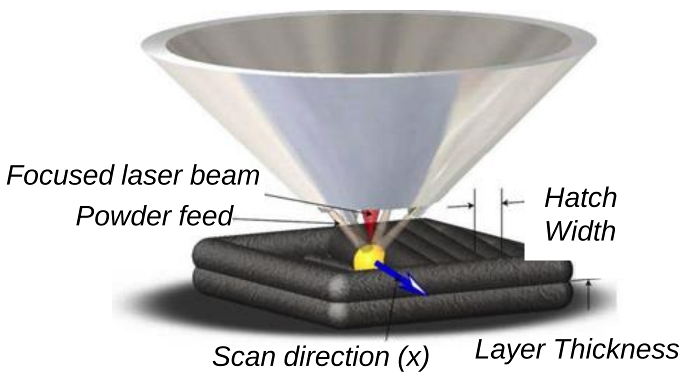

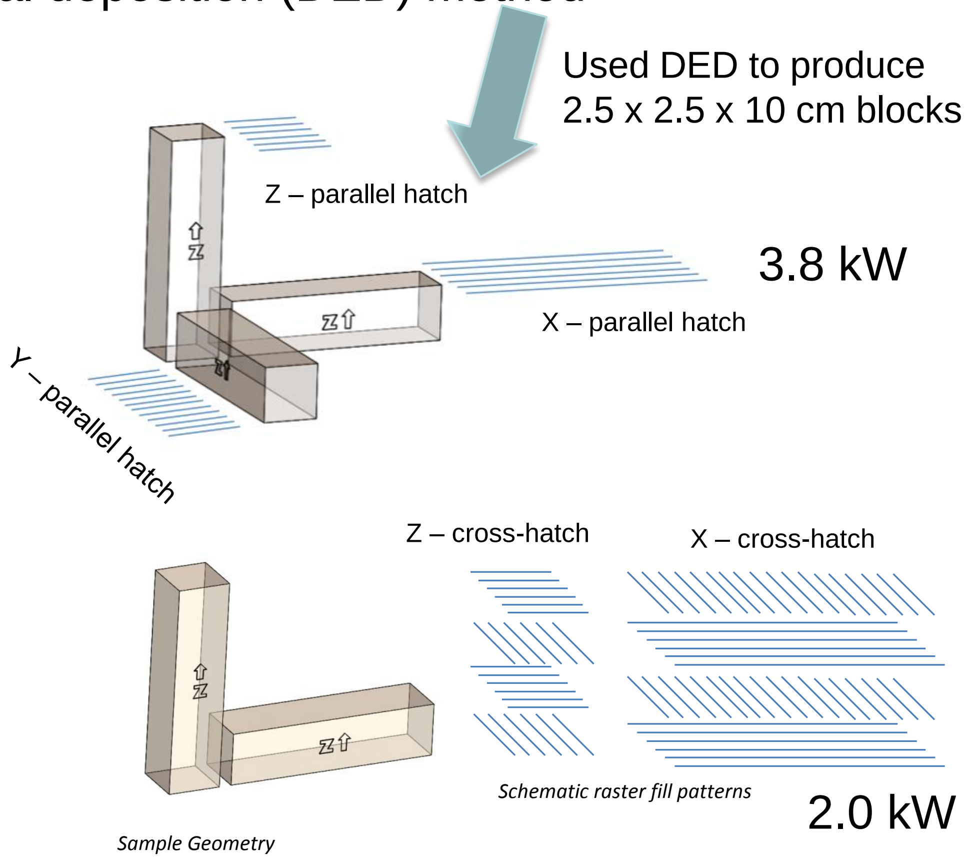

Large area views of microstructure of AM SS304L (2.0 kW)

- **Electron backscatter diffraction maps of electropolished surface.**
- **Example shown to right was built with a cross hatch approach.**

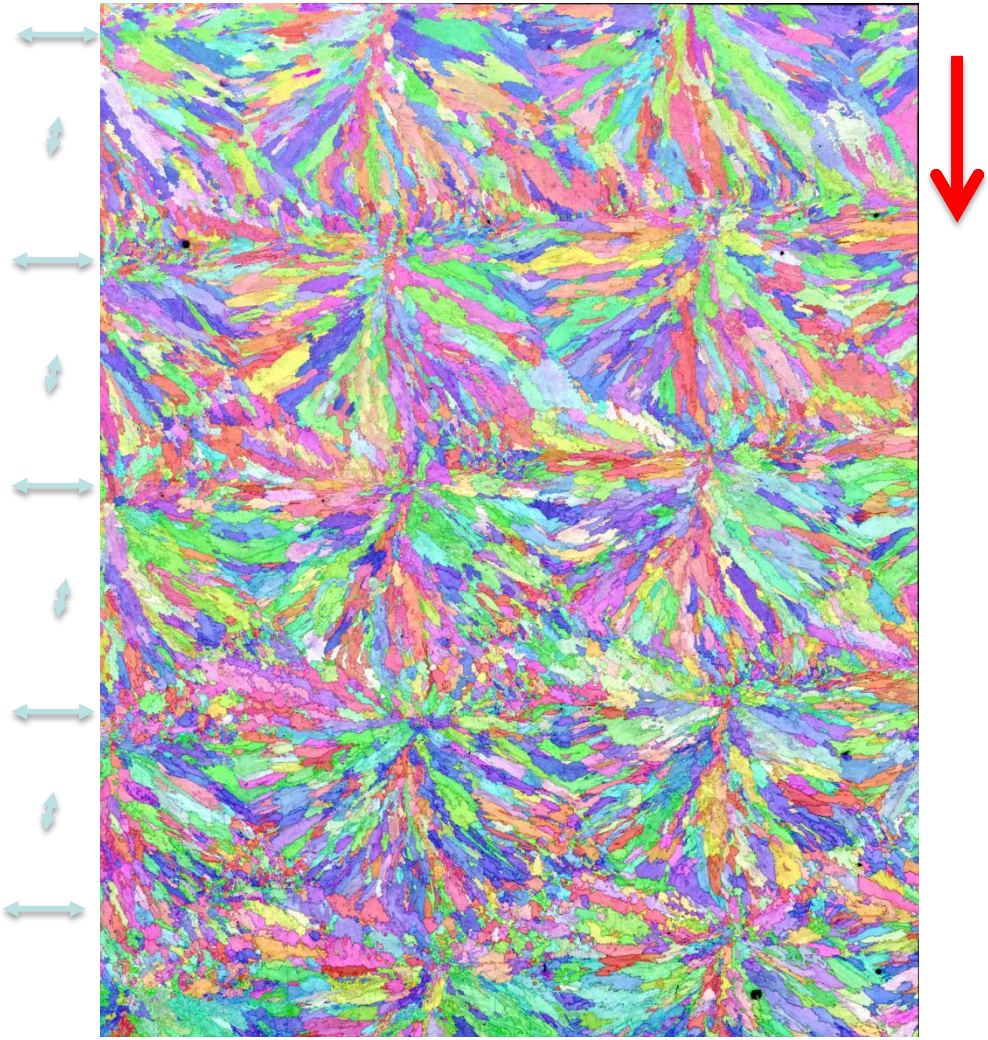

IPF X + BC

6 mm wide by 10 mm high

Primary Ferrite or Primary Austenite Solidification?

As-deposited structure is a mix austenite with fine ferrite precipitates.

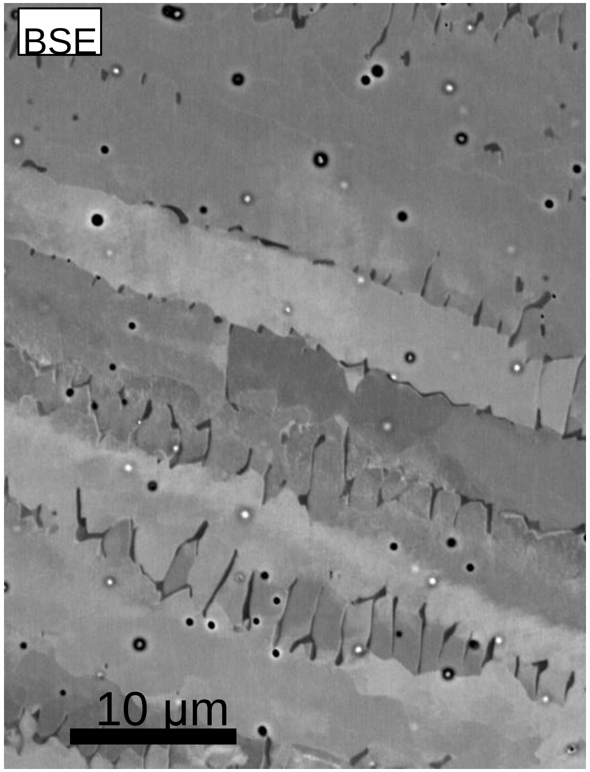

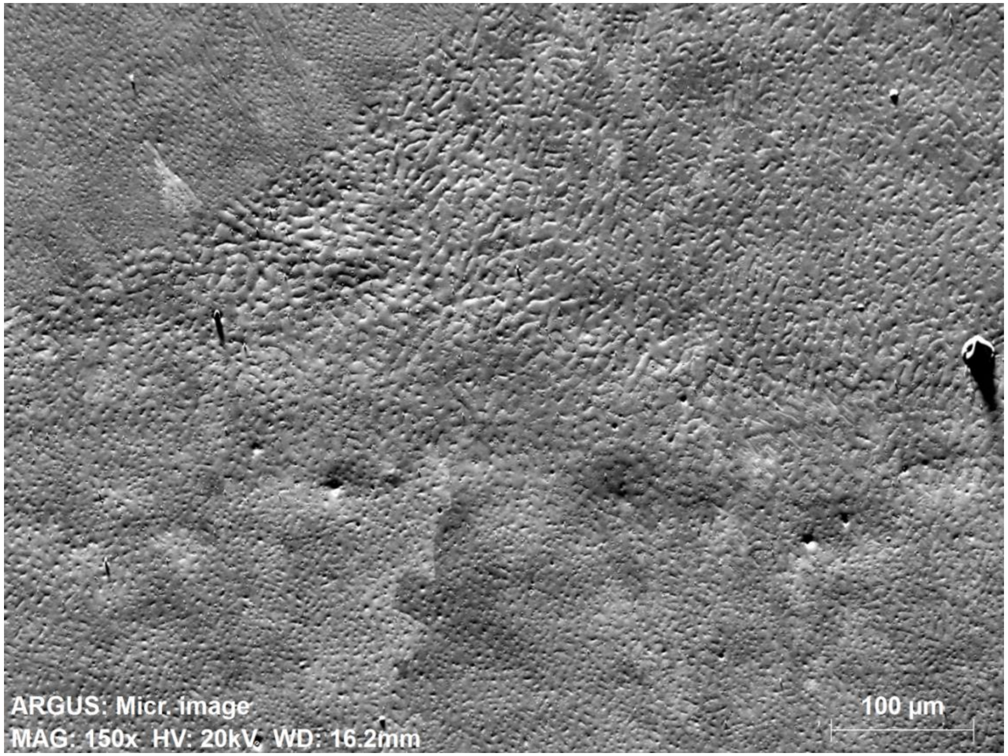

Primary Ferrite or Primary Austenite Solidification?

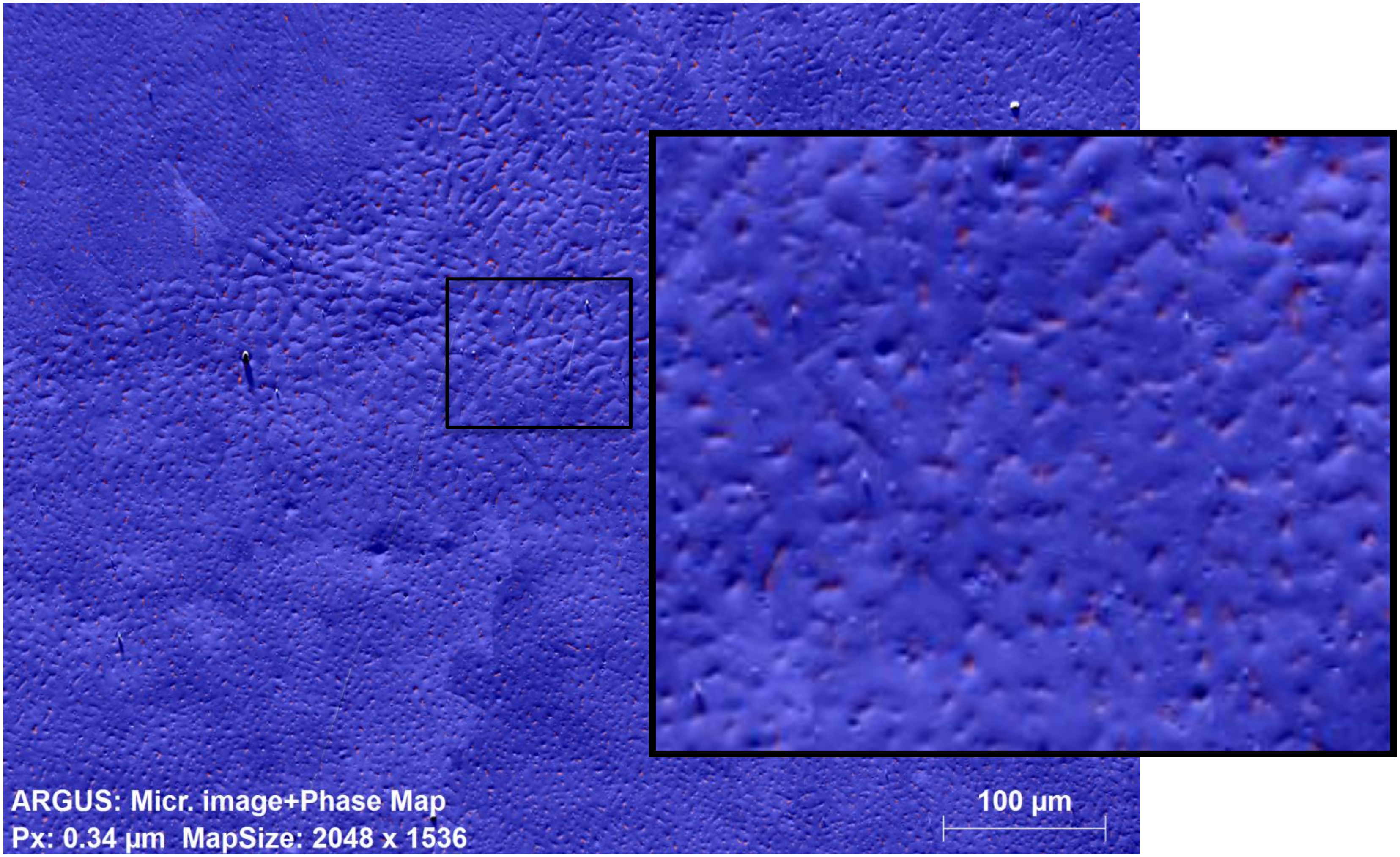

Image + austenite (blue)+ferrite (red)

EBSD reveals the fine ferrite precipitates in the austenite matrix.

Primary Ferrite or Primary Austenite Solidification?

EBSD orientation of Austenite and Ferrite

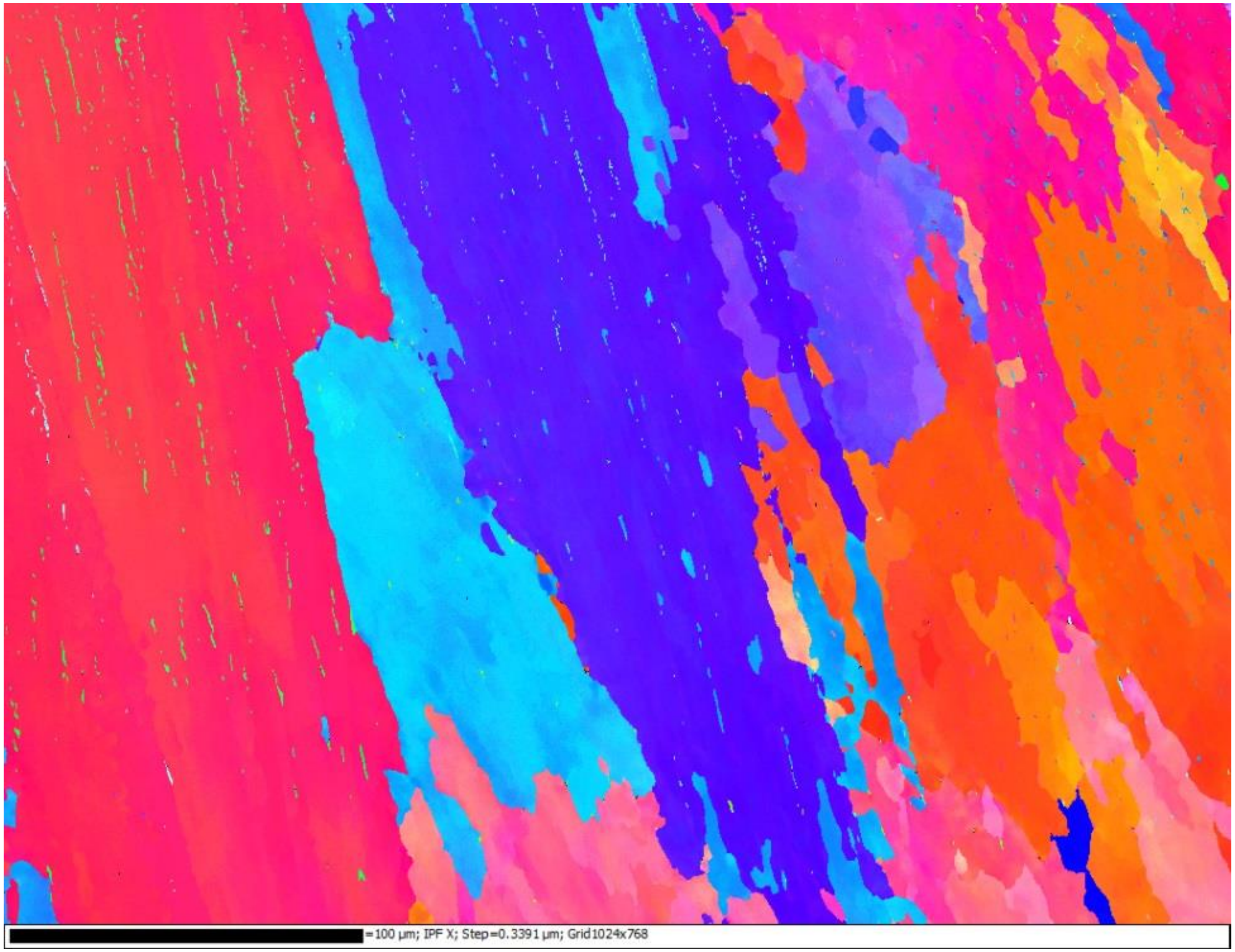

Common Ferrite Orientation Within the Solidification Subgrains
Indicative of Primary Ferrite Solidification

Primary Ferrite or Primary Austenite Solidification?

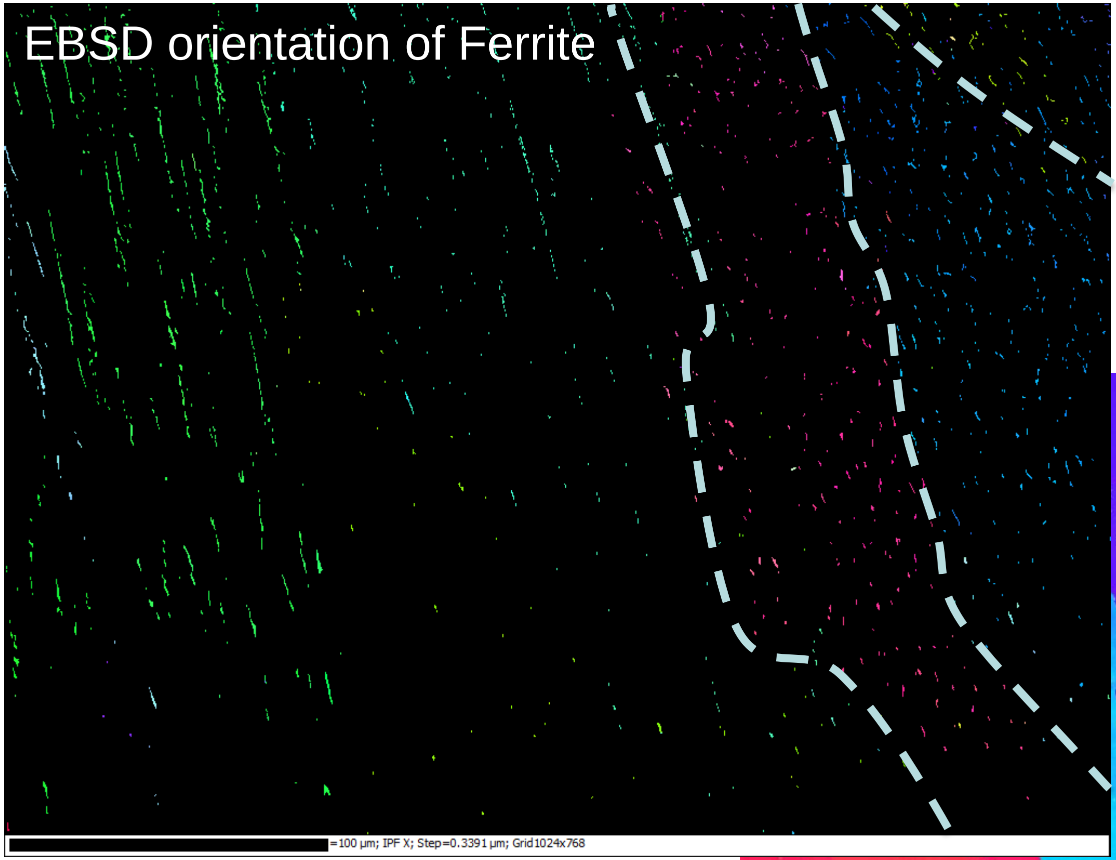

This is primary ferrite solidification and can be used to inform microstructural development models.

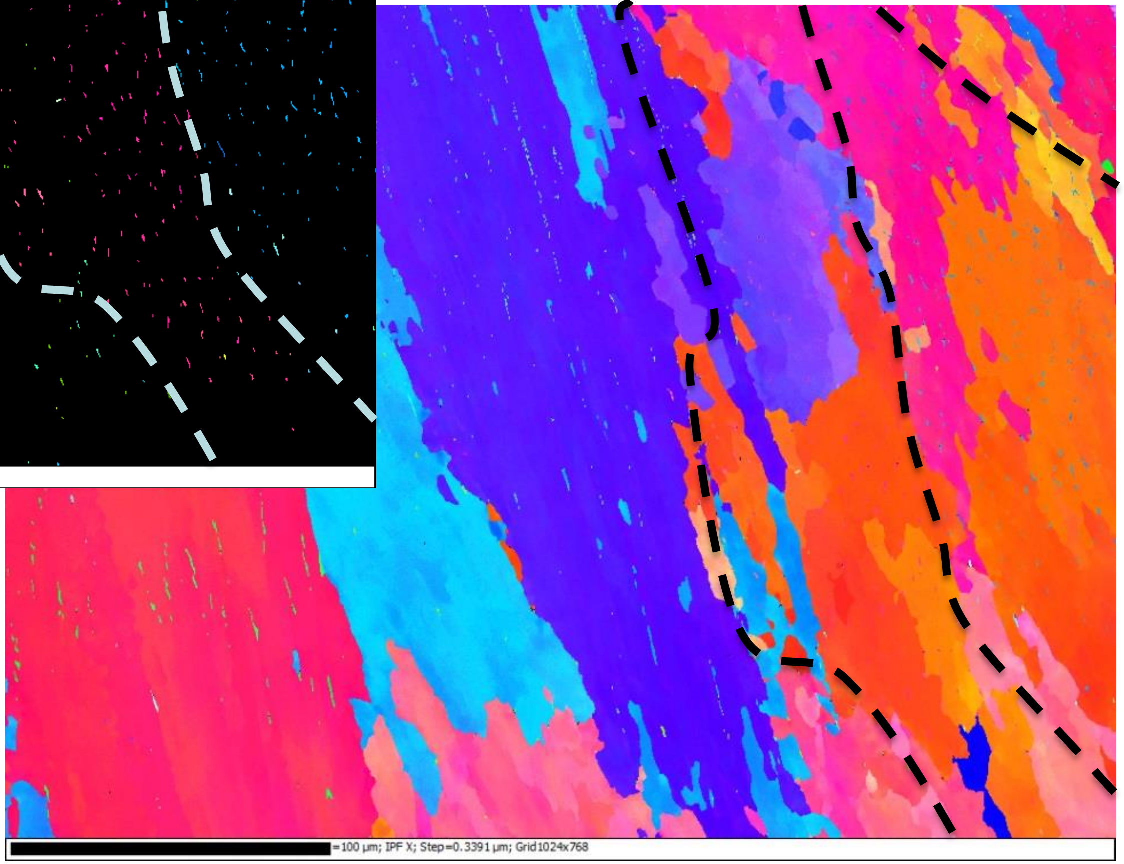

Common ferrite orientation allows prior ferrite grains (high temperature) to be visualized.

Understanding of friction using EBSD

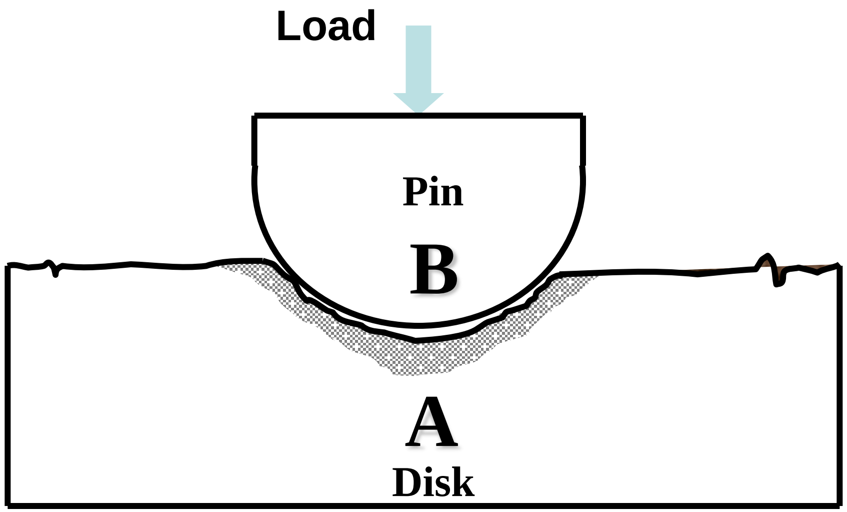

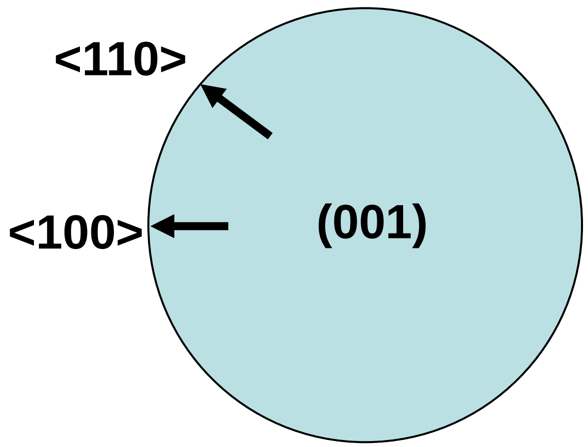

Use EBSD in FIB to orient sample and then mark directions with FIB

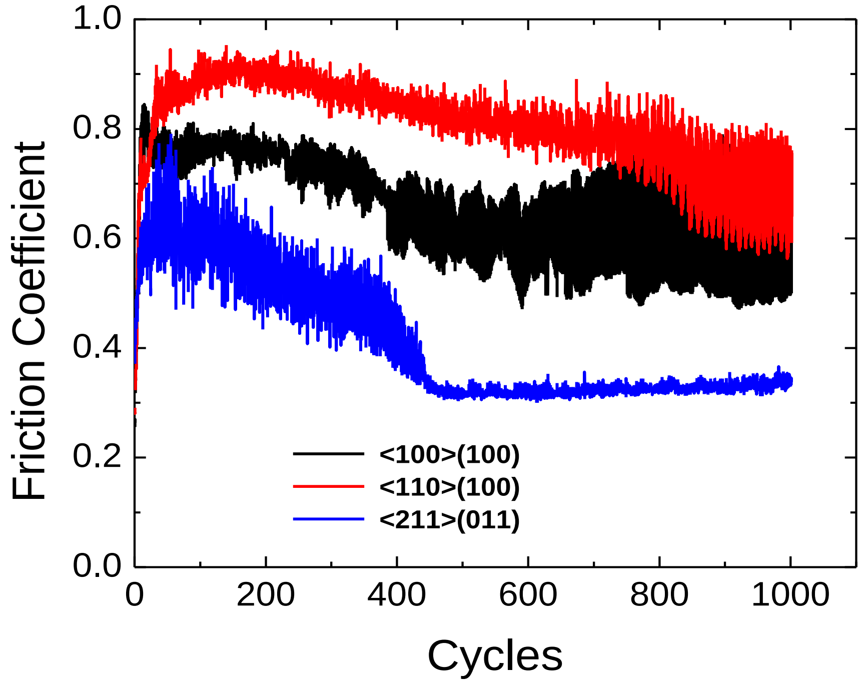

FIB sample preparation for EBSD and TEM

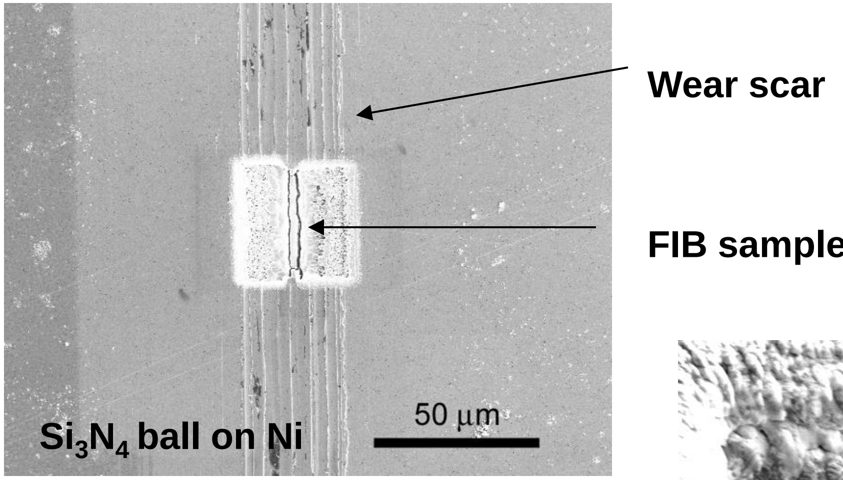

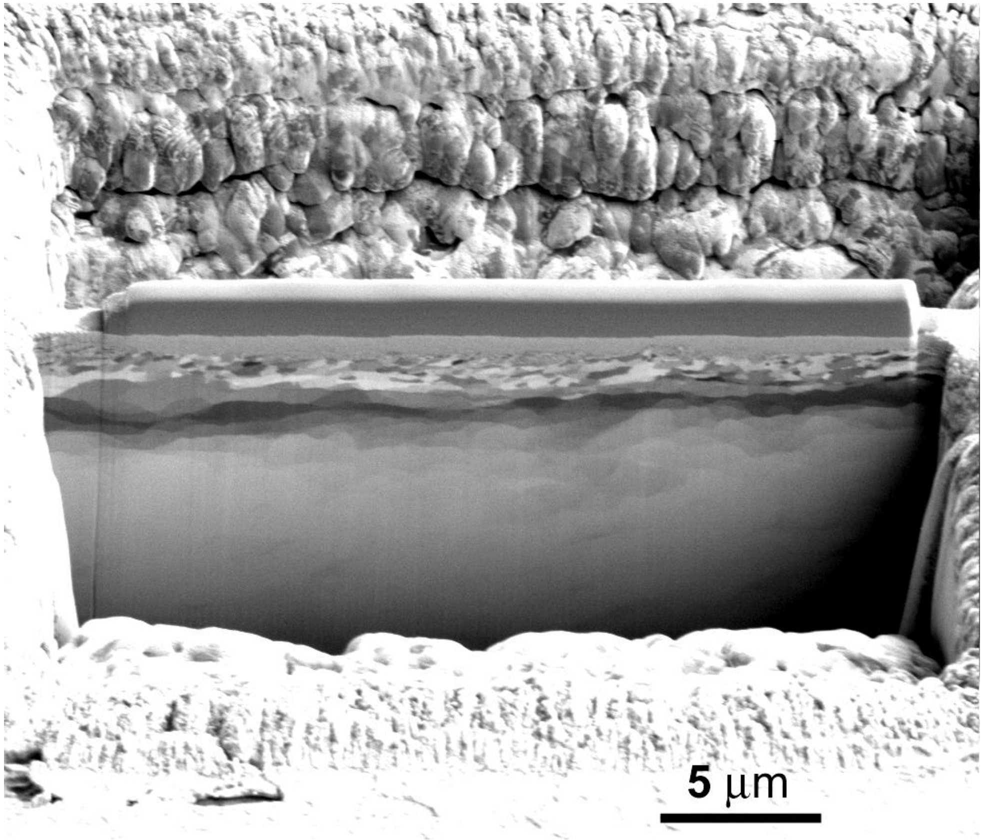

Ion channeling contrast image of wear scar

<211> on (111) Ni single crystal

EBSD provides quantitative information (<110> on (111) Ni

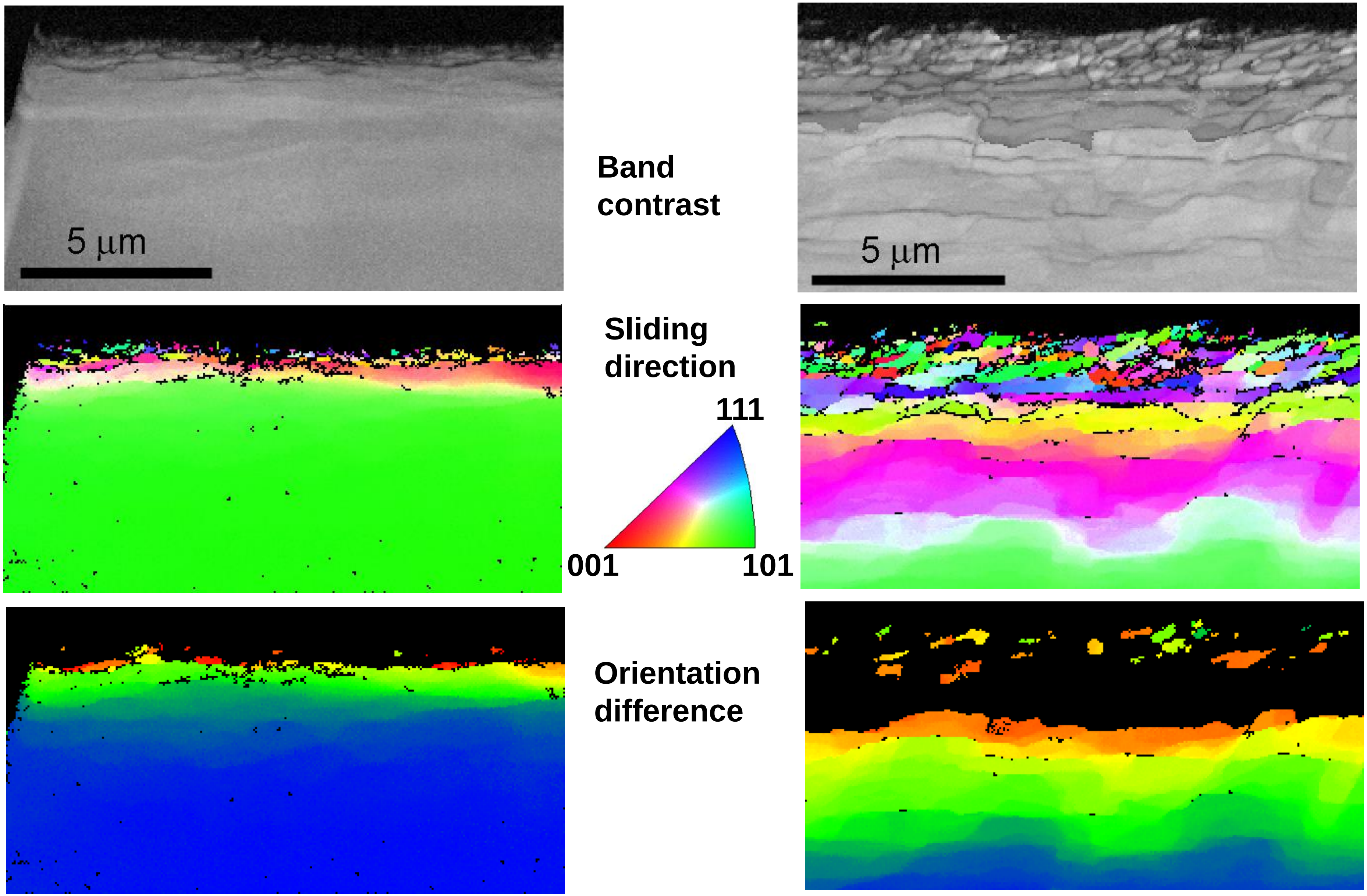

10 gram load for 1000 cycles

100 gram load for 1000 cycles

Relationship between crystallography, deformation and friction

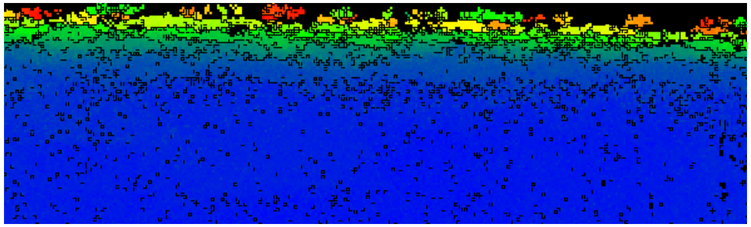

<100>(001)

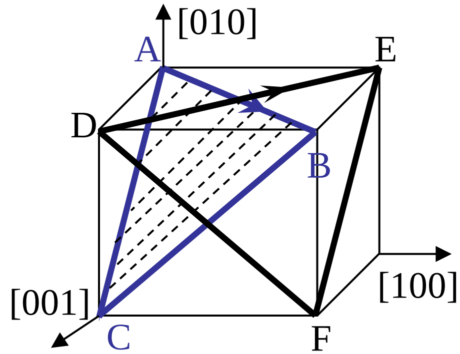

Strong dislocation interactions- high work hardening – low friction

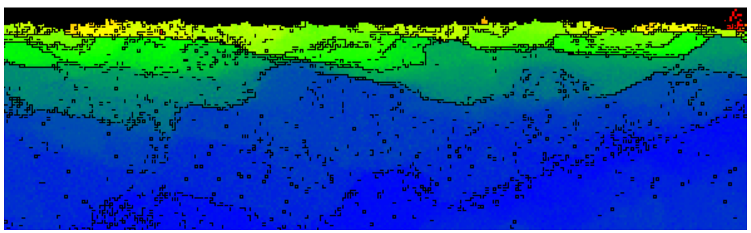

<110>(001)

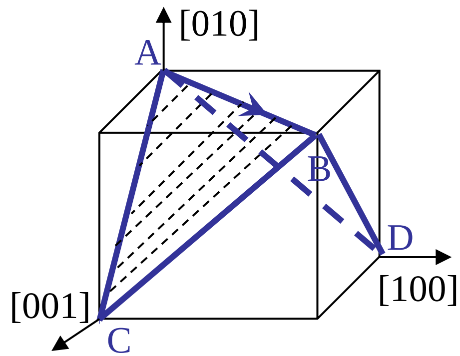

Weak dislocation interactions- low work hardening – high friction

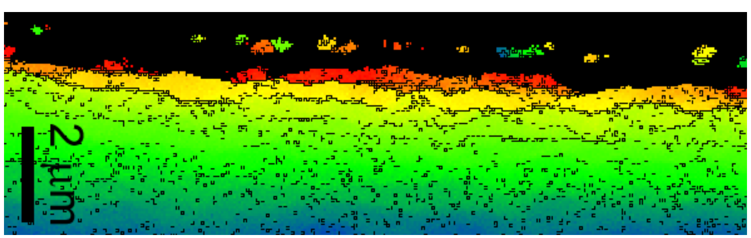

<211>(011)

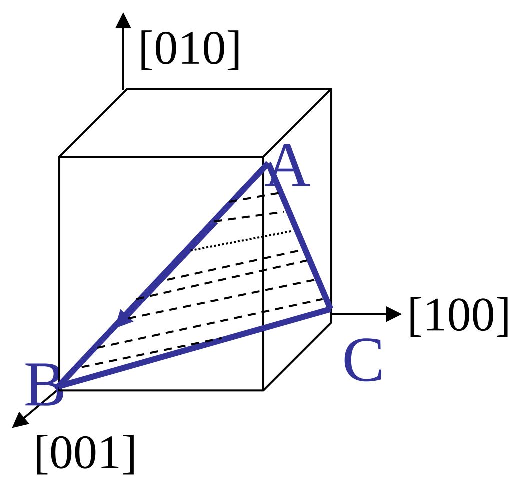

Very weak dislocation interactions- low work hardening – rapid recrystallization – low friction

Courtesy: Bhaskar Majumdar NM Tech

Application of wear studies to electrical contacts (TKD)

1 gm load 1000 cycles

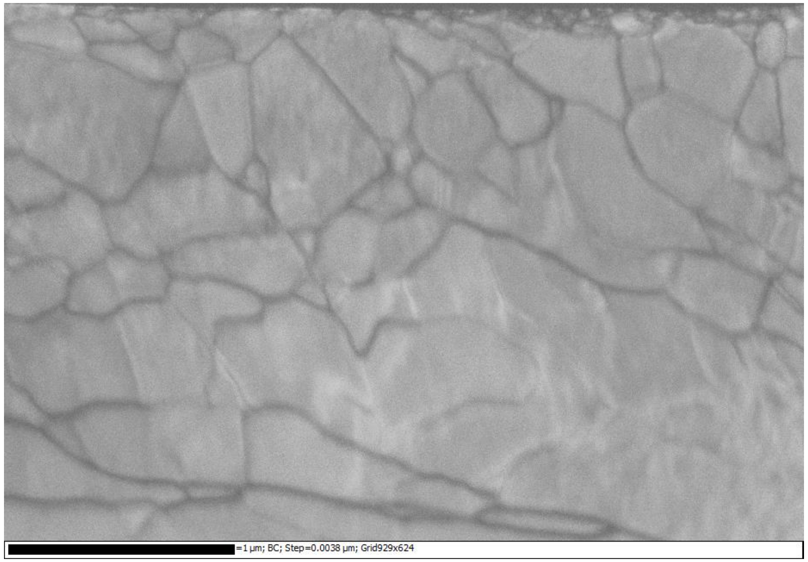

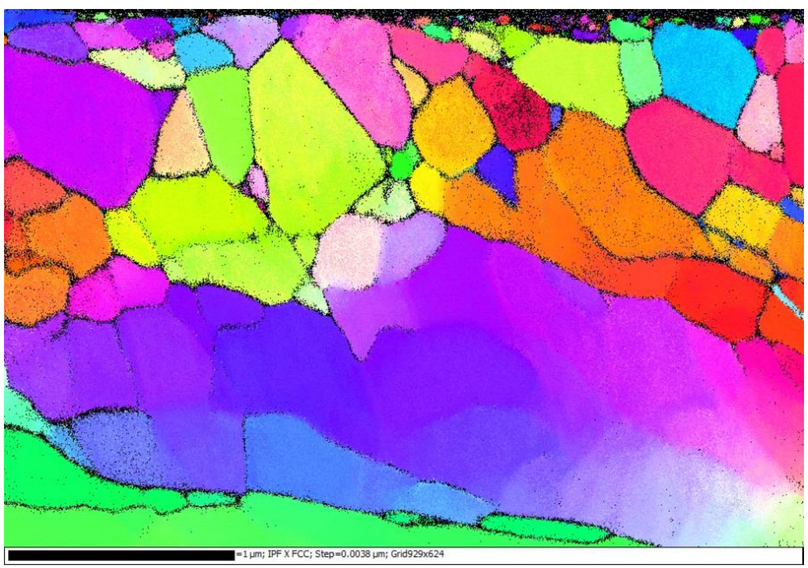

50 gm load 1000 cycles

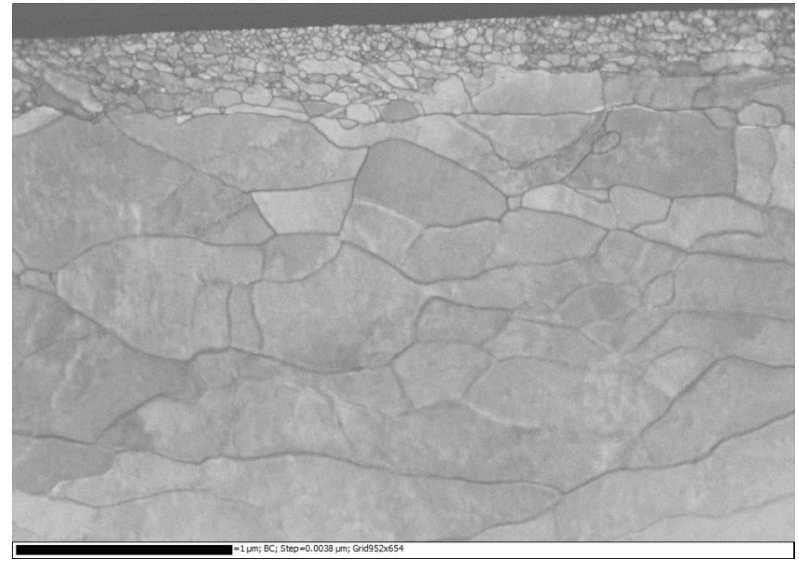

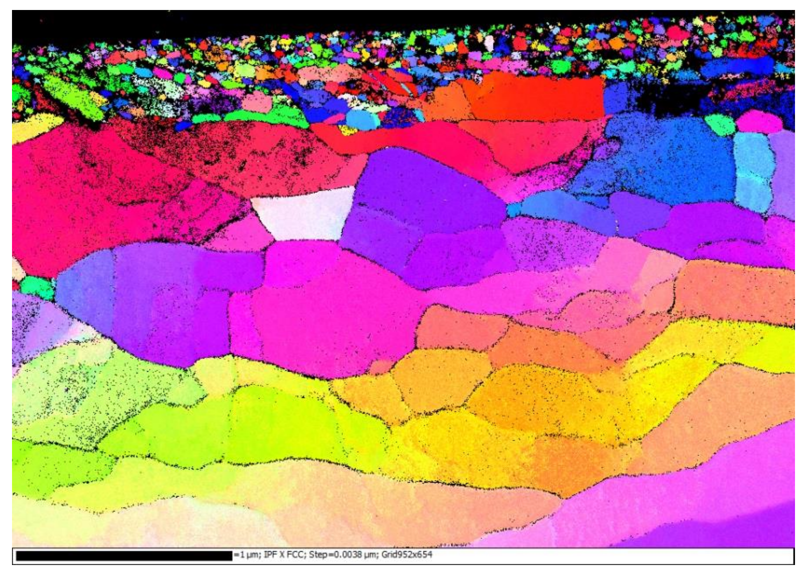

FIB prepared thin samples TKD 4 nm step size

Development of PVD ZnO hardened Au for electrical contacts

- Inexpensive electrically conductive structural alloys are prone to oxidation and poor tribological performance.
- Electroplated hard gold thin films have been traditionally used to improve the tribological and contact resistance of these alloys.
- PVD provides an economical environmentally favorable approach to replace electroplated coatings
- Coatings must remain microstructurally stable during elevated temperature use
- Additions of ZnO through electron beam co-deposition provides a stable coating for long term applications in electrical contacts

For details see: Argibay, et al. *J. Appl. Phys.*, vol. 117, 2015, 145302.

Development of PVD ZnO hardened Au for electrical contacts

Typical pure Au microstructure obtained through e-beam deposition

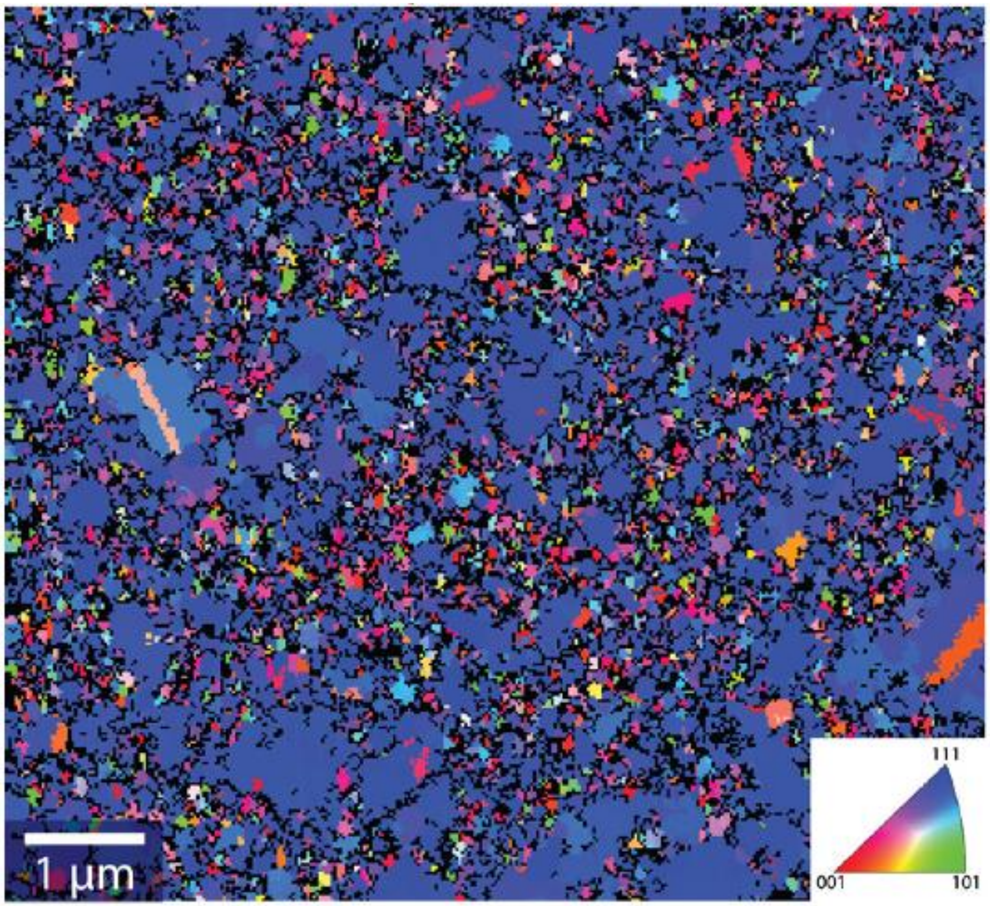

Highly textured coarse grained coatings that are prone to rapid grain growth are a result of pure Au deposition.

Microstructural instability can result in varying contact performance during long term use.

Development of PVD ZnO hardened Au for electrical contacts
As-deposited Au-ZnO microstructures

1 vol% ZnO

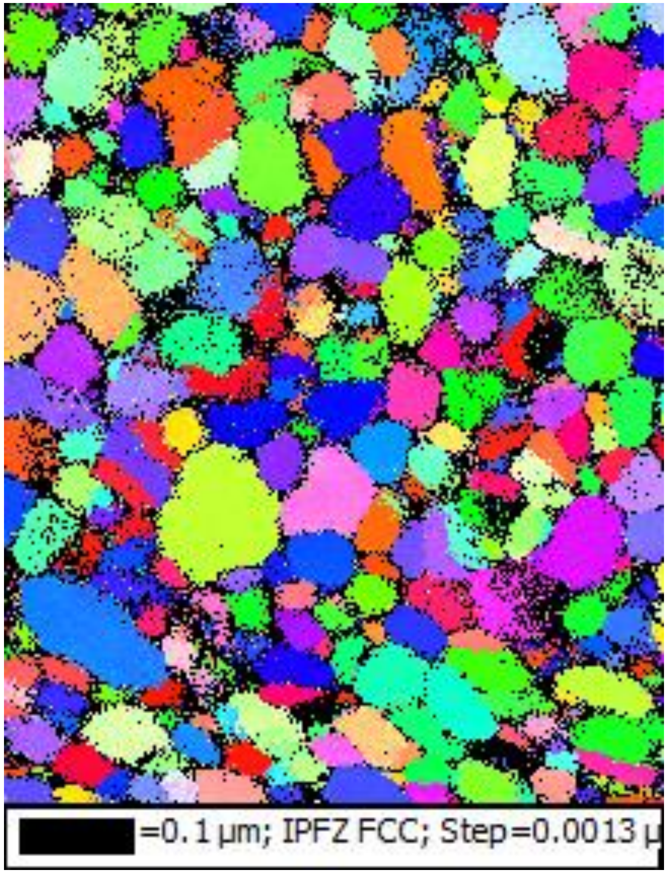

2 vol% ZnO

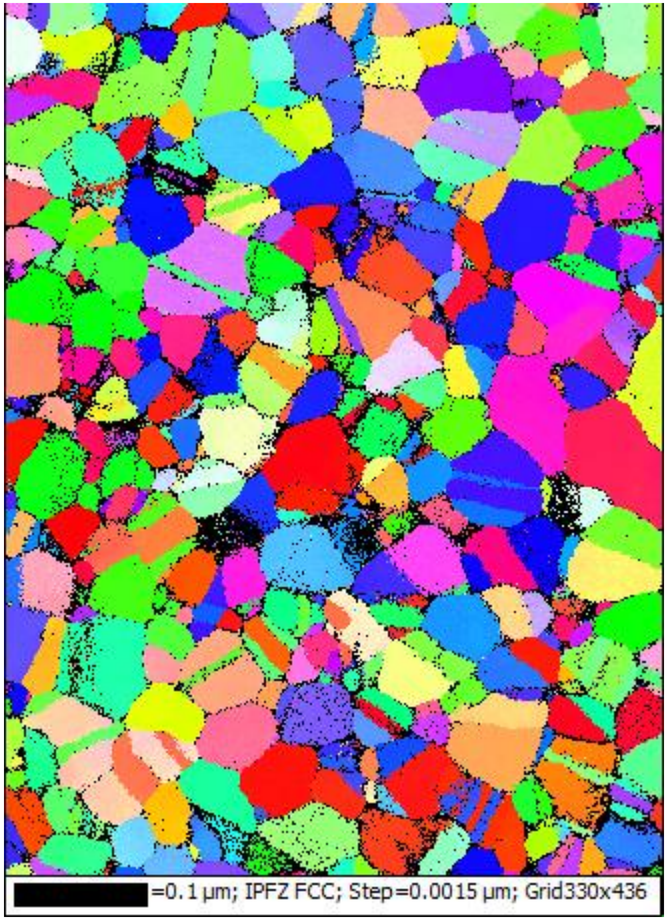

TKD was required to allow the grain structure to be observed. Note lack of texture in the as-deposited condition.

Plan view samples were prepared via Ga ion beam milling

Development of PVD ZnO hardened Au for electrical contacts

200 C

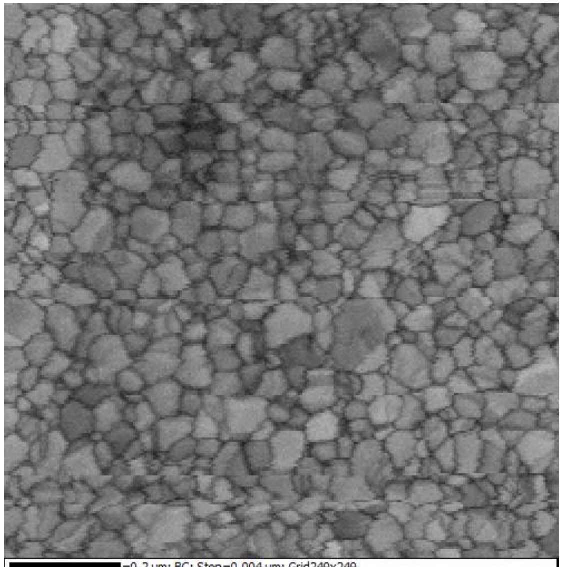

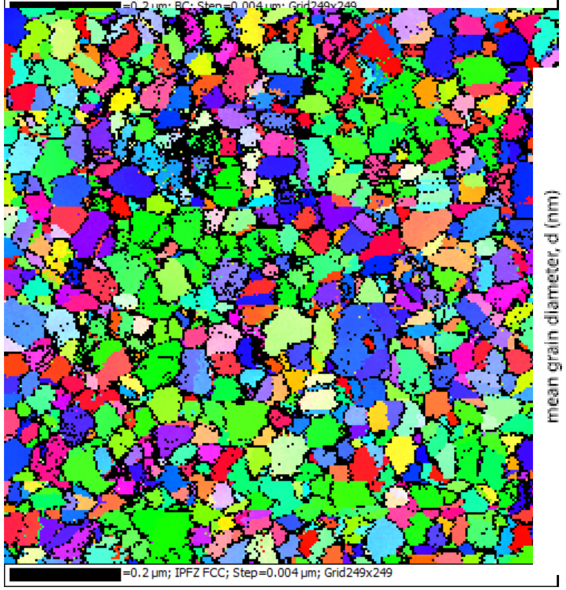

Au-2% ZnO exhibits slower grain growth kinetics as compared to typical hard gold coatings.

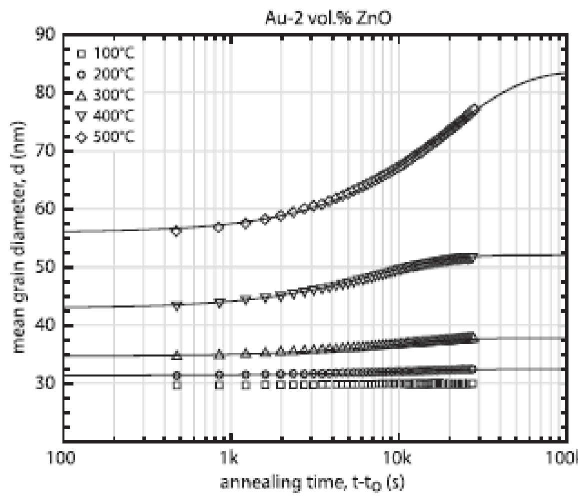

500 C

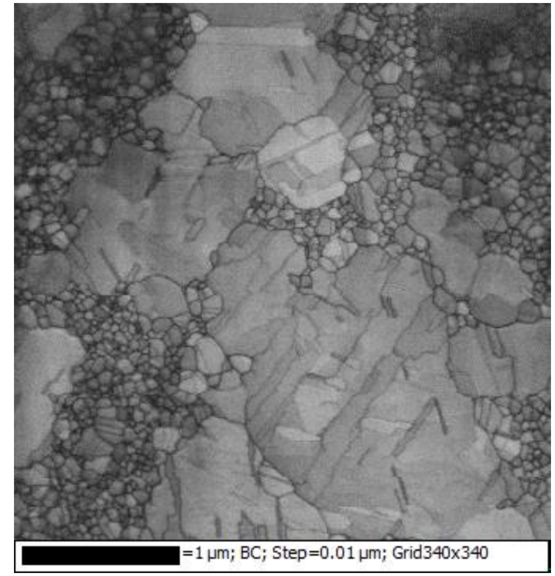

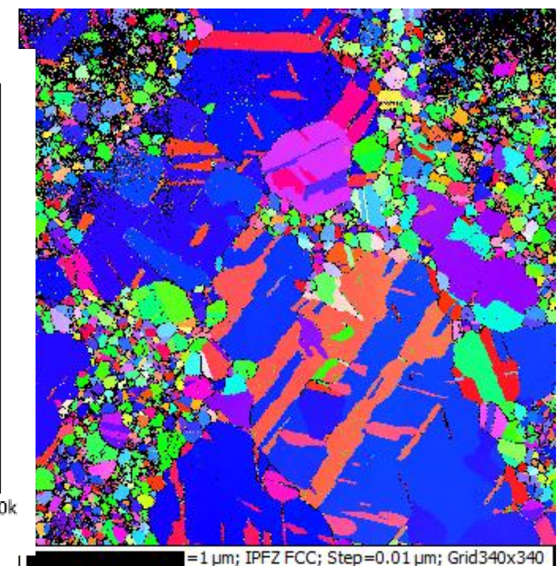

Plan view TKD of 2 % ZnO samples

3D Electron Backscatter Diffraction

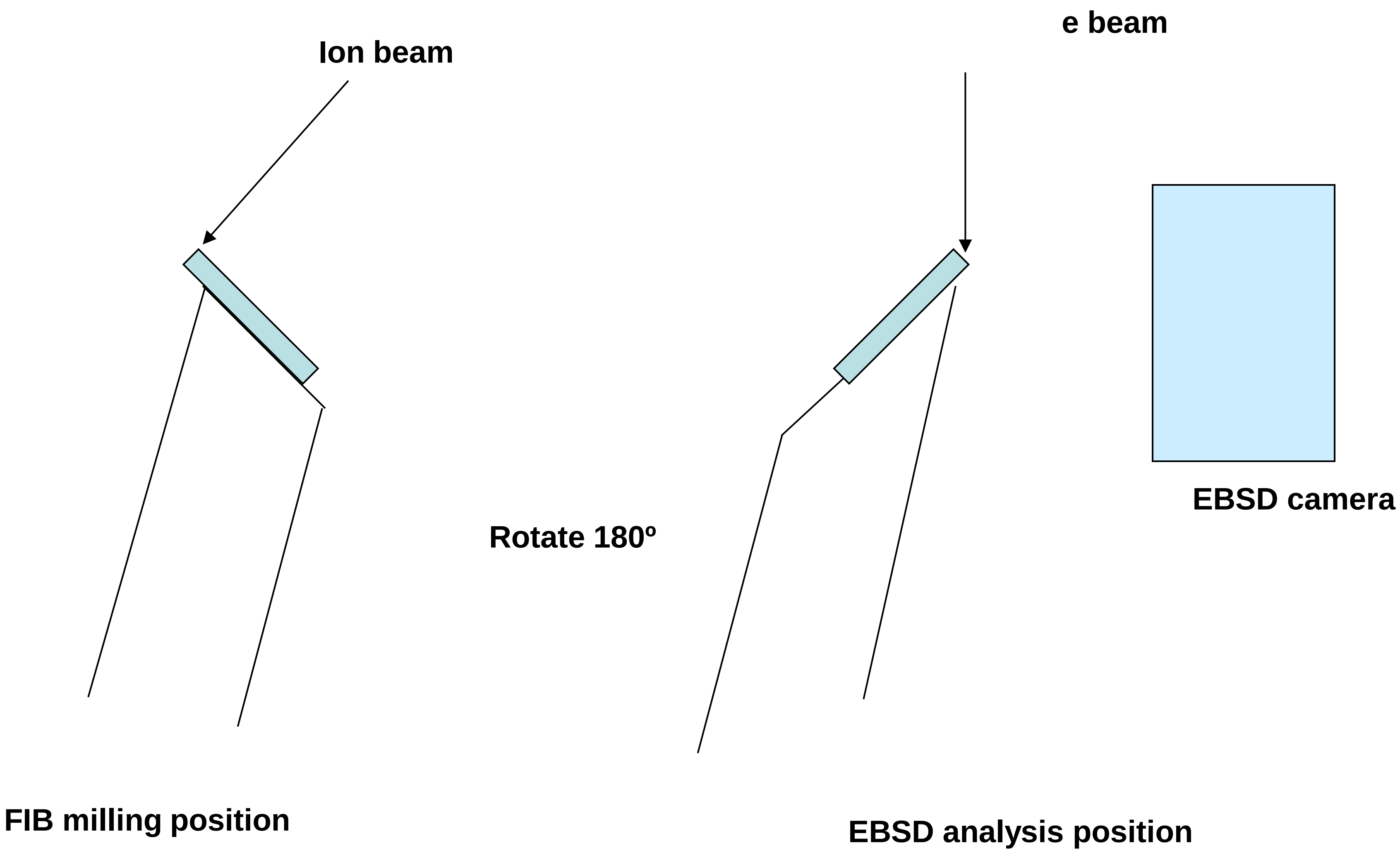

Geometry allows moving from FIB miling position to EBSD position with a simple 180º rotation.

FIB enabled 3D Electron Backscatter Diffraction

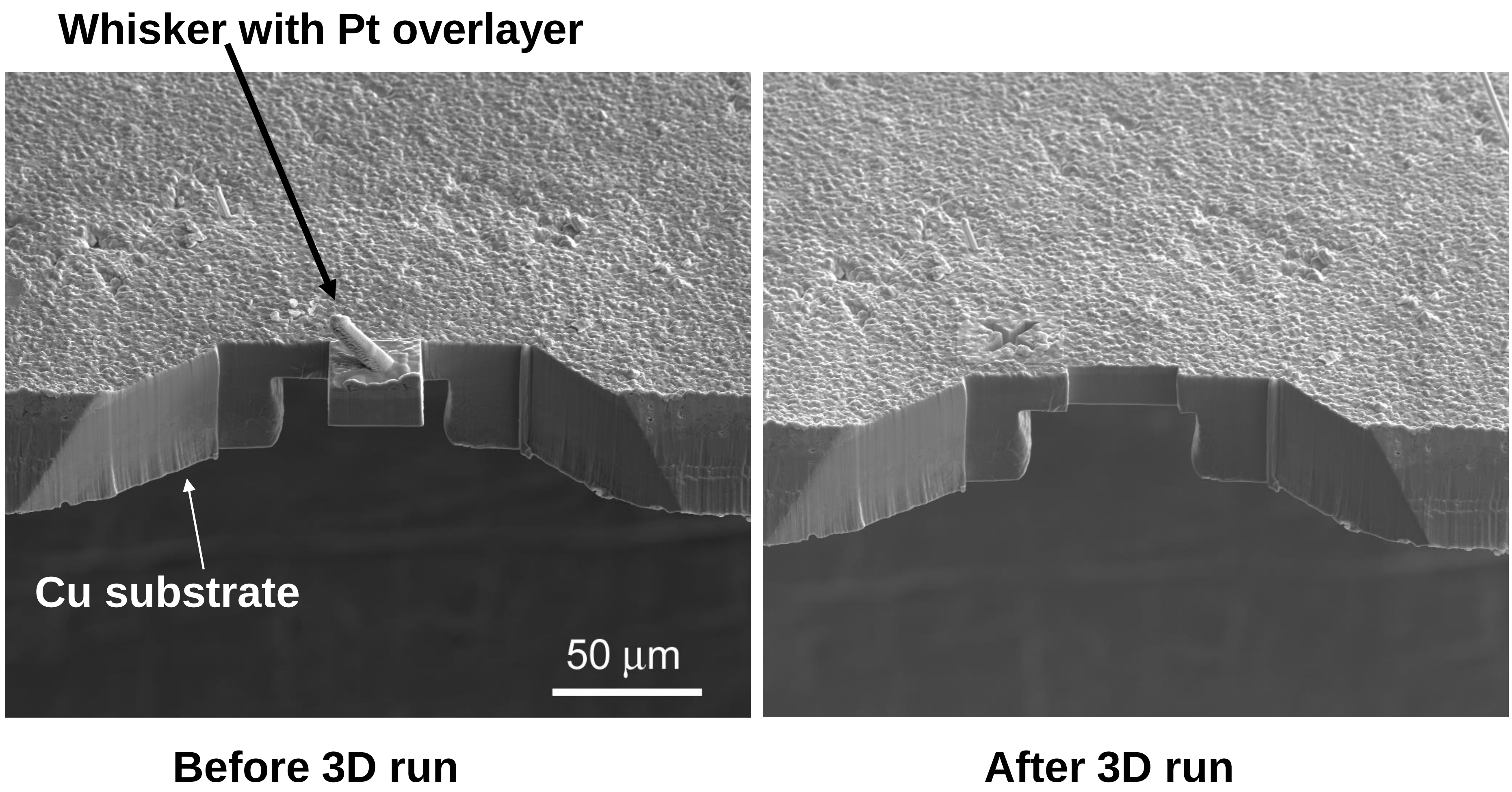

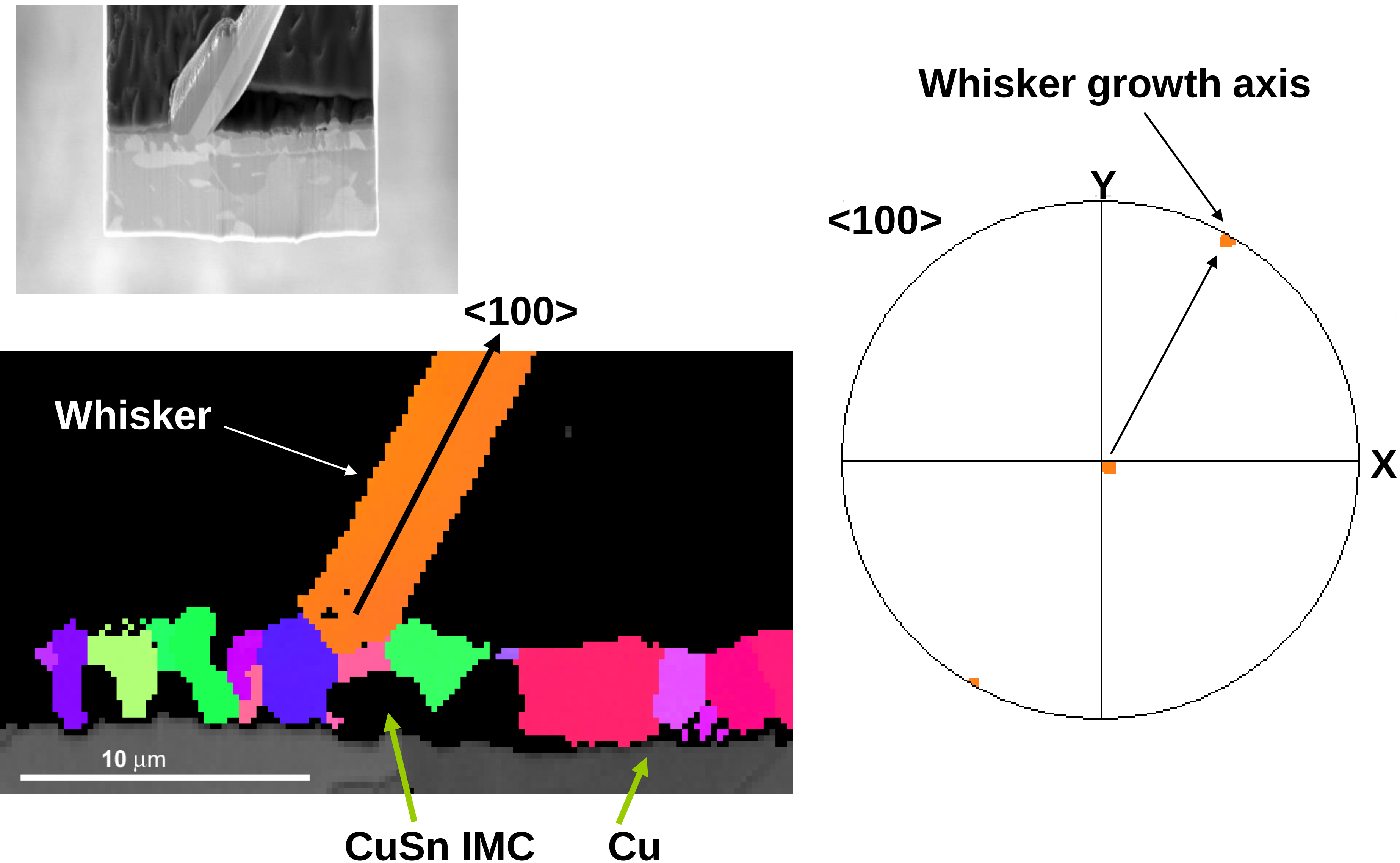
<100>
Whisker
10 µm
CuSn IMC
Cu
Whisker growth axis
<100>
Y
X

3D EBSD using FIB/SEM may help!

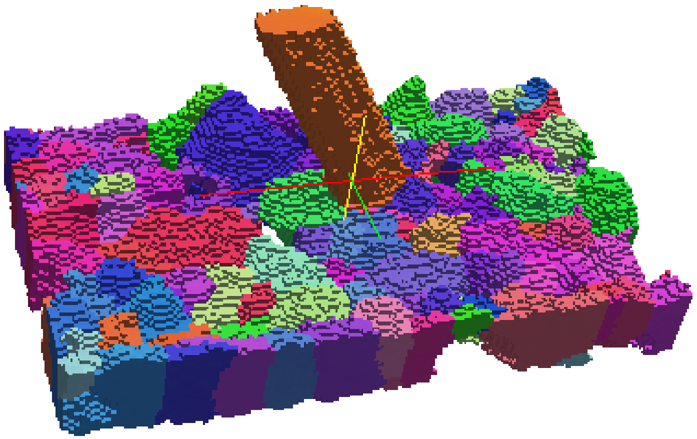

IPF-X

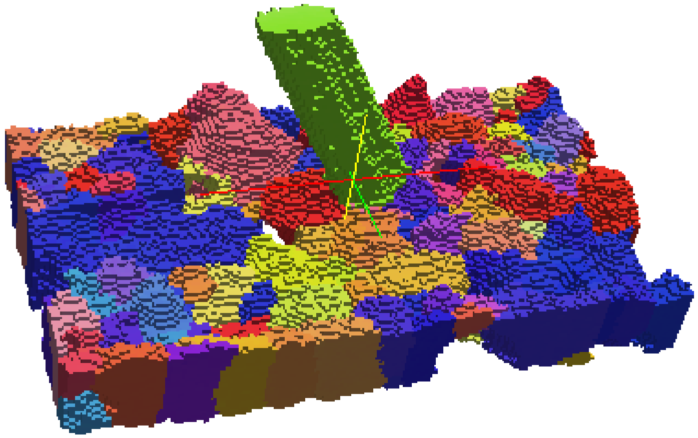

IPF-Y

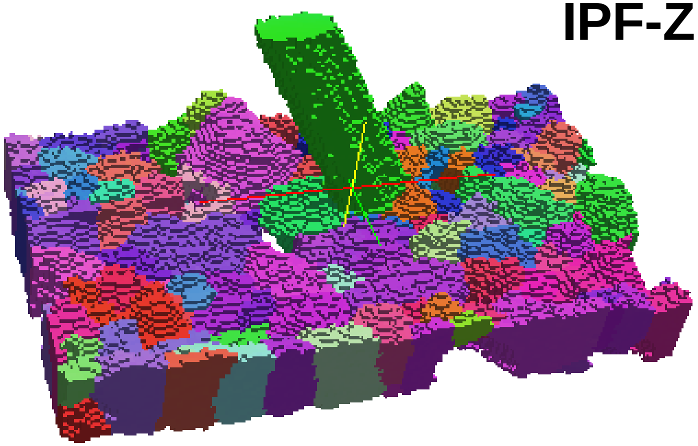

IPF-Z

Data reconstructed from 75 slices 200 nm thick (each pixel 200 nm^3).

Total time was about 48 hours.

Data constructed using DREAM.3D

3D EBSD using FIB/SEM may help!

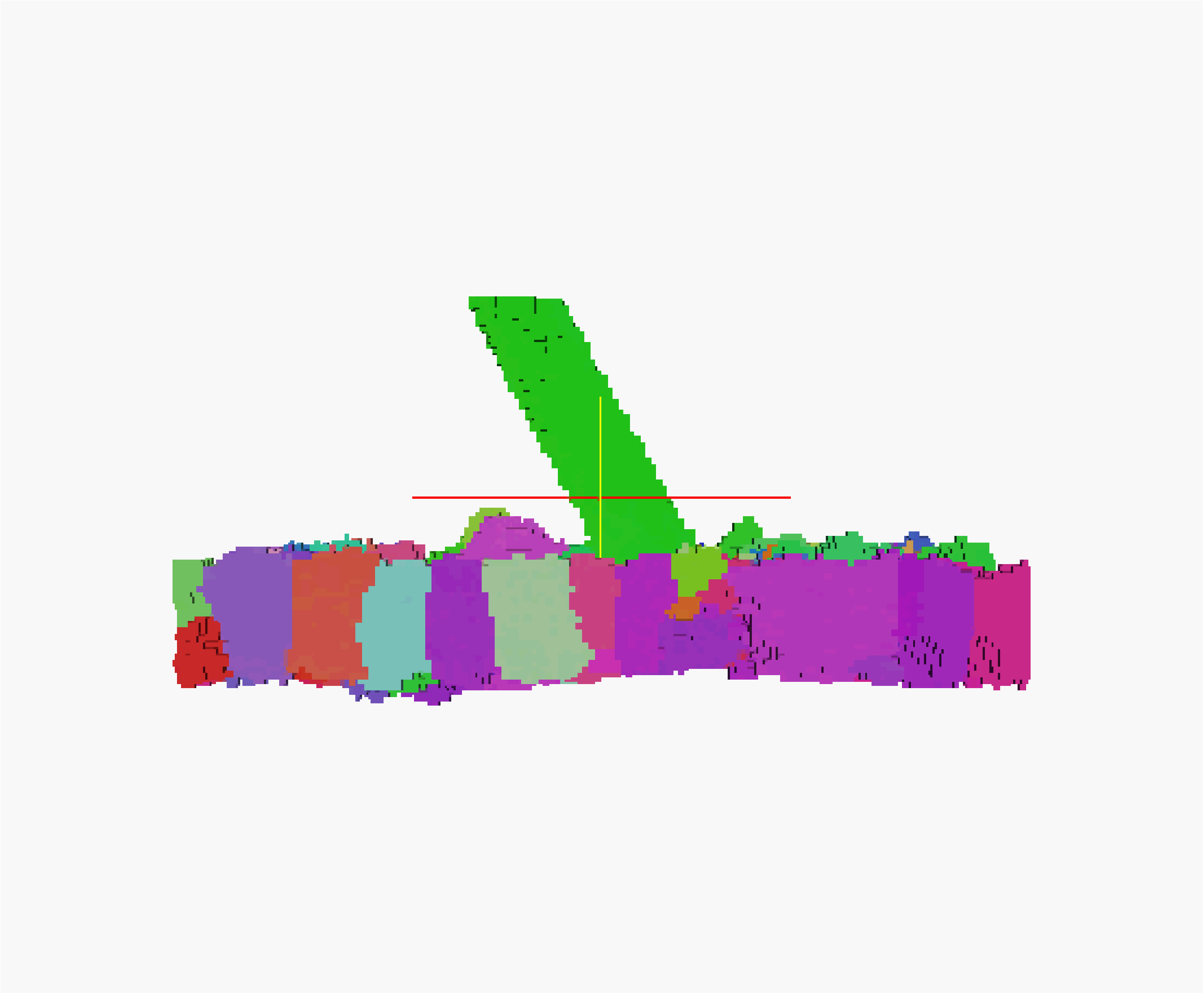

3D EBSD of large hillock on electroplated tin

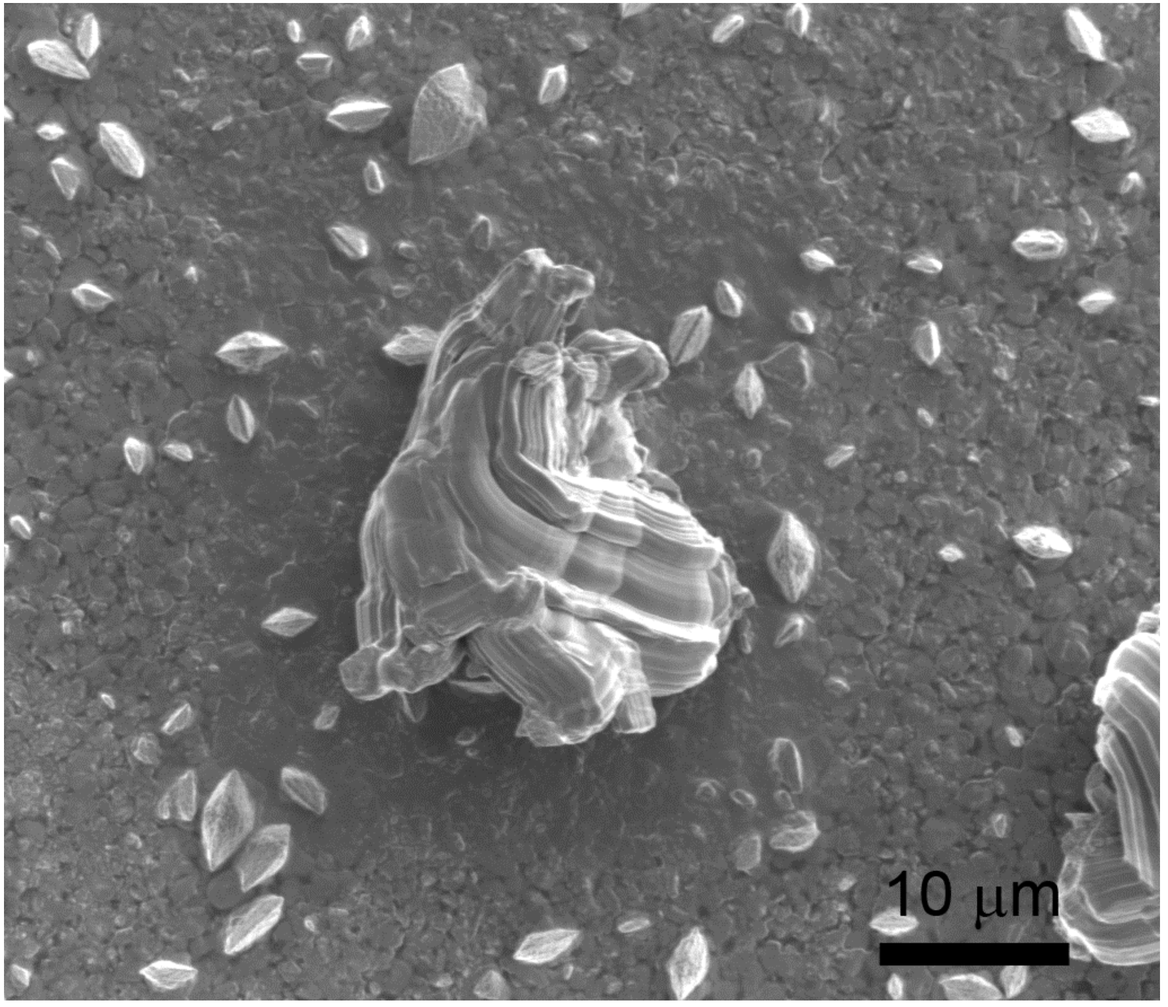

3D EBSD of large hillock on electroplated tin

IPF-X

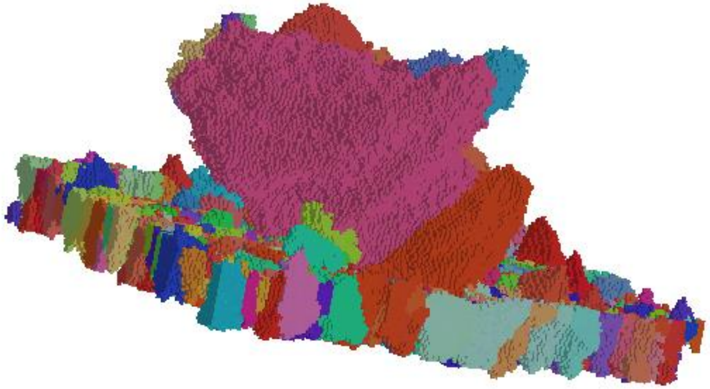

IPF-Y

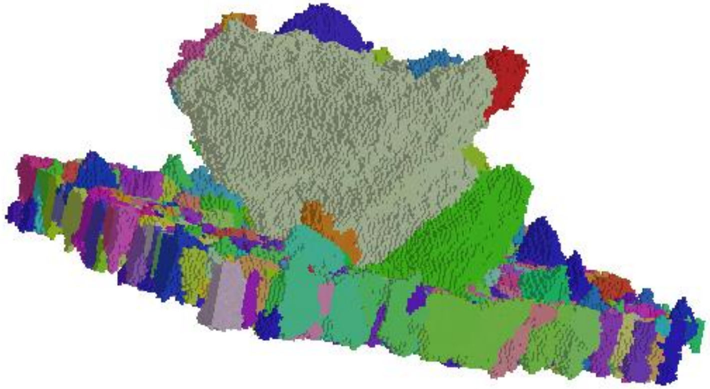

IPF-Z

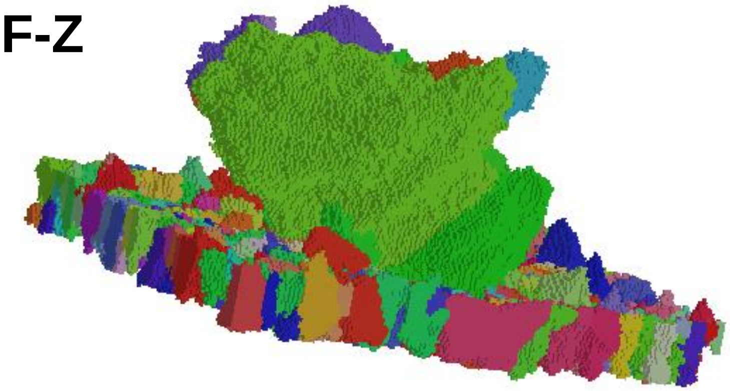

3D EBSD of large hillock on electroplated tin

Cross section

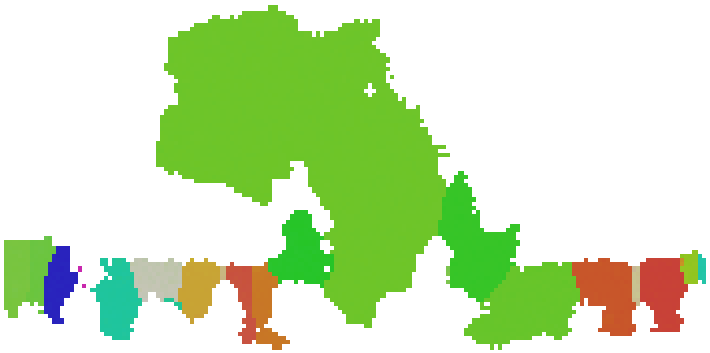

Plan view of tin film

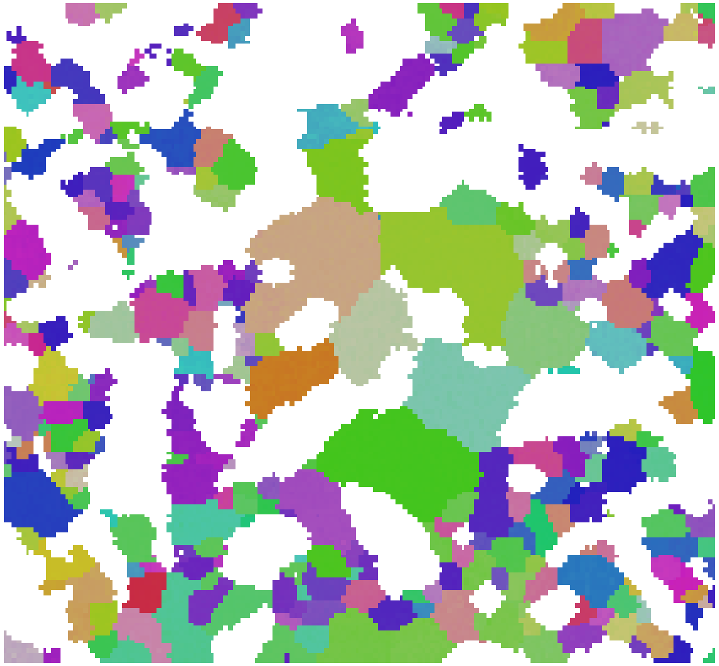

Slices through 3D data of hillock demonstrates that the hillock is mostly a single crystal and there are large grains due to recrystallization in the tin film.

Application of EBSD in materials science:

Applies to many materials

- ✓ Metals
- ✓ Ceramics
- ✓ Whiskers
- ✓ Mechanical testing
- ✓ Materials processing
- ✓ Use FIB for 3D EBSD

Acknowledgements:

Meteorite studies:
Joe Goldstein

AM and Stainless Steel Artifacts:
Jeff Rodelas
Michael Maguire

Wear studies and Contact materials:
Somuri Prasad
Nic Argibay

Tin whiskers:
Don Susan

Expert technical help:
Bonnie McKenzie –SEM and EBSD
Alice Kilgo - Metallography
Michael Rye – FIB sample preparation